Universidade Estadual Paulista "Júlio de Mesquita Filho"

Instituto de Física Teórica

Dynamics of Structured Populations

Renato Mendes Coutinho

Advisor:
Prof. Dr. Roberto André Kraenkel

Thesis presented to IFT in order to obtain the title of Ph.D. in Physics.
IFT T.001/15

Examining Committee:
Prof. Dr. Marcos Amaku (Universidade de São Paulo)
Prof. Dr. Fernando Fagundes Ferreira (Universidade de São Paulo)
Prof. Dr. Mark Lewis (University of Alberta, Canada)
Prof. Dr. Alexandre Souto Martinez (Universidade de São Paulo)

São Paulo

February 2015

ABSTRACT

This thesis broaches the dynamics of structured biological populations. These structures consist of anything that distinguishes individuals of the same population: sex, age, stage, size, spatial location, individual characteristics, etc. We explored a wide range of ecological systems and modeling approaches, working closely with biologists and ecologists in problems arising in specific contexts.

We studied some spatially explicit models for dispersal in connection with stage structure. Those include an integrodifference model for a blowfly invasion in Brazil during the 1970s, parametrized with laboratory and reanalyzed field data to predict *a posteriori* the invasion speed, obtaining a reasonable agreement. We also study the phenomenon known as habitat split, where immature individuals of species with complex life history, such as amphibians dependent on water streams to reproduce, are physically separated from their adult habitat, what can increase their mortality dramatically and lead to sharp extinction thresholds. We also investigate a model for population migration from a patch in a scenario of strong seasonality, where dispersal is possible only during part of the year, leading to distinct scenarios depending on that duration relative to the characteristic time for diffusion into the matrix.

Then we look at problems involving coexisting species in communities, beginning with the dynamics and coexistence of two species engaging in intraguild mutualism, in which they are both specialist predators on a common, shared resource, but benefit from each other's presence because of increased predation efficiency, leading to stable coexistence. We also develop an eco-epidemiological model for malaria transmission in the Atlantic Forest that incorporates feedbacks from ecological factors into biting rate and mosquito population size. Parametrized with data, it explains the absence of malaria transmission in the area, in contrast to the Ross-MacDonald model.

We introduce a novel framework to predict the population dynamics of cold-blooded animals taking into account temperature variation and stage structure. We use individual life-history traits (birth, death and development rates) and their response to temperature to parametrize the population dynamics model, applying it to two sets of questions: population viability and (temperature-dependant) intra-specific competition.

Finally, we explore the dynamics of predator-prey communities in which each population is composed by many species, characterized by their traits. Prey can invest more in defense against predators, at the cost of slower growth, while predators can be more or less selective on which prey it feeds on, but selective predators are more efficient. These traits can vary along a range of values, each species corresponding to a trait value. While traditional theory simplifies the description of the system by modeling only the aggregate measures of the distribution of traits in the population, we follow the dynamics of the whole system in order to learn how trait distributions with large variance, especially bimodal ones, change the outcomes of the community dynamics. We observe a range of behaviors, and characterize under which circumstances we expect to see drastic deviations from the usual aggregate models.

RESUMO

Esta tese aborda a dinâmica de populações biológicas estruturadas. Essas estruturas podem ser quaisquer características que distinguam indivíduos da mesma população: sexo, idade, estágio, tamanho, localização espacial. Exploramos uma variedade de sistemas ecológicos e estratégias de modelagem, trabalhando com biólogos e ecólogos em problemas específicos.

Estudamos alguns modelos espaciais explícitos para dispersão em conexão com estrutura de estágio. Isto inclui um modelo de equações integrais a diferenças para a invasão de moscas varejeiras no Brasil durante os anos 70, parametrizado com dados tanto de laboratório quanto de campo para prever *a posteriori* a velocidade de invasão, obtendo boa concordância. Também estudamos o fenômeno conhecido como desconexão de *habitat*, em que indivíduos imaturos de espécies com história de vida complexa, tais como anfíbios dependentes de cursos d'água para reproduzir, são fisicamente separados do seu *habitat* adulto, o que aumenta sua mortalidade drasticamente e pode levar a um limiar de extinção. Investigamos ainda um modelo para migração a partir de uma mancha em uma paisagem com forte sazonalidade, onde a dispersão é possível somente durante uma parte do ano, levando a regimes distintos dependendo da duração dessa estação em relação ao tempo característico de difusão na matriz.

Atacamos também problemas envolvendo a coexistência de espécies em comunidades, começando com a dinâmica de coexistência de duas espécies relacionadas por mutualismo intraguilda – predadores de um recurso comum compartilhado, mas que se beneficiam da presença uma da outra devido ao aumento da eficiência de predação, levando a coexistência estável. Além disso, desenvolvemos um modelo eco-epidemiológico para a transmissão de malária na mata Atlântica, que incorpora fatores ecológicos na taxa de picadas e tamanho da população de mosquitos. Este modelo é parametrizado com dados e explica a ausência da transmissão de malária nesta região, em contraste ao modelo de Ross-MacDonald.

Introduzimos um novo quadro teórico para prever a dinâmica populacional de animais de sangue frio levando em conta a variação de temperatura e a estrutura de estágios. Em particular, incorporamos características de história de vida (taxas de nascimento, morte e desenvolvimento) e sua resposta à temperatura a um modelo de dinâmica de populações, aplicando-o a duas questões: viabilidade da população e competição intra-específica dependente de temperatura.

Finalmente, exploramos a dinâmica de comunidades predador-presa nas quais cada população é composta por muitas espécies. Presas podem investir mais em defesa contra predadores às custas de uma menor taxa de crescimento, ao passo que predadores podem ser mais ou menos seletivos, porém os mais seletivos são mais eficientes. Essas características variam ao longo de um eixo contínuo, com cada valor correspondendo a uma espécie. Embora a teoria tradicional simplifique o sistema modelando apenas médias e variâncias, nós seguimos a dinâmica do sistema completo para descobrir como distribuições de características com grande variância, especialmente as bimodais, alteram os resultados da dinâmica de comunidades. Observamos vários tipos de dinâmica, e determinamos sob quais circunstâncias espera-se ver diferenças drásticas entre os modelos usuais e o nosso.

It can be very dangerous to see things from somebody else's point of view without the proper training.
— Douglas Adams, Mostly Harmless

ACKNOWLEDGMENTS

I thank the São Paulo Research Foundation (FAPESP) for the fellowship that supported me through my Ph.D.

I am very grateful to my advisor Roberto Kraenkel. I also thank my colleagues Gabriel Maciel, Franciane Azevedo, Juliana Berbert, and Natarajan Rethinavel, for many interesting discussions.

I am very indebted to the group from Potsdam University, particularly to my supervisor there, Ursula Gaedke, and to Toni Klauschies.

I thank all my collaborators, especially Priyanga Amarasekare, Frithjof Lutscher, Gabriel Laporta, Gilberto Corso, Marcio Zikan, Carlos Fonseca, Wesley Godoy, Cláudia Pio, and Paulo Inácio Prado, from whom I had much to learn.

I was lucky to always count on the support and affection of my girlfriend Fabiana, as well as her mother's care.

In closing, I thank my mother, Nadimi, for the love and encouragement through all my endeavours, and further my family, especially my brother and my father (*in memoriam*).

CONTENTS

1 INTRODUCTION

Ecology has a long tradition of attracting physicists and mathematicians. Population dynamics, in particular, often presents challenges that are appealing to the modeler's impulse to look for mechanisms based on few key assumptions that can be formalized in simple equations. Ecology, in turn, has greatly benefited from the theory-building efforts of many former physicists and mathematicians, besides biologists themselves.

Why does ecology need so much theory? In view of the tremendous diversity of organisms, environments, and ecosystems, it is hard to generalize any knowledge on the basis of experimental or observational evidence. It is thus necessary to develop general ideas that can be applied to many different situations – in other words, theory, even though it does not have to be mathematical. The application of mathematical concepts and methods becomes central to population ecology because its object of study, populations, are most usefully characterized by a single number, their size, whose change over time is one of the main preoccupations of the discipline. Other important derived quantitative central to ecology include reproduction and mortality rates, distribution of the population over space, ratio of males to females, and many others.

Mathematical models can be used to make accurate quantitative predictions. This is often thought to be the main (sometimes only) role of models, and their utility is defined only in terms of their validation compared to data. This is feasible, however, only on very specific circumstances, when the system at hand has been exhaustively studied and measured. Ecological processes and measurements present so many sources of noise or unexpected variation that "strong" prediction[1] is often precluded. This shows a strong contrast to physics, which has two properties that make it much easier to deal with: the first is that one can, for all practical purposes, isolate physical systems from the rest of the world, something not possible for biological systems (nor desirable, since we want to study how they work *in natura*); secondly, in most cases physical entities are all identical, and have few kinds of interactions between each other, so classical reductionism tends to work well.

Mathematical modeling has other roles. In its simplest approach, it can be used to provide a bare caricature of a system, which answers basic questions like: can such mechanism generate the expected qual-

1 Broadly speaking, precise quantitative prediction of effects independent of previously measured parameters.

itative patterns, as hypothesized? In this context, a well-thought-out model checks and reinforces our understanding of the processes and mechanisms behind the patterns.

Models can also play a role unifying disparate phenomena that behave in a similar way. For instance, Chesson (2000) classified the many mechanisms of species coexistence into stabilizing and equalizing, which act together to determine when two (or more) species coexist. Although the framework is broadly applicable, the mechanisms can be easily understood analyzing the classical Lotka-Volterra competition model.

Research on interdisciplinary areas presents several challenges. The first is simply communication: different backgrounds and training result in incompatible jargon and canned ways of thinking, which can be hard to overcome initially. From a broader perspective, the main issue is: what is the effective contribution of that research? Entering an interdisciplinary field presents two complementary risks: by ignorance or lack of communication, we may work on topics that are not useful for that field at all; on the other hand, we are somewhat disconnected from the research on the original area, even if the methods used are still the same. All those issues can be greatly mitigated by working close to people across the disciplinary boundary.

The topic of this thesis is the dynamics of structured populations. These structures consist of anything that distinguishes individuals of the same population: sex, age, stage, size, spatial location, individual characteristics, etc. Although these are all common subjects in mathematical biology, there are still many unexplored aspects to investigate. Our approach was to work closely with biologists and ecologists in problems arising in specific contexts, which is also reflects the philosophy of the mathematical biology working group at the Institute for Theoretical Physics (IFT). This gave the thesis a somewhat fragmented nature, being composed of several research projects. The net result, however, is a comprehensive formation that provides flexibility for dealing with an array topics.

The thesis is structured in four main chapters. Each one broaches specific topics, based on research done at different times, with several different collaborators, and distinct goals. Therefore, the chapters are independent, each containing its own introduction. Their structure follow closely the articles published or in preparation.

Chapter 2 deals with spatially explicit models for dispersal in connection with stage structure, and describes three distinct projects. In section 2.2 we develop an integrodifference model for a blowfly invasion which occurred in Brazil in the 1970s, using laboratory and reanalyzed field data to find all parameters and predict *a posteriori* the invasion speed. The second work (section 2.3) formalizes the phenomenon known as *habitat split*, where immature individuals of species with complex life history, such as amphibians dependent on

water streams to reproduce, are physically separated from their adult habitat, which can increase their mortality dramatically and lead to sharp extinction thresholds. Finally, in section 2.4, we investigate a model for population migration from a patch in a scenario of strong seasonality, where dispersal is possible only during a limited part of the year, leading to distinct regimes depending on that duration relative to the characteristic time for diffusion into the matrix.

Chapter 3 comprises two works: the first, detailed in section 3.2, is on the dynamics and coexistence of two species engaging in *intraguild mutualism*, in which they are both specialist predators on a common, shared resource, but benefit from each other's presence because of increased predation efficiency, leading to stable coexistence – something usually surprising in view of traditional consumer-resource theory. Section 3.3 presents an eco-epidemiological model for malaria transmission in the Atlantic Forest. It incorporates some relevant ecological factors – diffuse competition between vector and non-vector mosquito species, dilution effect due to the presence of non-competent (which do not carry the disease) warm-blooded animals, and also the possibility that mosquito population is limited by blood supply from humans and animals. That model is parametrized with data collected at Ilha do Cardoso (Southeast litoral of São Paulo State), and explains the absence of malaria transmission in the area, in contradiction to the traditional Ross-MacDonald model.

Chapter 4 describes a novel framework to predict the population dynamics of cold-blooded animals taking into account temperature variation and stage structure. In particular, we use individual life-history traits (birth, death and development rates) and their response to temperature to parametrize the population dynamics model, applying it to two sets of questions: population viability and (temperature-dependant) intra-specific competition.

Finally, chapter 5 explores the dynamics of predator-prey communities in which each trophic level is composed by many species, characterized by their traits. Prey can invest more in defense against predators, at the cost of slower growth, while predators can be more or less selective on which prey they feed on, but selective predators are more efficient. These traits can vary along a range of values, each species with a different trait value. Traditional theory simplifies the description of the system by modeling only the aggregate measures of the distribution of traits in the population – their means and variances. We choose to model the full distributions in order to learn how distributions of large variance, especially bimodal distributions, change the outcomes of the system dynamics. We observe a rich dynamics, and characterize under which circumstances we expect to see drastic deviations from the usual aggregate models.

2

SPATIO-TEMPORAL DYNAMICS AND STAGE STRUCTURE

2.1 INTRODUCTION

The traditional formulation of mathematical models describing population dynamics is done by means of differential equations. In the simplest case, of a single population of size N, a general formulation is just:

$$\frac{dN}{dt} = f(N) \,, \tag{2.1}$$

where t is time, and the function f defines the net growth rate, and includes all relevant processes that can affect the population.

The extension of such models to a spatial context was first treated by Skellam (1951), using a diffusion-reaction equation. It consists of a non-spatial part, also called the *local* term, and a diffusion term, which describes the population dispersal:

$$\frac{\partial N(x,t)}{\partial t} = f(N) + D\frac{\partial^2 N}{\partial x^2} \,, \tag{2.2}$$

This diffusion approach assumes that, at the spatial scale relevant to the model, the density of the population over space is well approximated by a continuous function, that is, it is not patchy. This will certainly not hold if the scale is small enough, as individuals are usually discrete. The derivation of reaction-diffusion equations is based on a random walking process without bias, being identical to that from the study of random particle movement. Many other kinds of population redistribution models have been proposed, taking into account particular movement patterns, such as chemotaxis, aggregation of individuals, pursuit of prey, etc. (Murray, 2002).

The model (2.2) requires also the definition of boundary and initial conditions. Invasion problems usually focus on the pattern and speed of invasion, and therefore tend to use an infinite domain with zero population at one end ($x \Rightarrow \infty$) and some other fixed point in the other direction ($x \Rightarrow -\infty$). In the context of limited habitat, we define a restricted domain and impose boundary conditions based on the behavior of the individuals near the border (Maciel and Lutscher, 2013).

Discrete-time models are defined by mappings, equations like

$$N_{t+1} = f(N_t) \,, \tag{2.3}$$

where the variable t is now a non-negative integer, and refers to the generation number. These kinds of models are particularly appropriate when populations have well defined generations, that is, individuals can be assigned in a sensible way to a generation together with other individuals born around the same time. This is the case, for instance, for annual plants, that reproduce only once a year. In extreme cases, we have non-overlapping generations, in which the old generation is gone by the time the new one matures.

The introduction of space into discrete-time models is less well-known than the reaction-diffusion equations, but is simpler to understand and interpret. Given the density of the population over space at generation t, $N_t(x)$, we compute the total population density at a given point y using a *redistribution kernel* K (Kot, 1992):

$$N_{t+1}(y) = \int_{-\infty}^{+\infty} N_t(x)K(y,x)dx \,, \tag{2.4}$$

where $K(y,x)$ denotes the probability density function of migration from x to y. K is normalized, that is $\int_{-\infty}^{\infty} K(y,x)dy = 1$, so that there is no non-biological leaking of population. K is any probability density function (i.e, a non-negative function), although it is usually written as a function of the distance between the two point, $K(y,x) \equiv K(|y-x|)$. This formulation allows much more flexibility in choosing or modeling specific movement patterns than continuous-time models.

Coupling population dynamics with dispersal is also straightforward: we assume a growth phase, during which the local populations grow ($N_{t+\text{growth}}(x) = f(N_t(x))$ and a dispersal phase, in which we apply the equation above to this intermediate population.

In what follows, we present three problems involve spatially extended populations. The first section studies the invasion of a blowfly species, a project developed in collaboration with Wesley Godoy, currently a professor of Ecology at the University of São Paulo in Piracicaba. This work was published in the article "Integrodifference model for blowfly invasion" (Coutinho et al., 2012). We propose a stage-structured integrodifference model for blowflies' growth and dispersal taking into account the density dependence of fertility and survival rates and the non-overlap of generations. We assume a discrete-time stage-structured model. The spatial dynamics is introduced by means of a redistribution kernel. We treat one and two dimensional cases, the latter on the semi-plane, with a reflective boundary. Using laboratory data for fertility and survival parameters and dispersal data of a single generation from a capture-recapture experiment in South Africa, we obtain an estimate for the velocity of invasion of blowflies of the species *Chrysomya albiceps*. This model predicts a speed of invasion which was compared to actual observational data

for the invasion of the focal species in the Neotropics. Good agreement is found between model and observations.

Section 2.3 shows the result of a collaboration between our mathematical biology group, including Juliana Berbert and Franciane Azevedo, besides our advisor Roberto Kraenkel and myself, and Carlos Fonseca, professor of Ecology at the Federal University of Rio Grande do Norte (UFRN), and Gilberto Corso, professor at the Department of Biophysics also at UFRN. It was published in "Modeling habitat split: landscape and life history traits determine amphibian extinction thresholds" (Fonseca et al., 2013). Habitat split has been recently proposed as an important threat for organisms exhibiting marked ontogenetic habitat shifts. For most amphibian species, for instance, habitat alteration can potentially create a disjunction between the terrestrial habitat of the adults from the aquatic habitat of the larvae, leading to population decline and, eventually, local extinction. Here, we develop a model concerning the effect of habitat split on population size and persistence. Our diffusive model, inspired on forest-associated amphibians with aquatic larvae, shows that habitat split alone is able to generate extinction thresholds. The model predicts that species with higher reproductive success and higher diffusion rate of post-metamorphic juveniles will have larger critical split distances[1] for species persistence in forest fragments. Furthermore, it predicts that negative effects of habitat split can be compensated by positive effects of fragment size, but only up to a given point. The model has relevant implications for landscape design for species conservation.

Another collaboration with Gilberto Corso, together with Marcio Zikan Cardoso, professor of ecology at UFRN, led to the work described in section 2.4, still unpublished, on the effects of strong seasonality in dispersal rates on the maximum colonization distance expected from colonizers out of a patch. Functional connectivity between habitat patches is influenced by the nature of the intervening matrix and how organisms respond to it. Models usually treat the matrix as a fixed category and fail to appreciate the possibility of dynamic matrix types. Given that matrix quality differs between dry and wet seasons in the seasonal tropics, the role of seasonal changes in matrix quality have not been explored. The duration of the favorable period for dispersal, the species' ability to disperse and the distance between patches could be important factors determining patch connectivity. We explored these connections by employing a diffusion model to a one-dimensional landscape subjected to periodical fluctuations in matrix quality; diffusion was curtailed in the dry season and permitted in the wet season. Our model predicts that, given a particular organism's lifetime and diffusion constant, connectivity will be a function of the diffusion distance during the favorable disper-

1 The distance between the breeding site and the patch, as will be explained later.

sal season. We parameterize our model with demographic data from *Heliconius* butterflies, finding that the model successfully describes connectivity between habitat patches, so it could be used to model dispersal of other organisms in seasonal environments and to help guide restoration efforts and design of protected areas in the tropics.

2.2 BLOWFLY INVASION AND INTEGRO-DIFFERENCE EQUATIONS

Invasive species are thought to be one of the greatest causes of loss of biodiversity in the world (Williamson, 1999), along with habitat destruction and overexploitation of natural resources. Many different aspects of invasions have been object of attention in the last decades. Among those, the spatial dynamics of invasions is one aspect that has attracted a great amount of interest (Shigesada and Kawasaki, 1997). The mathematical theory to understand and predict how invasions take place has been studied to a great extent, and features a variety of mathematical formulations, from reaction–diffusion to integrodifference equation models. Although the assumptions behind each treatment may be different, there are some general results, such as that – in the absence of Allee effects – the spread velocity depends only on dispersal capacity and net reproductive rate at low densities (Kot et al., 1996).

Comparison of models with data is in general harmed by the lack of observations about the main parameters present in the models. Although growth ratios can in many cases be inferred from laboratory experiments, the dispersal ability of a given species is difficult to determine. Frequently, models are adjusted to data by fitting the parameters related to dispersal. However, this weakens the model's validity and precludes testing the model. In this section we overcome these difficulties in a specific case: we give a model where the parameters determining the speed of invasion are completely fixed by either laboratory experiments or by field observations. With the velocity determined by the parametrized model, we test the predictions in a geographically distinct region, relying on historical data.

Around 1975, *Chrysomya albiceps* (Calliphoridae), a blowfly species, was brought from Africa to South America by Angolan refugees during the Civil War (Guimarães et al., 1978). Although there are records of previous introductions (Baumgartner and Greenberg, 1984), only on that occasion did the species establish. Afterwards, *C. albiceps* invaded South America tropical regions in the following decade, displacing other native blowfly species.

Blowflies, as many insects, are an stage-structured species. The larval phase accounts for the population regulation, as the population level is essentially determined by the resource availability (in this case, carrion). On the other hand, dispersal is related to the adult stage.

We formulate a model incorporating stage-structure and dispersal that is capable of predicting the speed of invasion for blowflies of the *C. albiceps* species using as input parameters fertility and survival data, measured in laboratory, and one-generation dispersal data, assessed by means of capture-recapture techniques in an experiment performed in the 80's in South Africa. This provides us with a definite speed that is not fitted to the realized invasion, so we are able to compare it to the actual speed of invasion observed in South America.

Although the data used in this case mixes laboratory experiments with field data from different geographical locations, the results about the invasion speed are close to the observed velocity, a point which renews hope that even simple models, taking care of biological particulars and noisy data, can provide meaningful information about the dynamics of invasions.

Finally, we point out that the model presented below also displays an interesting mathematical structure, which has already been seen in previous works, (Kot, 1992; Andersen, 1991). In fact, as the dynamical (non-spatial) stage of the model shows a bifurcation route to chaos, when space is incorporated the resulting model reveals the formation of spatial non-stationary structures.

2.2.1 *Model*

C. albiceps life cycle consists of egg, larvae, and adult stages. The female adults deposit large masses of eggs onto carrion or feces, which are consumed by the larvae after eclosion. The larvae go through three instars before emerging as adults, which are able to fly and search for new carcasses.

These blowflies are known to display intraguild predation as well as cannibalism in the larval stage (Ullyett, 1950), which contributes to a strong density dependence during the larval period with overcompensation (Godoy et al., 2001), that is, declining recruitment with increasing density of larvae, affecting both survival and fertility rates.

Successful invasive species are expected to be regulated by bottom-up processes: the release from predatory pressure in a given region – taking the species out of a self-regulated community – makes the population level dependent on the available resources (Sakai et al., 2001). This fact simplifies the mathematical modeling of invasions, as relevant results can be obtained by means of single-species models.

The local dynamics

Let us begin by building our model presenting the local dynamics equations. We consider a simple, two-stage difference model, following the results of Prout (Prout and McChesney, 1985). It accounts for

growth and competition for resources in the larval stage, without any spatial dynamics yet:

$$u_t = S^* \nu_t \, e^{-s\nu_t} \quad , \tag{2.5}$$

$$\nu_{t+T} = \frac{1}{2} F^* u_t \, e^{-f\nu_t} \quad . \tag{2.6}$$

The larvae at generation t, of density ν_t, survive to adulthood at a maximum survival rate of S^*, at very low densities. At higher densities, this survival decreases exponentially. This is due to *scramble competition*, in which resources are divided roughly equally among competitors, rendering almost all of them unable to develop. The adults (of density u_t) that do develop will have also lower fecundity due to this lack of resources during larval stage, and so fecundity of adults will also decrease exponentially with larval density. The next generation of larvae will be equal to this adult population multiplied by the fecundity. The parameters s and f quantify the density effects on those rates. Also, each time step corresponds to a complete generation time, the egg-to-egg interval T.

C. albiceps is a semelparous species, that is, it oviposits only once. Also, it feeds on ephemeral resources, so that competition tends to be important only between individuals of the same generation. This indicates that the assumption of discrete time dynamics is a sensible choice.

The spatial dynamics

We proceed by introducing spatial dynamics into the model through a redistribution kernel $K(x, x'; y, y')$. In the case at hand, only the adult population is responsible for the dispersal, since the spread of larvae occurs at a much smaller scale. The redistribution kernel should thus describe the contribution of adults emerging at (x', y') at time t to the larvae at (x, y) at the next next generation (at time $t + T$), through oviposition. Adopting a discrete-time, continuous space description, the equations will read (Kot, 1992):

$$u_t(x, y) = S^* \nu_t(x, y) \, e^{-s\nu_t(x,y)} \quad , \tag{2.7}$$

$$\nu_{t+T}(x, y) = \frac{1}{2} F^* \iint u_t(x', y') \times e^{-f\nu_t(x',y')} K(x, x'; y, y') \, dx' dy' \, , \tag{2.8}$$

where the parameters are the same as in equations (2.5) and (2.6).

Spatial Homogeneity

In the above equation we have assumed that the parameters F^*, S^*, s and f do not depend on the spatial location. This cannot be true on every spatial scale as, for instance, f and s are related to the carrying

capacities which, in turn, are related to the availability of resources. We certainly have fragmentation at small scale, since carcasses are distributed heterogeneously in space, but the invasion's spatial scale is much larger than that. In view of that, we will treat space as homogeneous, taking all parameters as some average (not necessarily arithmetic), which corresponds to the homogenization limit (Shigesada et al., 1986). Accordingly, variability in small spatial scale is not to be predicted by our model.

Spatial heterogeneity on a larger scale may have a large effect, but for that the problem would have to satisfy two conditions (Pachepsky and Levine, 2011): (a) discrete number of individuals, that is, insufficient size of propagules, such that it is necessary that the population build up in order to be able to go forward [2]; and (b) inhospitable barriers between patches. None of them are verified, since (a) a single female blowfly may propagate the invasion, having a very high recruitment, such that the number of propagules is always as high as it can be; and (b) blowflies are generalists, feeding on all kinds of decaying organic material, from feces to carcasses, so that they are able to survive in most places (Richards et al., 2009). Therefore, we expect heterogeneity effects to be relatively small.

Ricker-like Model

The system of equations can be rewritten as a single equation for larvae only, where adults are not explicitly modeled, but may be seem as a means of propagation from one generation to the next:

$$\nu_{t+T}(x,y) = \frac{1}{2}F^*S^* \iint \nu_t(x',y') \times e^{-(f+s)\nu_t(x',y')} K(x,x';y,y')\,dx'dy' \,. \quad (2.9)$$

It is clear that this model is of the Ricker form (Ricker, 1954), so its local dynamics, which is well known (May and Oster, 1976), exhibits complex behavior for high values of the product S^*F^*, presenting a period-doubling bifurcations route to chaos as the product of those parameters increases.

The redistribution Kernel

In order to progress, an assumption has to be made about the form of the redistribution kernel. We will consider, in what follows, two cases. First, we will look at the one-dimensional case. This will allow us to get a simplified view of the dynamics and use previous results to calculate the speed of the invasion front. Next, we will look to the two-dimensional case on the semi-plane, with zero-flux conditions on the border. This represents additional biological realism, as the actual

2 That is, an Allee effect

invasion process for *C.albiceps* in the Neotropics was initiated at a coastal zone and directed inland.

For the one-dimensional case, we make the simplifying assumption that the redistribution kernel is Gaussian. Even though it is usually argued that real populations tend to show leptokurtic kernels (Okubo and Levin, 1989; Neubert et al., 1995; Kot et al., 1996), we seek to keep behavior-related assumptions to a minimum, though keeping in mind that we may be underestimating dispersal. Such choice yields the following model:

$$v_{t+T}(x) = \frac{F^* S^*}{2\sqrt{\pi}\sigma} \int_{-\infty}^{+\infty} v_t(x') \times e^{-(s+f)v_t(x')}\, e^{-(x-x')^2/\sigma^2} dx' , \quad (2.10)$$

where now we have another parameter, σ, which measures the typical distance an adult individual roams before ovipositing. On this interpretation, we neglect the effect of another female oviposition besides the first.

For the two-dimensional case, we assume independence of the x and y directions. This allows us to consider a product kernel, $K(x, x'; y, y') = K_x(x, x')K_y(y, y')$. Considering the semi-plane defined by $x \geqslant 0$, the kernel reads:

$$K_y(y, y') = \frac{1}{\sigma\sqrt{\pi}}\, e^{-\frac{(y-y')^2}{\sigma^2}} \quad (2.11)$$

$$K_x(x, x') = \begin{cases} \dfrac{1}{\sigma\sqrt{\pi}} \left[e^{-\frac{(x-x')^2}{\sigma^2}} + e^{-\frac{(x+x')^2}{\sigma^2}} \right] & \text{if } x' \geqslant 0 , \\ 0, \text{ otherwise.} \end{cases} \quad (2.12)$$

$K_y(y, y')$ is the Gaussian kernel in the unbounded direction. The expression for $K_x(x, x')$ can be derived under the same assumptions used to derive a Gaussian kernel, but with a reflexive boundary at $x = 0$. Indeed, both expressions can be obtained from the assumption that the underlying process is Markovian, with equal probabilities in each direction (Chandrasekhar, 1943). We note furthermore that with this kernel, the integral appearing in Eq.(2.9) is not a convolution anymore, as $K_x(x, x')$ does not depend only on the difference $x - x'$.

2.2.2 *Results*

One-dimensional case

The model defined by the kernel given in Eq.(2.10) leads to complex spatial and temporal dynamics for sufficiently large F^* and S^* parameters as can be seen in figure 2.1. This was to be expected, since the local dynamics already showed such complex behavior(Kot, 1992;

Andersen, 1991). The population density oscillates irregularly both in space – if we look at a "snapshot" in time – and in time – given a fixed spatial location. It is not, however, our intention to reassess the typical dynamics of the Prout model. Rather, we proceed to consider the spatial effects that are connected to observations.

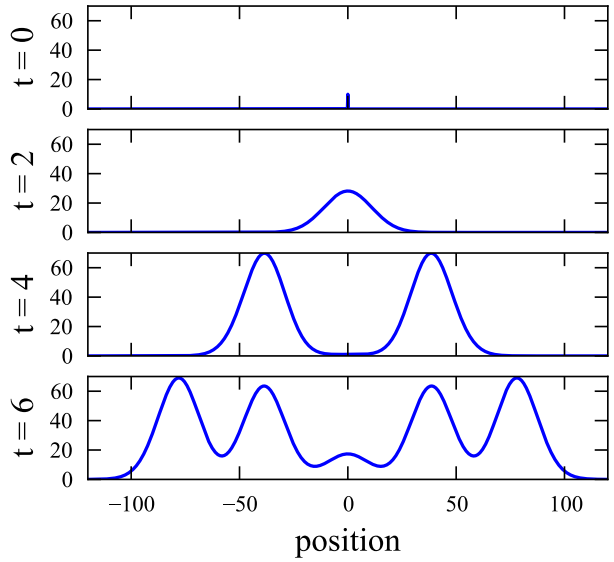

Figure 2.1: Population density evolution, with realistic parameters for *C. albiceps* invasion: $F^*S^* = 130$, $s + f = 0.1$ and $\sigma = 10.8$. In the first plot we show the initial condition, a small, localized population.

We turn now to the calculation of the speed of invasion. As in many models with the same ingredients, dispersal and nonlinearity, we have essentially two solutions – one is the null solution, and the other shows complex dynamics, (Kot, 1992). Connecting both of them, there is a wave front. After a short interval, the speed of invasion converges to a constant, as can be seen by numerically integrating the equations. We point out that the spatial scale is fixed by the parameter σ, so that the space units are fixed with respect to it, and so it is expected that the invasion speed should be proportional to σ, as it will indeed turn out.

The upper bound of the velocity, c, of the front of invasion in terms of the model parameters was given by Kot et al. (1996):

$$c = \sigma\sqrt{\log\frac{F^*S^*}{2}} \tag{2.13}$$

For sake of completeness, in Figure 2.2 we display also how the maximum fertility and survival rates affect invasion velocity.

It is worthy to emphasize that the front velocity does not depend on the parameters f and s. These parameters, which measure fertility and survival drop rates when population density increases, come into play only at higher densities and do not interfere in the velocity

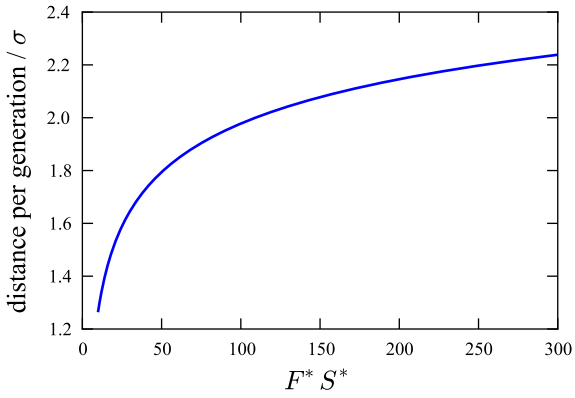

Figure 2.2: Analytical upper bound for the invasion speed as a function of the parameter's product F*S*, for both one and two-dimensional cases.

of invasion. We note, however, that it has been argued recently that density dependence can play a role in spread velocity (Pachepsky and Levine, 2011) when the landscape is fragmented and populations are discrete, that is, when the approximation of continuously varying, infinitesimal populations is not sensible.

Two-dimensional case

The two-dimensional case has been treated numerically and the solution is displayed in Fig.(2.3). The results have been obtained using realistic parameters.

In the full nonlinear case, we show numerically that, after a transient, the distance travelled per generation along any ray with origin in (0,0), is constant. Therefore the invasion speed is also constant, and indeed has the same value as in the one-dimensional case.

The general aspect of the spatial configuration of the solutions corresponds to non-stationary patterns with a spatially complex dynamics, just as in the one-dimensional case, Fig.(2.1). In the next section we comment on the actual detectability of such patterns.

2.2.3 *Parameter estimates and comparison with observations*

In this section, we reuse data from the literature to feed the model developed in the last subsection in order to obtain a prediction of the velocity of invasion. In using and analyzing that data, it is crucial to bear in mind that predictability may be hindered by "founder effects" (Melbourne and Hastings, 2009), so that the variability of the relevant life-history traits must be taken into account. In that spirit, what we provide is a range of values for the invasion speed.

Godoy *et. al.* (Godoy et al., 2001) measured fertility and survival data for *C. albiceps*, finding S^* to be approximately 0.5 ± 0.1 and F^*

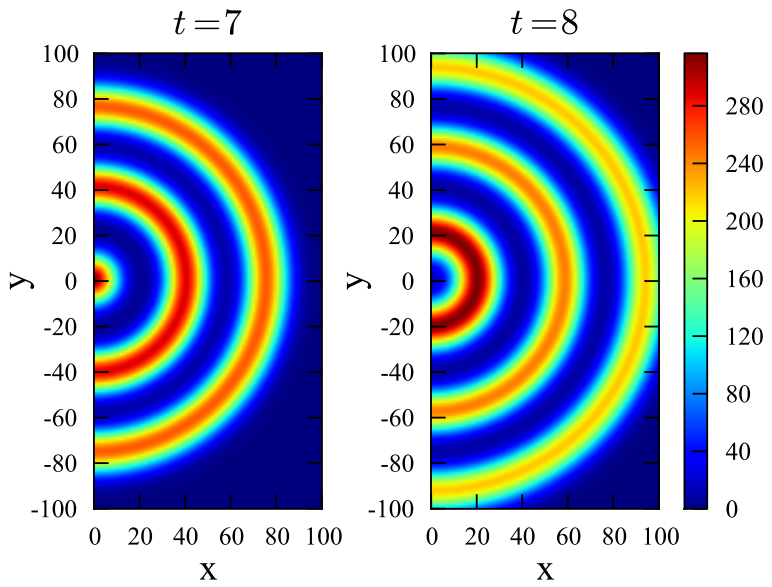

Figure 2.3: Solution of the two-dimensional model results, with $F^*S^* = 130$, $s + f = 0.1$ and $\sigma = 8$. We can see the front of invasion expanding in one generation, as well as a pattern of peaks and valleys in the region already occupied by the population. At $t = 0$ the initial condition consists of a localized population around the origin.

260 ± 40 total eggs/female in 10 days. They also validate the Ricker form of the local population dynamics, although the parameters f and s found are related to the amount of resources used in their particular experiment.

To estimate σ, we use data from a capture-recapture experiment performed by Braack and Retief (1986). The experiment consisted of releasing 16000 radioactively marked *C. albiceps* blowflies in a central point of the northern Kruger National Park, South Africa. After one week, 69 traps were placed throughout the park, and the number of flies, both marked and unmarked, were counted. The raw data are presented in the first four columns of table 2.1.

The redistribution kernel $K(x, x')$ gives the probability of an adult emerging at point x' to oviposit at x. The experiment had been set up so that the captures occur when flies try to oviposit in the meat inside the trap.

The typical time until oviposition was also carefully considered, since *C. albiceps* oviposits only 5 to 7 days after emerging. Thus traps had been set only after this interval, which also contributes to avoid overcrowding of non-marked blowflies in the samples.

To estimate the redistribution kernel, we must account for several effects, such as area of measurement, sampling effort and attractiveness of traps.

The area of the park has been divided by Braack and Retief (1986) in several rings – distance ranges from the center – of different areas.

Since we are interested in the density of captures, we need to divide the number of catches by each ring's area.

We must also counterbalance the sampling effort – related to the number of traps employed in each area – and the fact that the environment is heterogeneous at the scale considered, in such a manner that some traps might have been placed in more favorable or accessible places than others. Both biases can be corrected by looking at the total amount of *C. albiceps* blowflies captured, including the non-marked ones, which should be a proxy for how attractive the traps were. This quantity incorporates the sampling effort as well, since the total number of catches will also be related to the number of traps in each region. Therefore, we divide the number of marked blowflies by the total amount of blowflies to obtain the corrected proportion of marked blowflies in each region.

In view of the above, the reworked density proportion y in each distance range can be calculated by:

$$y = \frac{\text{marked flies}}{\text{total flies} \times \text{area}}$$

Table 2.1: Dispersal data for *C. albiceps* in the Kruger National Park, South Africa. The first four columns are published data (Braack and Retief, 1986), followed by the results of the analysis.

Distance ranges from central release point (km)	Number of traps	Total number of *C. albiceps* captured	Number of *C. albiceps* re-captured	Area (km^2)	Density of captured flies corrected by total catches (10^{-5} flies/km^2)
0–4	12	4066	8	50.3	3.91
6–10	19	14270	65	201.1	2.27
12–18.5	16	10801	40	622.8	0.59
20–29	8	5992	9	1385.4	0.11
30–40	12	10455	10	2199.1	0.04

Although these values do not give the actual scale of population density, they do represent the proportion of radioactively marked blowflies at different distance ranges. The result is presented in the last column of table 2.1 and also in the reflected histogram in Fig.(2.4).

We calculate σ fitting the best Gaussian with a least squares method, shown in figure 2.4, along with the histogram of the data treated as described. The estimative is rough, given the limitations of the measurement, but it is taken on the field instead of in the lab, so the data is more likely to reflect the characteristics of the population *in natura*.

Figure 2.4 shows that σ is about 10.8 km, in the range $7 - 14$ km. Using these value for σ along with the data for F^* and S^*, we find

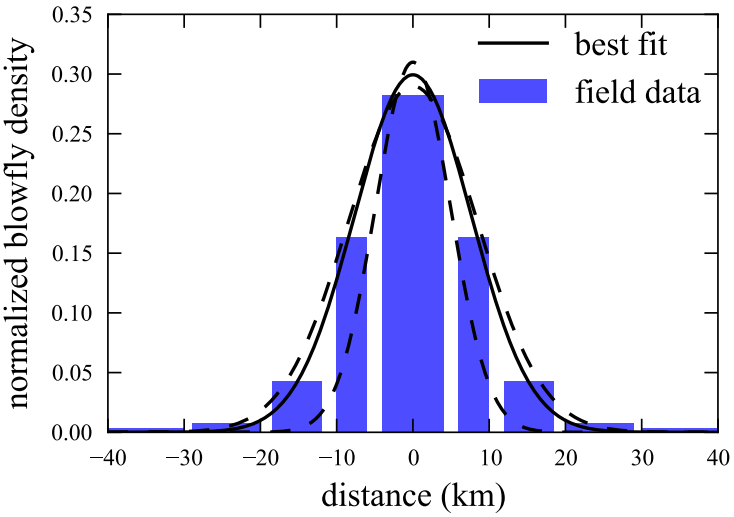

Figure 2.4: Least squares fit of analyzed dispersal data from Braack and Retief (1986). Dotted lines indicate minimum and maximum acceptable width parameter.

that the velocity per generation is about 20 km/generation, with the range between 14 and 30 km/generation.

To calculate the actual velocity, we need to estimate the generational time of the blowflies in the field. Laboratory experiments show that time from hatching to eclosion is highly dependent on temperature, ranging from 10 to 30 days for temperatures between 17 and 25°C (Al-Misned et al., 2002; Richards et al., 2008). Also, from the field experiment performed by Braack in the Kruger Park (RSA) (Braack and Retief, 1986), which presents temperatures similar to the State of São Paulo, we can estimate that the flying stage lasts between 5 and 10 days, which leads to an egg-to-egg time of 15 to 35 days.

Table 2.2: Summary of parameter ranges used.

parameter	range
F^*	220 – 300 eggs/female
S^*	0.4 – 0.6
σ	7 – 14 km
T	15–35 days

Using the previous results and taking into account these estimates for generational time, our models predict dispersal velocity between 0.4 and 2.0 km/day for *C. albiceps* invasion in the Neotropics.

In order to compare these results with the actual invasion in the Neotropics, we resort to historical data published in the 70's and early 80's. Baumgartner and Greenberg (1984) estimated *C. albiceps* invasion velocity between 1.5 and 1.8km/day. We also retrieved data

stating the first observation of *C. albiceps* in 73 locations in Brazil (Guimarães et al., 1979). This allows us to estimate the upper bound for the invasion velocity, which turns out to be 2.0km/day. The estimated range that we had calculated above, between 0.4 and 2.0km/-day, is in agreement with the actual invasion speeds.

Finally, we notice that the spatio-temporal patterns observed in the dynamics of the models (see, for instance, figures 2.1 and 2.3) are not expected to be observable in field experiments, as they occur in a spatial scale close to σ, which is the scale in which the homogenization limit, discussed in section 2, breaks down.

2.2.4 *Conclusions and Final Comments*

Invasive species present a rich variety of situations where the use of mathematical models is helpful to provide a theoretical setting, allowing to assess questions such as invasibility and the dynamics of actual invasions.

The results that we have obtained combine laboratory parameters (fertility and survival) with dispersal data from a field experiment for one-generation, leading to prediction of the invasion speed of the species. The agreement of this result with the velocity of an actual invasion in another geographical range is by no means trivial. The combination of data obtained at different spatial and temporal scales could have hampered the applicability of the models. Indeed, that has been the case, for instance, with the model predictions for an invasive shrub in North America studied by Neubert and Parker (2004). Although observations connected to the pattern of spread have showed agreement with theory (Nash et al., 1995; Kot et al., 1996; Mistro et al., 2005), quantitative predictions have seldom been tested. Even in continuous time models, more often it is the spread pattern, such as a front of constant velocity, that has been verified, but see Giuggioli et al. (2005).

The fact that the model predictions are supported by data is probably related to the generalist behavior of the *C. albiceps* species with respect to the use of habitat, being found in wide climatic and geographical ranges (Richards et al., 2009). This not only makes the application of data collected in Africa to the Neotropics sensible, but also strengthens the case for the assumption of homogeneous space, as in the models presented above. The spatially homogeneous model yielded consistent results at a scale of 10^2-10^3 kilometers.

In this work we have introduced a two-dimensional redistribution kernel defined on the semi-plane, thus breaking radial symmetry of the equations. With the assumption of a completely reflective boundary, the solutions of the model, obtained numerically, give results similar to the one-dimensional case. To our knowledge, two-dimensional

kernels have been explored only in a few cases, as for example in Lindström et al. (2011).

2.3 HABITAT SPLIT EXTINCTION THRESHOLD

Habitat loss and fragmentation are considered to be the most important landscape traits affecting biodiversity loss (Laurance and Bierregaard, 1997). Many models have been proposed to capture the complexity of such process, from the theory of island biogeography (MacArthur and Wilson, 1967; Fahrig, 2003) to complex spatially explicit metapopulation models (Hanski, 1991; Hanski and Thomas, 1994; Hanski and Hanski, 1999). The basic predictions of these models have been corroborated for different taxa, including protozoa (Holyoak and Lawler, 1996), butterflies (Harrison et al., 1988; Hanski and Thomas, 1994), birds (Ferraz et al., 2007), and mammals (Lomolino, 1986) (but see (Harrison and Bruna, 1999; Marsh and Trenham, 2001; Harrison, 1991)). Organisms exhibiting marked ontogenetic habitat shifts, however, can be strongly affected by another landscape metric, called *habitat split* (Becker et al., 2007).

Habitat split is defined as human-induced disconnection between habitats used by different life history stages of a species (Becker et al., 2007). For forest-associated amphibians with aquatic larvae, deforestation causes spatial disjunction between the habitat of the larvae, the streams, and the habitat of the adults, the forest fragments. At the local scale, habitat split compels adults to transpose the anthropogenic matrix to reach breeding sites and recently metamorphized juveniles to walk haphazardly through the matrix searching for an isolated forest fragment. This compulsory bi-directional migration causes drastic declines on amphibian populations (Becker et al., 2010).

At the landscape scale, habitat split decreases the richness of the amphibian community due to the extinction of aquatic larvae species (Becker et al., 2007). This process causes bias in communities towards amphibians with terrestrial development, since these species are able to breed successfully in forest fragments even in the absence of a water source (Fonseca et al., 2008). More importantly, the richness of amphibians with aquatic larvae has been demonstrated to be more strongly affected by habitat split than by habitat loss and habitat fragmentation (Becker et al., 2007).

Empirical evidence suggests that any taxon with complex life history can be affected by habitat split. For insects with indirect development, such as dragonflies and damselflies, alterations in the physical structure of riparian vegetation disconnect the aquatic habitat of the larvae from the terrestrial habitat of the adults (Remsburg and Turner, 2009).

We formulate the first model for habitat split. A simple diffusion model shows that habitat split generates critical distances for species

persistence in forest fragments. The model predicts how life history traits affect the extinction thresholds. Furthermore, it predicts how population size is affected by landscape configuration, particularly fragment size and distance from the breeding habitat. The model has relevant implications for landscape design for species conservation.

2.3.1 *Model*

In this section we develop a model designed to capture the main consequences of a habitat split on populations of amphibians. This means a model that has enough ingredients to provide a basis for predictions but without taking into account particularities of any specific amphibian species. The main point the model is set to address is that of population decline and local extinction.

The spatial configuration of the model is shown in figure 2.5. The reproductive site of the amphibians is at the river, $x = 0$, the forest fragment starts L_1 apart from the river and has a size $s = L_2 - L_1$. We have chosen to work in a one-dimensional context. Extensions to a two-dimensional space could be implemented, but the main features are already present in our model.

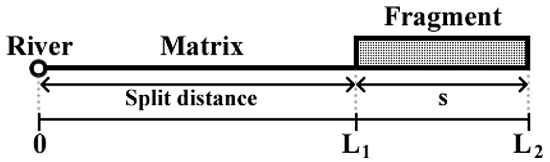

Figure 2.5: The spatial configuration for the model of habitat split with its three main ingredients: the river (or any aquatic reproduction site), the inhospitable matrix and the forest fragment.

Habitat split consequences on the amphibian population are directly connected to the fact that the population is stage-structured. Accordingly, we introduce two variables, $J(x,t)$ and $A(x,t)$, representing juveniles and adults densities respectively. We will assume that the juvenile amphibians move in a hazardous way through the matrix. From the modeling point of view, this suggests that a diffusion equation is appropriate to describe the spatial aspects of the juveniles in the matrix. In the fragment, we will posit that the adults also obey a diffusion equation.

Juveniles that reach the fragment are dynamically equivalent to adults, so that we will assume that there are no juveniles in the fragment, $J(x,t) = 0$, if $L_1 < x < L_2$. On the other hand, adults migrate through the matrix back to the river for reproduction. This however, is a directed movement, similar to advection rather than diffusion. Mathematically, these assumptions translate into two diffusive equa-

tions. The first equation is defined for juveniles in the matrix and the second for adults in the forest fragment:

$$\frac{\partial J}{\partial t} = D_J \frac{\partial^2 J}{\partial x^2} - \mu_J J \tag{2.14}$$

$$\frac{\partial A}{\partial t} = D_A \frac{\partial^2 A}{\partial x^2} - \mu_A A \, , \tag{2.15}$$

where D_J and D_A are the diffusion coefficients for juveniles and adults in the matrix and the forest and μ_J and μ_A the respective mortality rates. At the fragment border L_2 , several scenarios are possible, depending on the landscape beyond L_2: the boundary may be completely absorbing if there is a very hostile matrix, or totally reflexive if the environment is as good as in the fragment, or it can be something in between. This point will be discussed in detail in the next section and for now we consider a general formulation (Cantrell et al., 1998):

$$-D_A \frac{\partial A}{\partial x}\bigg|_{x=L_2} = bA\bigg|_{x=L_2} \, , \tag{2.16}$$

If $b = 0$, we have a completely closed patch at L_2 and the adults will turn back towards the fragment interior. This condition is used when we do not want to take into account size effects of habitat patch, that is, when the patch is large. The opposite limit, $b \to \infty$, corresponds to the situation in which all individuals that reach the border L_2 will leave the modeled landscape.

When juveniles reach the fragment, they become adults and, since adults cannot turn into juveniles, the border $x = L_1$ represents a completely absorbing boundary for juveniles. Although describing a different system, the derivation of this las boundary condition is similar to the one presented in (Ananthasubramaniam et al., 2011). Moreover, the rate at which new adults arrive at the fragment must be the same as the rate of juveniles leaving the matrix. These conditions are expressed in the following boundary conditions:

$$D_A \frac{\partial A}{\partial x}\bigg|_{x=L_1} = D_J \frac{\partial J}{\partial x}\bigg|_{x=L_1} \tag{2.17}$$

$$J\big|_{x=L_1} = 0 \, . \tag{2.18}$$

The fourth and last boundary condition models the reproductive behavior of the amphibians. For simplicity, adults are assumed to exhibit a constant recruitment rate r, which comprises the fertility of adults, the survival of adults crossing the matrix, and the survival of tadpoles. We also take into account that it takes a certain time, t_1, for the influx of juveniles to respond to a variation in the number of adults. This time t_1 is interpreted as the sum of the times spent by adults to cross the matrix (a movement taken to be advective),

mate, reproduce, plus the time until eggs mature and develop into juveniles capable of crossing the matrix. Population size is controlled by competition at the river, so we introduce a saturation parameter K, which can be interpreted as the maximum rate of juveniles that can be generated. The mathematical expression of this condition is the following:

$$-D_J \frac{\partial J}{\partial x}\bigg|_{x=0} = \frac{rN}{1+\frac{r}{K}N} \tag{2.19}$$

where r is the recruitment and N is the total population of adults at a previous time, given by:

$$N = \int_{L_1}^{L_2} A(x, t-t_1)dx \tag{2.20}$$

2.3.2 *Results*

Qualitative analysis

Equations (2.14,2.15) do not contain any density dependent terms: they are linear. As discussed above, the population control term appears only in the boundary conditions, namely in (2.19). On the other hand, the fact that this condition includes a time delay makes it impossible to obtain explicit solutions in terms of both space and time. However, when we seek for stationary solutions, that is, solutions such that: $\partial J/\partial t = 0$ and $\partial A/\partial t = 0$ the time delay plays no role anymore and we can find the fixed points and – more importantly – the existence and stability criteria for non-zero solutions.

The stationary solution of equations (2.14,2.15) are derived from:

$$D_J \frac{d^2J}{dx^2} = \mu_J J \tag{2.21}$$

$$D_A \frac{d^2A}{dx^2} = \mu_A A\,, \tag{2.22}$$

where we have changed partial derivatives for ordinary ones as J and A depend only on x. The couple of linear equations (2.21,2.22) have the trivial solution:

$$\begin{cases} J(x) &= c_1 e^{\omega_J x} + c_2 e^{-\omega_J x} \\ A(x) &= f_1 e^{\omega_A x} + f_2 e^{-\omega_A x}\,, \end{cases} \tag{2.23}$$

where $\omega_i^2 = \frac{\mu_i}{D_i}$, $i = J$ or A; and c_1, c_2, f_1 and f_2 are integration constants. Using the boundary conditions we are able to find explicitly their values, although the expressions are messy. [3]

Equations (2.23) make sense only for real positive solutions. From the expressions, we can show that the stationary solution does not change sign, so we derive a positivity condition from $J\big|_{x=0} > 0$. If this condition is not satisfied, the population will go extinct as the null solution turns out to be the only stable one in this case. This condition is equivalent to:

$$\frac{r}{\mu_A \cosh(\omega_J L_1)} \left[1 - \frac{1+\beta}{\beta e^{\omega_A s} + e^{-\omega_A s}}\right] > 1 \,. \tag{2.24}$$

This condition has a standard interpretation in population dynamics: the recruitment should be large enough to replace the population, otherwise, the population disappears. In the special case where we take b to be zero (so $\beta = -1$), we have simply

$$\frac{r}{\mu_A \cosh(\omega_J L_1)} > 1 \tag{2.25}$$

Further, notice that $b = 0$ is equivalent to the limit $s \to \infty$, where the patch is arbitrarily large.

Stationary solutions

In Fig.(2.5) we depict the general form of the stationary solution as a function of x, the distance from the reproduction site. To help the visualization we plot the juveniles and adults in the same figure; for $0 < x < L_1$ the density in the y-axis refers to juveniles while for $L_1 < x < L_2$ the density of the adults is plotted. As a first approach we assume that diffusion coefficients of adults and juveniles are the same: $D_J = D_A = 1$. On the other side we suppose a large difference in mortalities of juveniles and adults, we put $\mu_A = 0.5 << \mu_J$, the values of μ_J are depicted in the picture. In this and the following graphics we use $L_1 = s = 0.1$ and $r = t_1 = K = 1$. The general

3

$$c_1 = -c_2 e^{-2\omega_J L_1} \,,$$
$$c_2 = -f_1 \frac{\sqrt{\mu_A D_A}}{\sqrt{\mu_J D_J}} \frac{e^{\omega_J L_1} e^{\omega_A L_2} \left(e^{-\omega_A s} + \beta e^{\omega_A s}\right)}{2} \,,$$
$$f_2 = -f_1 e^{2\omega_A L_2} \beta \text{ , with } \beta = \frac{b + \sqrt{\mu_A D_A}}{b - \sqrt{\mu_A D_A}} \,.$$

$$f_1 = \frac{K}{\sqrt{\mu_A D_A} e^{\omega_A L_2}} \times \left\{ \frac{\mu_A}{r} \left[\beta \left(e^{\omega_A s} - 1\right) + e^{-\omega_A s} - 1\right]^{-1} - \left[\cosh(\omega_J L_1) \left(\beta e^{\omega_A s} + e^{-\omega_A s}\right)\right]^{-1} \right\} .$$

behavior of this solution points to a population that decreases in the matrix and tend to stabilize in the fragment.

We also explore in this figure the dependence of juvenile mortality in the model. We plot three distinct μ_J as indicated in the figure. As expected an increase in the mortality leads to smaller populations and, as a preview of next subsection, this trend suggests the existence of a threshold in this model. As juveniles mortality exceeds a given threshold, or if the split distance does, the amphibian population collapses.

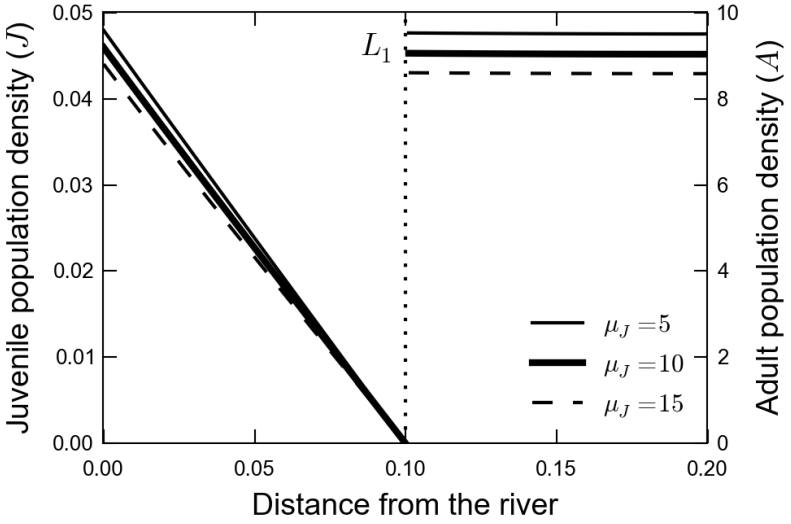

Figure 2.6: The stationary solutions of the model, as a function of space, measured as a distance from the reproduction site. Each curve refers to a given juvenile mortality in the matrix.

Critical split distance

The distance from the reproduction site to the fragment, L_1, is an important landscape metric which has great influence on the existence of a stationary solution of the model. At this point we explore the most important conceptual result of this work. The model introduced produces an extinction threshold for L_1. That means, there is a typical distance $L_1 = L_1^*$ above which the amphibian population is not viable and a local extinction takes place.

In figure 2.7 we show the amphibian density as a function of the split distance L_1, for three different values of the juvenile mortality μ_J as indicated in the figure. It can be view in these curves the presence of a critical split distance L_1^* that fix a maximal distance the adult population can survive apart from the river. In the case L_1 exceeds such limit the next generation of juvenile population will not reach the forest fragment to perpetuate the population. This figure also explores the influence of μ_J on L_1^*, as expected there is an inverse relation be-

tween L_1^* and μ_J. A more inhospitable matrix (large μ_J) will make the critical split distance smaller.

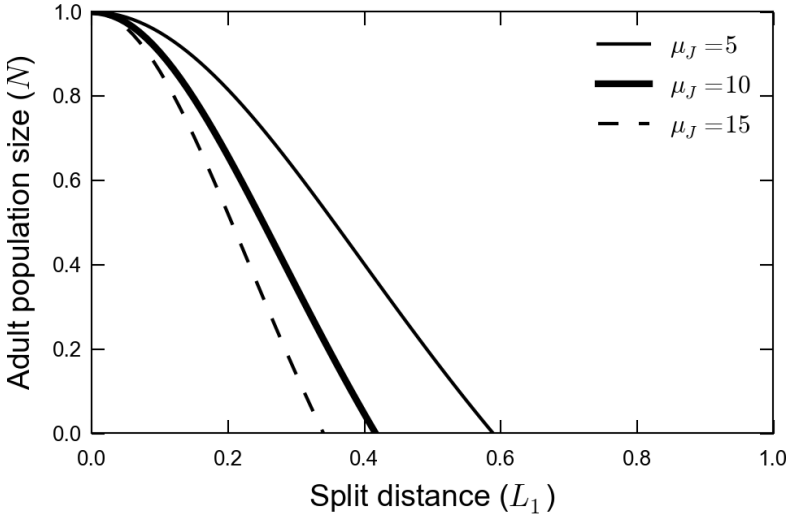

Figure 2.7: The total population of adults in the fragment function of the split distance, L_1. This picture points a critical split distance L_1^* above which the population vanishes. The three curves indicated in the figure represent different values of the juvenile mortality.

Dependence of the critical split distance on life-history parameters

One of the most relevant life-history traits for our analysis is the recruitment r, a parameter that measures the reproductive success of the amphibians. Indeed, in our model r summarizes three quantities: fertility of the reproductive adults, the survival of the tadpoles until they emerge from the aquatic medium to became able to cross the matrix and the adult success in going back to the river to reproduce. In figure 2.8 we explore the critical split distance, L_1^*, versus the recruitment, r, for three distinct values of diffusion coefficients of the juveniles D_J. The point $(L_1^* = 0, r = \mu_A)$ is a limit case, for this situation the recruitment is the minimum to maintain the population ($r = \mu_A = 0.5$) when the favorable habitat is connected to the reproduction site ($L_1 = 0$). The curves of figure 2.8 show an increase of L_1^* with recruitment, that means, an increment in the reproductive success permits larger split distances. The reason of this behavior is that the recruitment compensates the mortality in the matrix. The three curves in the figure examine the influence of the diffusion of the juveniles, D_J; for a given r, larger diffusion coefficient allows a larger split distance for the population. In this way D_J also counterbalance the mortality in the matrix and the consequent habitat split effect.

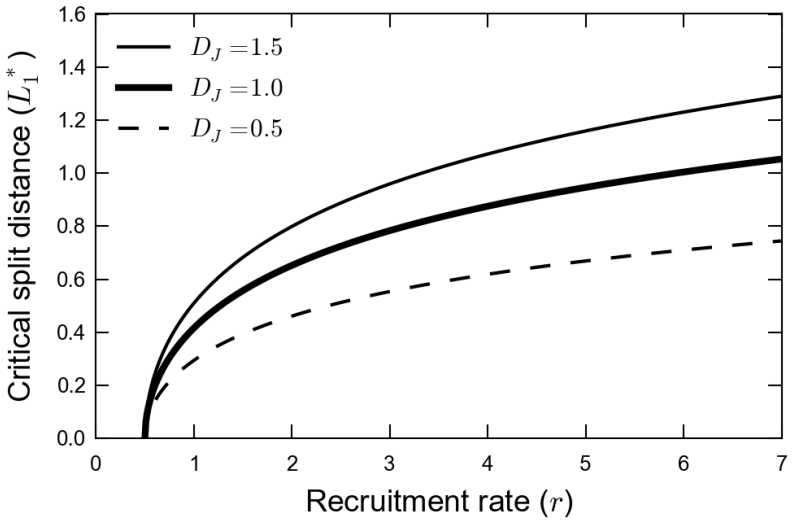

Figure 2.8: The critical split distance as a function of the recruitment parameter for three diffusion constant of juveniles. This figure explores two factors that counterbalance the habitat split effect: the recruitment and the diffusion coefficient of the juveniles.

Dependence of the critical split distance on landscape metrics

As we have seen in the previous sections, a critical split distance appears. When we took the border of the fragment as completely reflexive ($b = 0$), the dependence of the critical split distance on the size of the fragment disappeared: no matter how large the fragment, once a critical split distance is attained, the population goes locally extinct. On the other hand, we can introduce a non-zero value for b, representing a partially absorbing boundary at L_2 . In this case, a flux of adults to the outside of the fragment exists, making it still more difficult for the population to persist. To illustrate this point, we plotted in Fig. 2.9 the adult population in the fragment as a function of the split distance for three different fragment sizes in the case where $b = 1$. It is clear that the population is always smaller the smaller the fragment is, representing a typical area effect.

2.3.3 *Discussion*

Amphibian populations are declining worldwide (Alford and Richards, 1999; Beebee and Griffiths, 2005). Several non-exclusive hypotheses have been proposed to explain such a widespread pattern, including the emergence of *Batrachochytrium dendrobatidis*, a highly virulent fungus (Lips et al., 2006), climate change (Pounds et al., 2006), ultraviolet-B radiation (Blaustein and Belden, 2003), pollution (Relyea, 2005), introduction of exotic species (Kats and Ferrer, 2003), habitat loss and fragmentation (Stuart et al., 2004; Cushman, 2006; Gardner et al., 2007), and, more recently, habitat split (Becker et al., 2007). We

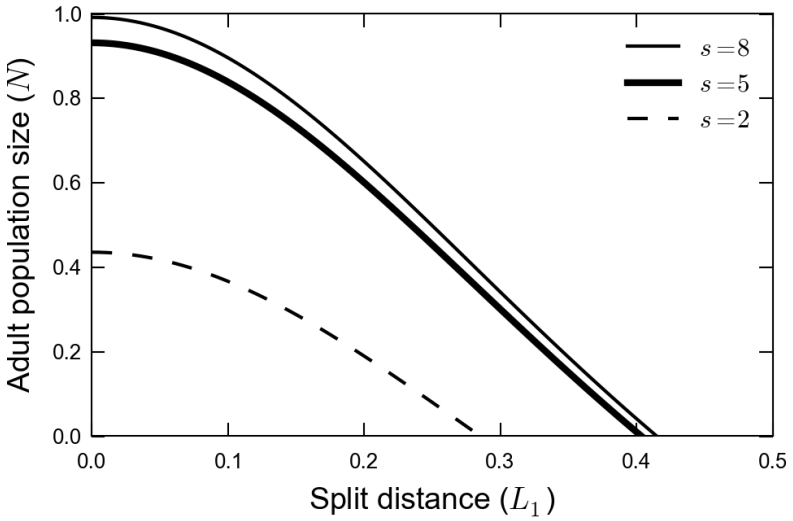

Figure 2.9: Population size versus split distance. In this figure we point the effect of the size of the fragment s on the critical split distance. This figure show that large forest fragments have only a limited effect to reduce the habitat split local extinction prevision.

explore the theoretical consequences of habitat split for the conservation of organisms with ontogenetic habitat shifts, such as aquatic larvae amphibian species.

Our diffusive model reveals that habitat split alone can generate extinction thresholds. Fragments located between the breeding site and a given critical split distance are expected to contain viable amphibian populations. In contrast, populations inhabiting fragments farther from such critical distance are expected to be extinct. The theoretical existence of extinction thresholds has been also demonstrated for habitat loss and fragmentation (Fahrig, 2003; Swift and Hannon, 2010). In this case, increase in the proportion of habitat loss above a certain level causes an abrupt non-linear decay in population size. Simulation models based on percolation theory suggest that this can be simply attributed to structural properties of the fragmentation process (Orbach, 1986). However, biological mechanisms such as minimal home range, minimal population size, and the Allee effect contribute to such extinction thresholds (Swift and Hannon, 2010).

The model can be also interpreted from a breeding site perspective. Split distance is expected to have a negative impact on the occupancy of matrix-inserted ponds. Indeed, a field study with *Rana dalmatina* demonstrated that the number of egg-clutches in ponds declines exponentially with increasing distance from a deciduous forest. Ponds less than 200 m from the forest edge were pointed as the most valuables for the species conservation (Wederkinch, 1988). For *Rana temporaria*, the occupancy of ponds for breeding purposes is influenced by the distance from suitable summer habitats (Loman, 1988). Furthermore, some studies have shown that the richness of amphibians

in ponds is positively related by the distance to forest patches (Laan and Verboom, 1990; Lehtinen et al., 1999).

The habitat split model predicts that amphibian species with different life history traits will exhibit different extinction proneness in response to a given landscape setting. One key feature determining the critical split distance is the diffusion rate of the post-metamorphic juveniles in the matrix. Amphibian species with higher diffusion rate are expected to exhibit farther extinction thresholds. Therefore, for a given fragmented landscape submitted to habitat split, species with lower diffusion ability are expected to be present in a smaller number of fragments and ultimately be regionally extinct earlier. Additionally, the probability to extinction in response to a habitat split gradient can be expected to be higher for species with lower diffusion ability.

Amphibians vary considerably in dispersal ability. Across species, the frequency distribution of maximum dispersal distance fits an inverse power law (Smith & Green 2005). While 56% of the amphibian species presented maximum dispersal distances lower than one kilometer, 7% could disperse more than 10 km (Alex Smith and M Green, 2005). However, those are data for adults dispersing advectively through the landscape. For the habitat split model, the main parameter to be estimated is the diffusion rate of the post-metamorphic juveniles. Although such data is more difficult to be obtained, one expects that it should be at least one order of magnitude smaller than for the adults due to their smaller body size, lower energetic reserves and higher sensitivity to environmental stress (Wells, 2010).

The reproductive success is also a crucial life history parameter determining the critical split distance. In the model, reproductive success is the average number of pos-metamorphic juveniles produced per adult living in the fragment. Across species, higher reproductive success leads to farther extinction thresholds. Reproductive success is positively correlated to clutch size but also a function of the survival rate of the aquatic larvae before metamorphosis. Body size is possibly a good inter-specific predictor of reproductive success. Body size has a strong positive inter-specific relationship with clutch size, even after controlling for the phylogeny (Cooper et al., 2008). Furthermore, for pond-breeding anurans of four different families (Bufonidae, Hylidae, and Ranidae), there is a positive relationship between body size and egg-diameter (Wells, 2010). Therefore, species with larger body size can be expected to exhibit larger critical split distances. The survival rate of the aquatic larvae, however, depends on biotic interactions, such as predation and competition. Furthermore, riverine systems are nowadays submitted to multiple anthropogenic generated stressors (Tockner et al., 2010), agrochemicals (Relyea, 2005), and emerging diseases (Lips et al., 2006) that can alter dramatically mortality rates. The model predicts that the extinction threshold can be pushed away from the breeding site only at the cost of increasing the size

of the fragment. The gain in the critical split distance, however, is a non-linear function of fragment size. Therefore, small fragments can only keep viable amphibian populations if it is positioned in the adjacency of the river or nearby. If a fragment is located far away from the river, it must be large enough to compensate for the negative habitat split effect. But, beyond a given point, increases in fragment size with bring only a marginal gain in the critical split distance. The implications of such results for conservation are straightforward. When habitat loss is intense and small fragments are the rule, the best landscape scenario for the conservation of forest-associated amphibians with aquatic larvae is the preservation of the riparian vegetation.

In biodiversity hotspots (Mittermeier et al., 1999), in particular, landscape design is expected to play a crucial role in the conservation of the aquatic larvae species. For instance, the Brazilian Atlantic Forest is home of one the most species rich amphibian fauna of the world (Mittermeier et al., 1999), containing at least 300 endemic amphibian species (Haddad and Castro, 1998). Nowadays, only 11.7% of its original cover is left (Ribeiro et al., 2009). The remaining area is distributed in 245,173 forest fragments from which 83.4% are smaller than 50 ha (Ribeiro et al., 2009). However, although the protection of the riparian vegetation is insured by the Brazilian Forest Code (4771/65), habitat split is a common feature in the landscape (Becker et al., 2007). Not surprisingly, several amphibian populations have declined recently (Heyer et al., 1988; Weygoldt, 1989; Eterovick et al., 2005). The habitat split model reinforces the view that the conservation and restoration of riparian vegetation should be properly enforced (Wuethrich, 2007).

The quality of the matrix is also a key element defining the critical split distance. Higher quality matrix generates lower mortality rates of post-metamorphic juveniles enabling recruited individuals to reach successfully forest fragments that are further away. For empirical studies this parameter is critical since anthropogenic matrix vary widely in quality, from ecologically-managed tree monocultures (Becker et al., 2007; Fonseca et al., 2009) to intensively used cattle and crop fields (Joly et al., 2001). Furthermore, roads are also important matrix elements that can jeopardize the bi-directional migration of amphibians (Glista et al., 2008). Metapopulation models assume disjunct breeding patches containing individual populations that exist in a shifting balance between extinctions and recolonisations via dispersing individuals (Hanski and Hanski, 1999). Realistic models on metapopulations have incorporated patch area, shape, isolation besides the quality of the intervening matrix (Hanski and Hanski, 1999). The application of metapopulation models for amphibians, however, has been questioned on several grounds (Marsh and Trenham, 2001; Alex Smith and M Green, 2005). We envisage that future metapopulation models, when applied to species exhibiting marked ontogenetic

habitat shifts, will generate more accurate predictions by the incorporation of habitat split effects.

2.4 DIFFUSION AND CONNECTIVITY UNDER STRONG SEASONALITY

Matrix quality plays an important role in determining patch connectivity because organisms may need to move through it to reach other suitable patches (Baum et al., 2004; Goodwin and Fahrig, 2002; Kuefler et al., 2010). Recent studies with butterflies have shown that matrix type influences movement between habitat patches (Ricketts, 2001; Roland and Fownes, 2000) and the movement in the matrix itself (Kuefler et al., 2010). Theoretical developments have tried to unify models for patchy populations and classic metapopulation, where matrix quality plays a small role (Ovaskainen and Hanski, 2004). Understanding the role of matrix habitats in metapopulation and landscape dynamics represents an important advance both empirically and conceptually and provides a more realistic view of animal behavior in complex landscapes (Wiens, 1989; Lima and Zollner, 1996; Prevedello and Vieira, 2010).

Recent conceptual models have tried to understand the rules and scale of animal movement (Nathan et al., 2008). Yet, in most models of animal dispersal and interpatch movement, it is common to treat matrix habitats as static nominal variables with little change in time. This misses the dynamic nature of matrix habitats, which may be a relevant feature depending on the time-scales involved (Blaum and Wichmann, 2007). Consider, for instance, the dynamic nature of a matrix habitat such as an abandoned pasture bordering a forest fragment in the Amazon. The development of this pasture into secondary growth brush makes it more permeable to movement of birds from nearby forest fragments (Antogiovanni and Metzger, 2005; Sberze et al., 2010).

Habitats may also change on a much shorter time-scale, such as seasonal variations. The timing of annual cycles in tropical regions, for example, leads to the existence of well-defined dry and rainy seasons. Because seasonal factors are expected to influence and affect animal dispersal, we focus our modeling approach at this time-scale.

To illustrate a scenario of seasonal variation, let us consider the coastal Atlantic Forest of South America. Near its northern limit, this biodiversity hotspot is subjected to a seasonal climate that alternates dry hot summers and wet winters (Nimer, 1972; Pennington et al., 2000). During the dry season ("summer"), plant growth in open areas is stunted and few plants are in bloom: herbs die out and leaf loss is common in many trees, even within forest patches (Silva et al., 2008). During the rainy season ("winter"), plant growth and biomass production increase everywhere, including open areas, where there is

an abundance of flower resources for butterflies and bees. Conditions are also milder, with lower temperatures, higher humidity, and an increase in rainfall. This dynamic nature is the norm in most places with clear seasonal variations and is to be clearly differentiated from the more iconic tropical rainforest biome (Kricher, 1997).

Here we focus our questions on the role of seasonal variations in matrix quality and its effect on patch functional connectivity. We hypothesize that seasonal improvement in matrix quality allows animals to diffuse into it and eventually colonize other suitable habitat patches during a time period of favorable conditions. However, due to the cyclic nature of the system, matrix quality will diminish as the unfavorable (in our case, the dry season) period takes hold, thereby halting movement. To our knowledge, movement models have not explored the implication of this seasonal variation in detail and have not incorporated this dynamics into diffusion models.

We explored these concepts using *Heliconius* butterflies as our model system. *Heliconius* butterflies are found in forested habitats in the Neotropics and have a long tradition of ecological and evolutionary studies (reviews by Brown (1981) and Gilbert (1991) provide details on the biology of *Heliconius*). Like many butterflies in the Neotropics, *Heliconius* takes advantage of ephemeral micro-habitats in the matrix during the rainy season (Brown Jr and Freitas, 2002; Muriel and Kattan, 2009). Our model considers the ecology of *Heliconius* occupying forest patches in a fragmented landscape in the highly seasonal region of the Brazilian northeast (Kayano and Andreoli, 2009).

2.4.1 *Model*

We posit a model of *Heliconius* diffusion based on Fickian diffusion (for the general context, see Cantrell and Cosner (2003)). The population in the matrix is described by its density $N(x,t)$ which depends on location (x) and time (t). Our model focuses on the dynamics of the population of colonists in the matrix and ignores within-patch behavior by assuming that butterfly density at the border is constant. *Heliconius* populations are known to be relatively stable over time (Ehrlich and Gilbert (1973); Ehrlich (1984); Gilbert (1984) but see Ramos and Freitas (1999)) and we felt justified to use this assumption. The use of a constant flux into the matrix instead does not change the results substantively. For the sake of simplicity, we model a one-dimensional system, with the matrix as a line and the habitat patch as a point (Figure 2.10).

The dynamics of the population in the matrix is driven by the flux of butterflies into it. There, the only significant processes in action are diffusion and mortality. Adults moving into the matrix are able to survive owing to nectar sources (or, alternatively, stored energy

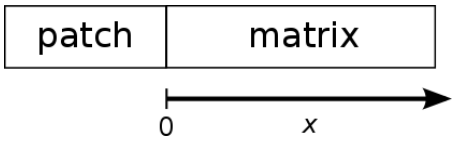

Figure 2.10: Schematic representation of the one-dimensional landscape used in the model. Axis x indicates distance from the border of the patch into the matrix.

reserves) but there is no reproduction (egg-laying) because the matrix does not contain larval host plants.

The equation that describes the density $N(x,t)$ in the matrix is

$$\frac{\partial N(x,t)}{\partial t} = D(t)\frac{\partial^2 N(x,t)}{\partial x^2} - \mu N(x,t)\ , \tag{2.26}$$

where $D(t)$ is the diffusion coefficient and μ is the mortality rate.

To simulate seasonal changes in the matrix, we divided the year into two periods, corresponding to the rainy (of duration T) and the dry seasons. We then incorporated seasonality by employing a periodic time-dependent diffusion coefficient of period 1 year, given by the following expression (see also Figure 2.12a):

$$D(t) = \begin{cases} D & \text{in the rainy season} \qquad 0 \leqslant t < T \\ 0 & \text{in the dry season} \qquad T \leqslant t < 1\,year \end{cases} \tag{2.27}$$

Equation (2.26) has to be supplemented with two boundary conditions. First, we assume that the density of individuals is constant at the border of the fragment during the whole year. Second, we also assume that population density is very low far from the fragment, i.e., the patch is the only significant source of individuals. Accordingly, boundary conditions are as follows:

$$N(0,t) = N_0 \tag{2.28}$$

$$\lim_{x\to\infty} N(x,t) \to 0 \tag{2.29}$$

The model contains three parameters: the diffusion coefficient D, the mortality rate μ and the duration of the favorable season T. The mortality parameter μ is written as $\mu = 1/T_L$, with T_L being the average adult lifetime. Notice that the only constant involving a length unit is D, whose units are given in squared length divided by time.

2.4.2 *Results*

Case 1: No seasonal variation

In order to set the background stage for future comparisons, we first consider the situation where no seasonal variation is present, with a

constant "dispersal-friendly" matrix, characterized by $D(t) = D$. The diffusion is thus maximal and leads to a constant coefficient equation. For large times, the solution will approach the stationary solution, i.e., the time-independent solution to Eq. (2.26) with $\frac{\partial N}{\partial t} = 0$:

$$D\frac{d^2N(x)}{dx^2} = \mu N(x), \tag{2.30}$$

Solutions to this equation obeying the boundary conditions will have the following form:

$$N(x) = N_0\, exp(-\sqrt{\mu/D}\, x) \quad , \tag{2.31}$$

where N_0 is the population density at the habitat border. The stationary solution has an exponentially decaying behavior, with a spatial decay rate equal to $\sqrt{\mu/D}$. We define a typical decay distance associated with the density at the stationary state, x_{max}. This connectivity measure is defined as the distance where density decays to a certain fraction $1/k$ (with $k > 1$) of its value at the border of the patch, considered roughly the minimum population necessary to establish connectivity. Using Equation (2.31) it follows that

$$x_{max} = \sqrt{D/\mu}\ln k\,. \tag{2.32}$$

This quantity represents the maximum distance the population can reach into the matrix during a very long period of favorable diffusion. Consequently, this value shows the natural range for the population's ability to diffuse into the matrix.

The factor $1/k$ is somewhat arbitrary and may be thought as gauging an effective exclusion threshold. We note that, since the dependence on it is logarithmic, changing its value has only a small impact on x_{max}, so that only its order of magnitude is relevant.

Case 2: Seasonal variation (time-dependent case)

Because conditions change seasonally, we expect that diffusion will be influenced by shifts in environmental conditions and, consequently, we will see changes in the population's ability to spread into the matrix. In order to evaluate these changes, we numerically solved equation (2.27) and calculated population density profiles in the matrix during favorable and unfavorable seasons.

The general form of the results for these calculations is depicted in Figure 2.11, which shows the spatial spread of the population into the matrix at equally spaced time intervals for the duration of the favorable period. At $t = 0$, the population density drops dramatically as one moves away from the fragment, while in times $t = 1$ and $t = 2$, a increasingly larger penetration distance into the matrix is attained due to the diffusion process. Times $t = 3, 4$ and 5 are not shown as

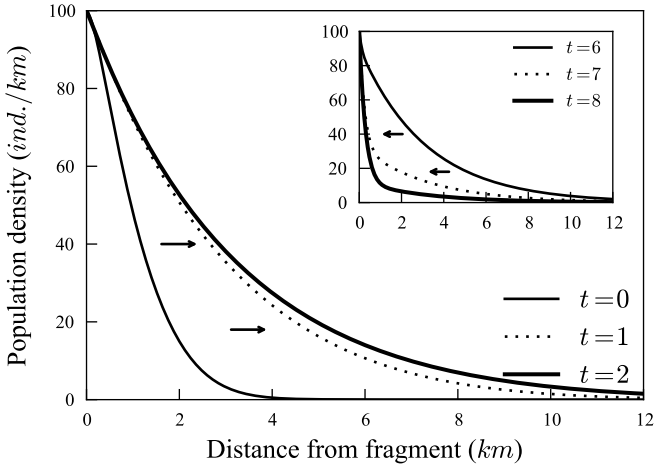

Figure 2.11: The distribution on $N(x,t)$ as a function distance from fragment (x) and season (t). The parameters used were $D = 10\,km^2/month$, $\mu = 1\,month^{-1}$, $N_0 = 100$ ind./km and $T = 6$ months. The main graph shows how the population spreads into the matrix as the season progresses. At time $t = 0$ (first month) there is little colonization, but as time goes on, at the third month ($t = 2$), there is a longer spread into the matrix as the arrows point. Notice that lines change less at the last transition because population is approaching x_{max}. In the inset, as we now move into the unfavorable season, at the beginning of month 6, then the population profile begins to recede as the arrows indicate, until there are no significant population density in the matrix at the end of the unfavorable season ($t > 8$) and individuals become rare in the matrix.

the plot practically superposes the one for $t = 2$. At $t = 6$ the diffusion constant switches to zero (see Eq. (2.27)) and the population contracts gradually towards the habitat fragment (Figure 2.11, inset). Population density is maximally spread at time $t = 6$; spread then recedes via mortality and curtailing of diffusion, at times $t = 7$ and $t = 8$, with the population now effectively surviving only close to the habitat patch. Thus, the favorable season allows a population expansion into the matrix with a subsequent contraction in the unfavorable season; the expansion-contraction dynamics is influenced by the duration of favorable and unfavorable seasons.

Due to seasonal constraints in diffusion, we expect that the effective spread will be less than that attained during an always favorable season (case 1 above, which we called x_{max}). We thus define the effective spread (x_{eff}) as the distance where the density decays to a fraction of its border value, or $N(x_{eff}) = N_0/k$. Therefore, in Figure 2.11, x_{eff} is shifting as a function of the effective diffusion into the matrix. We illustrate how seasonality affects x_{eff} and the cyclic nature of the population range expansion in Figure 2.12. The two populations displayed in the figure differ by their mortality. In case (b) the

maximal spread is attained during the wet season and the flat period indicates that x_{eff} is close to x_{max}. The drop in range is caused by the seasonal change in matrix quality. In case (c) the duration of the season does not allow the maximal potential spread to be attained, so the population will reach a value of x_{eff} below x_{max}. As before, the spread decreases during the unfavorable season.

The duration of the favorable season and the organism's ability to diffuse during its lifetime will influence the colonization of habitat patches. If the length of the adult lifetime is shorter than the duration of the favorable season, then the effective population spread (x_{eff}) will approach the maximum population spread (x_{max}) during the season as in Figure 2.12b. If suitable patches are located within this distance, i.e. their distance is smaller than x_{eff}, then colonization will be possible and the major determinant of colonization itself is the duration of the period during which diffusion is possible. In our case this is the duration of the season. This leads to fluctuations characterized by the population colonizing and then disappearing from the matrix in the unfavorable season. This expansion-contraction dynamics is found in populations located at the limit of the species distribution range, which experience expansion during the favorable season and contraction in the unfavorable season (Cardoso, 2010).

On the other hand, the duration of the favorable season could be too short in relation to the adult lifetime (Figure 2.12c) and constrain a population so that it would settle at a x_{eff} that is much lower than its maximum dispersal (x_{max}). This happens because changes that lower matrix quality come in before this limit is reached. Contrary to the preceding case, fluctuations may be less pronounced because the population has a longer lifetime, and so is able to persist longer in the matrix.

Dependence on the diffusion constant

The results above show how the dynamics of the population in the landscape is influenced by the duration of the season (T), the mortality rate (μ) and the diffusion constant (D). To what degree does the value of the diffusion constant (D) affect these results? Equation 2.32 makes that relationship explicit. On the other hand, if we define the effect of seasonality on a given species by the ratio $\frac{x_{eff}}{x_{max}}$, then this ratio will not depend on D. This comes from the fact that D is the only parameter whose units comprise length, so that a ratio of two lengths cannot depend on D.

Thus, rainy season length can curb dispersal distance, leading to a maximum dispersal reach limited either by season length or by diffusivity, but the latter cannot determine which is the case.

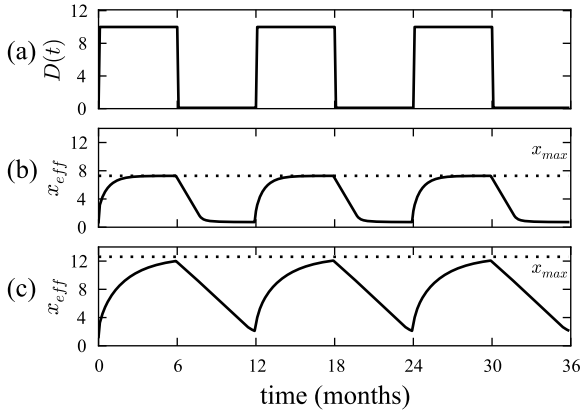

Figure 2.12: The effect of seasonality on the expansion of two hypothetical populations with differing diffusion abilities. (a) The discrete nature of the diffusion constant in our model. Diffusion in "on" during the favorable season (upper step) and "off" during the unfavorable season (lower step). (b) The maximal spread of the population is reached during the favorable season. In this case, the plateau represents the situation where $x_{eff} = x_{max}$. (c) The populations do not reach maximal spread before the end of the favorable period ($x_{eff} < x_{max}$). In both (b) and (c) the drop in range during the unfavorable season is caused by the mortality and reduced influx of individuals in the matrix. The parameters used were $N_0 = 100\,individuals/km$, $D = 10\,km^2/month$ and $k = 10$, with $\mu = 1\ month^{-1}$ in (b) and $\mu = 0.33\ month^{-1}$ in (c).

Parameter evaluation for Heliconius

The estimated average lifetime T_L for *Heliconius* butterflies is around 90 days (Turner, 1971; Ehrlich and Gilbert, 1973), which corresponds to a mortality $\mu = 1/90\,day^{-1}$. For the system with well defined dry and wet seasons we set T as approximately 180 days. Thus, *Heliconius* species and, for that matter, most of the other butterfly species in tropical regions with strong seasonality, could reach x_{max} during the season. In this case, the value for the length of the population spread in our one-dimensional model, i.e. the places where the population is expected to be found in the matrix, is well approximated by x_{max}.

In order to estimate x_{max} we used natal dispersal data from Mallet (1986) to parameterize our model. In this case, dispersal of young adults is expected during four days following eclosion and the square root of the mean quadratic distance travelled by individuals in four days is approximately 266m. The diffusivity constant D can be estimated as $\frac{(266m)^2}{4days} \approx 1.8 \times 10^4 m^2/day$. Hence, using $x_{max} = \sqrt{\frac{D}{\mu}} \ln k$, and a conservative value of $k = 10$, the maximum attainable dispersal distance in the favorable season (x_{max}) is around 3000m.

2.4.3 *Discussion*

Habitat loss and land conversion are among the main causes of biodiversity impoverishment. Recent estimates of extinction rates point to a "silent mass extinction" of specialist herbivores (Fonseca, 2010) in biodiversity hotspots such as the Brazilian Atlantic Forest. Thus it is important not only to know the composition of the biota but also to understand how the spatial patch configuration influences invertebrate populations and their long-term viability in the highly fragmented landscapes of biodiversity hotspots.

Our model provides answers to some of these concerns to an invertebrate species by providing a first approximation to the relationship between diffusion capability and landscape configuration in a seasonal tropical environment. Because most of the world's biodiversity is located in the tropics and high rates of habitat loss and conversion mean unknown effects on many species whose ecology is not known. Thus, a focus on tropical species and a tropical perspective on animal behavioral landscape ecology are fundamental. Many studies of butterfly movement deal with landscape configuration where forest patches are a barrier to diffusion rather than being the habitat of interest (e.g. Roland and Fownes (2000)). Our view is to use forest patches as the habitat of interest and the open, human-made intervening matrix as the force to be reckoned with.

One important feature of our model is that it explicitly deals with temporal variation in matrix quality as an effect on diffusion. Thus, we envision a system where we could parameterize not only patch configuration in the landscape but also the constraints in diffusion and dispersal in general caused by temporal changes in habitat quality.

The application of our diffusion model to *Heliconius* suggests that 3km is the upper ceiling for connectivity threshold. Given that this reflects a density that is one tenth of the original patch density, the distance between patches would have to be below this value to maintain population integrity. Patch distribution for Atlantic forest remnants is widely variable, but recent estimates point to a mean distance of 1.5km between fragments (Ribeiro et al., 2009). Thus, this average theoretical *Heliconius* could potentially colonize fragments within this range. However, *Heliconius* are usually found in low density populations in their native habitats and our threshold level of $N_0/10$ indicates that the effective spread is probably much smaller than this. Thus, the 3km limit is an optimistic view of the diffusion ability and does not take into account the possibility of increased mortality due to matrix of lower quality, for instance. Yet, for those areas where seasonal effects are less harsh, diffusion is probably easier and the functional distances between patches could potentially be attained.

This result corroborates population genetics studies that have found some differentiation between *Heliconius* populations in fragmented landscapes (Kronforst and Gilbert, 2008). In particular, estimates of genetic relatedness in *Heliconius* population in the seasonal forests of the Brazilian Northeast (Albuquerque de Moura et al., 2011) has found high levels of genetic variability populations in forest patches.

Our suggestion of matrix seasonal variation as a force determining animal diffusion is the main contribution of this model. As is the case of any model, we can add layers of complexity to make it more realistic, such as stochastic effects and a spatially explicit 2-D landscape. With the knowledge of spatial configuration of habitat patches and matrix we can then simulate x_{max} and x_{eff} for a variety of taxa and help design reserve location, restoration efforts and implementation of corridors/stepping stone. We hope our theoretical effort aimed at tropical species will contribute to conservation of tropical landscapes.

3

STRUCTURE AND PERSISTENCE OF COMMUNITIES

3.1 INTRODUCTION

Ecological communities are systems composed by more than one population in the same place, possibly interacting. They generalize single species models in a straightforward way – introducing an equation for each population, that can depend on any of the other variables, and affect the others as well, leading to a system of ordinary differential equations (ODEs). The simplest such models look like:

$$\begin{aligned} \frac{dN}{dt} &= f(N,P) \\ \frac{dP}{dt} &= g(N,P)\ , \end{aligned} \tag{3.1}$$

The most common issue in a community is to determine if there is coexistence, that is, if all species can keep nonzero populations indefinitely. This is tackled by employing the qualitative analysis of systems of ODEs: we calculate the fixed points (N^*, P^*) and find their local stability via the eigenvalues of the Jacobian matrix calculated at the fixed points. This procedure is often enough to get a good general picture of what the long-term solutions look like. For instance, a stable positive fixed point indicates coexistence, although it may not be resilient to large perturbations. Mutual invasion is in general a better, but much more strict, criteria, since it also allows for coexistence on oscillatory orbits.

We present in this chapter two works that look very dissimilar, one on the coexistence of species in an ecological setting and the other on the epidemiology of malaria, but at the essence they are quite similar: we look for conditions that assure coexistence or exclusion of one of the species – in the case of malaria, the elimination of the infected classes.

The work on intraguild mutualism, shown in section 3.2, originated during the ICTP-SAIFR Southern Summer School in Mathematical Biology, held January 19-28 of 2012 in São Paulo. It was a topic proposed by Roberto Kraenkel for one of the student groups, which included Florencia Assaneo, Yangchen Lin, and Carlos Mantilla. The results drew the attention of Frithjof Lutscher, professor at the Department of Mathematics and Statistics of the University of Ottawa, who was offering a mini-course at the School, and organized the group to push the results further and publish them after the School was over,

leading to the paper "Dynamics and coexistence in a system with intraguild mutualism" (Assaneo et al., 2012). It is a tenet of ecological theory that two competing consumers cannot stably coexist on a single limiting resource in a homogeneous environment. Many mechanisms and processes have since been evoked and studied, empirically and theoretically, to explain species coexistence and the observed biological diversity. Facilitative interactions clearly have the potential to enhance coexistence. Yet, even though mutual facilitation between species of the same guild is widely documented empirically, the subject has received very little theoretical attention. Here, we study one form of intraguild mutualism in the simplest possibly community module of one resource and two consumers. We incorporate mutualism as enhanced consumption in the presence of the other consumers. We find that intraguild mutualism can (a) significantly enhance coexistence of consumers, (b) induce cyclic dynamics, and (c) give rise to a bistability (a joint Allee effect) and potentially catastrophic collapse of both consumer species.

In section 3.3, we collaborated with Gabriel Laporta, then a Ph.D. student at the Departament of Epidemiology of the Public Health School of the University of São Paulo, and with Paulo Inácio Prado, professor of ecology at the University of São Paulo. This work led to the article "Biodiversity Can Help Prevent Malaria Outbreaks in Tropical Forests" (Laporta et al., 2013). This project aims to study how biodiversity affects the transmission dynamics of malaria in the Atlantic Forest region in São Paulo. Brazilian tropical rain forests encompass host- and vector-rich communities, in which two hypothetical mechanisms could play a role in the dynamics of malaria transmission. The first mechanism is the dilution effect caused by presence of wild warm-blooded animals, which can act as dead-end hosts to *Plasmodium* parasites. The second is diffuse mosquito vector competition, in which vector and non-vector mosquito species compete for blood feeding upon a defensive host. We developed a mathematical model to assess those two mechanisms in a pristine tropical rain forest, where the primary vector is present but malaria is absent. The Ross-MacDonald model and a biodiversity-oriented model were parameterized using newly collected data and data from the literature. The basic reproduction number (R_0) estimated employing Ross-MacDonald model indicated that malaria cases could occur in the study location. However, no malaria cases have been reported since 1980. In contrast, the model containing ecological feedbacks corroborated the absence of malaria transmission. In addition, we show how the diffuse competition mechanism decreases the risk of malaria transmission, which suggests a protective effect provided by the forest ecosystem. There is a non-linear, unimodal correlation between the mechanism of dead-end transmission of parasites and the risk of malaria transmission, suggesting a protective effect only under cer-

tain circumstances (e.g., a high abundance of wild warm-blooded animals).

3.2 INTRAGUILD MUTUALISM

Explaining coexistence of multiple species and finding mechanisms for the maintenance of biological diversity are two of the most fundamental questions in ecology, and are increasingly important issues in the face of global anthropogenic change and biodiversity loss. Theoretical results such as Tilman's R^*-rule (Tilman, 1982) and the generalized competitive exclusion principle (Levin, 1970) send the clear message that coexistence among competing species is difficult to achieve. Theoretical and empirical research has since focused on variability and trade-offs that promote coexistence, such as spatial extent, temporal variation, stochasticity and others, e.g. Levins and Culver (1971); Holt (1984); Chesson (1994); Hanski and Hanski (1999); Chesson (2000). Most of these efforts focus on models and experiments that consider only antagonistic interactions even though positive interactions also pervade ecological communities (Bruno et al., 2003). Positive interactions are a natural candidate mechanism to promote species coexistence, and to enhance the positive effects of diversity on ecosystem function (Cardinale et al., 2002), yet relatively little work has been done in this regard except for facilitation among plant species.

A form of facilitation of which very little is known is intraguild mutualism (Crowley and Cox, 2011), where consumers competing for the same resources also facilitate one another. The idea of predator mutualism goes back to Charnov et al. (1976), who theorized several mechanisms of predator mutual facilitation. When different predator species hunt in different locations or at different times, then a prey trying to avoid one predator could be more available to another. For example, mammals may hunt under dense cover and drive prey into the open where it is available for avian predators - and vice versa (Korpimaki et al., 1996; Eccard et al., 2008). Nocturnal predation by owls may drive prey to forage during daytime when hawks can spot them, and vice versa. Prey fish escaping predatory fish may rise close enough to the water surface that they are available to bird predation.

In general, increased feeding success and predator avoidance are the most commonly cited potential benefits between otherwise competing species (Dickman, 1992). Losey and Denno (1998) measured predation rates of two beetle species on aphids and showed that joint predation is greater than individual predation combined. Similar results of facilitation between predators were obtained, for example, by Cardinale et al. (2003); Meyer and Byers (2005); Bshary et al. (2006); Eccard et al. (2008); Fodrie et al. (2008) in other study systems. Mutual positive interactions also occur among plants (Callaway, 1995) for ex-

ample habitat amelioration through shading (Bertness and Leonard, 1997). The mutual positive effect of predator defense or avoidance is documented by Hay (1986); Hoeck (1989), among others.

A recent review by Crowley and Cox (2011) highlights the current increase in recognition of the importance and ubiquity of facilitative interactions in ecology (see also Bruno et al. (2003)). Specifically, they argue that there is ample empirical evidence for facilitative interactions and mutualism (reciprocal facilitation) within a guild, but that theoretical models of intraguild mutualism (IGM) are rare. Gross (2008) focused on the aspect of predator avoidance and studied a differential equations model of competing species whose death rates decrease in the presence of other species. He found that this mechanism produced stable multi-species communities with a single resource. Nathaniel Holland and DeAngelis (2009) consider a general two-species model where density-dependent rates can shift competitive interactions to mutualism, but the authors neither consider specific mechanisms nor address intraguild mutualism.

Here, we develop and analyze a model of resource competition, where consumption of each competitor can be enhanced by the presence of the other. Our general model consists of three equations, one for the resource and two for the competing consumers. Crowley and Cox (2011) suggest several community modules of varying topology, in which the effects of IGM should be explored. Our work here aims to shed light onto these effects for one particular module. We distinguish between two scenarios, the *chemostat scenario*, which is characterized by a constant supply rate of the resource and equal washout rates for all three species (Smith, 1995); and the *logistic scenario*, which is characterized by a logistically growing resource population and species-specific death rates. Our approach to understanding the dynamics of this three-dimensional system begins with simple linear predation and facilitation functions, and considers two special cases of parameter values. When the two consumers are identical, the system reduces to a two-dimensional model of a predator with self-facilitation (subsection 3.2.2). When facilitation acts in one direction only, the system remains three-dimensional but the number of parameters is greatly reduced (subsection 3.2.3). These two special cases help understand the dynamics of the general system, but they are worthy of study in their own right, as both of these cases are observed in nature. Finally, we briefly discuss the effect of nonlinear predation and facilitation functions (subsection 3.2.4), and we construct the possible dynamics of the full three-dimensional model from the results of the two previous subsections (subsection 3.2.5).

3.2.1 *Model*

We model the dynamics of two consumer species, x, y, and their resource, z. In the absence of the consumers, the resource grows according to some function G. Consumers reduce resource growth by a per-capita rate $h_i(z)$, modified to include consumer mutualism via functions f_i. There are linear death rates, d_i, of the consumers and yields $1/e_i$. Altogether, the model reads

$$\begin{aligned} \frac{dx}{dt} &= x(h_1(z)f_1(y) - d_1), \\ \frac{dy}{dt} &= y(h_2(z)f_2(x) - d_2), \\ \frac{dz}{dt} &= G(z) - e_1 x h_1(z)f_1(y) - e_2 y h_2(z)f_2(x). \end{aligned} \tag{3.2}$$

We distinguish two scenarios. In the *chemostat scenario*, we consider $G(z) = d(z_{in} - z)$ as the supply rate and outflow of the resource, and $d_1 = d_2 = d$ as the outflow rate of the consumers. In the *logistic scenario*, we choose logistic growth $G(z) = rz(1 - z/K)$, and we allow the consumer death rates d_i to be distinct. We also refer to the consumers as predators.

The functions h_i describe a non-decreasing functional response; they could be linear (type I) or saturating (type II) (Holling, 1959). Functions f_i are assumed positive and non-decreasing with $f(0) = 1$. For simplicity, we typically choose linear functions, but discuss nonlinear functions as well.

When the functions f_i are constant, then we have a classical situation. There is no stable coexistence, unless the two species are essentially identical (Kot, 2001). In the chemostat case, the species that can subsist on a lower resource level will drive the other to extinction. The lowest possible resource level is given by $h_i(z) = d_i$. In the logistic case, we may obtain coexistence between the predators in a stable limit cycle, provided h_i are saturating response functions (Koch, 1974; Kot, 2001).

3.2.2 *Identical consumers - reduced system*

We begin our analysis of system (3.2) with the special case that all parameters for the two consumer species are equal. With this assumption, the plane $\{x = y\}$ is invariant for the dynamics. On this plane, we can study the reduced system

$$\begin{aligned} \frac{dx}{dt} &= x(h(z)f(x) - d), \\ \frac{dz}{dt} &= G(z) - 2exh(z)f(x), \end{aligned} \tag{3.3}$$

where the factor of 2 in the last term reflects the fact that two consumer species of equal strength impact the resource. Alternatively, this system can be interpreted as a predator-prey system with predator intra-specific facilitation. Predator self-facilitation is quite common when predators hunt in packs, as in many canids. It also appears to be widespread in consumer–resource relationships in general, having been observed in terrestrial invertebrates (So and Dudgeon, 1989), aquatic invertebrates (Bertness, 1989) and parasites (Ogden et al., 2002). We refer to Berec (2010) for a recent in-depth study of the dynamic effects of self-facilitation in predators. For our model, we study the stability of the resource-only (semi-trivial) state as well as conditions for the existence and stability of a (positive) coexistence state.

The chemostat scenario

In the chemostat case, we choose $G(z) = d(z_{in} - z)$, as well as linear functions $h(z) = az$ and $f(x) = 1 + \alpha x$. After nondimensionalizing, the system reads

$$\begin{aligned} \frac{dx}{dt} &= x(Az(1 + Cx) - 1), \\ \frac{dz}{dt} &= 1 - z - xz(1 + Cx), \end{aligned} \tag{3.4}$$

where $A = az_{in}/d$ and $C = d\alpha/(2ea)$. The semi-trivial state is unstable if $A > 1$. A coexistence state is given by the relations

$$z = \frac{1}{A(1 + Cx)}, \qquad Cx^2 + (1 - AC)x + 1 - A = 0. \tag{3.5}$$

The explicit solution for x is

$$x = \frac{1}{2C}\left[AC - 1 \pm \sqrt{(AC - 1)^2 - 4C(1 - A)}\right]. \tag{3.6}$$

Now we see that there are three cases. (a) If $A > 1$, then the zero steady state is unstable; there is exactly one coexistence state. (b) If $A < 1$ and $AC < 1$ then there are no coexistence states. (c) If $A < 1$ and $AC > 1$, then there are two coexistence states, provided the expression under the square root is positive. The latter condition is equivalent to

$$C > C^* = \frac{1}{A^2}[2 - A + 2\sqrt{1 - A}], \tag{3.7}$$

which actually implies $C > 1/A$. We also get the relationship $\frac{1}{A}x + z = 1$.

The Jacobian at the positive steady state is

$$J = \begin{bmatrix} ACxz & x/z \\ -z(1+2Cx) & -1/z \end{bmatrix}. \tag{3.8}$$

It turns out that the trace of the Jacobi matrix is always negative at the positive steady state. When $A > 1$, this is easily seen from

$$\mathrm{tr}(J) = ACxz - \frac{1}{z} = \frac{Cx}{1+Cx} - A(1+Cx) < (1-A)Cx < 0. \tag{3.9}$$

For $A < 1$, we checked the condition numerically. In particular, there cannot be a Hopf bifurcation in this system. The sign of the determinant depends on the steady state. We have

$$\det(J) = x(1+2Cx-AC). \tag{3.10}$$

Substituting the explicit expression for x from (3.6), we see that the determinant is negative (a) if $A > 1$ and $x > 0$ or (b) if $A < 1$ and x is the larger of the two positive steady states.

In summary, when $A > 1$, then the semi-trivial steady state is unstable and the unique coexistence state is stable. When $A < 1$ and $C < C^*$, then the predator cannot persist in the system. When $A < 1$ and $C > C^*$, then the semi-trivial state is locally stable and there are two coexistence states. The one with the larger consumer density is stable. The consumer experiences an Allee effect, see Figure 3.1.

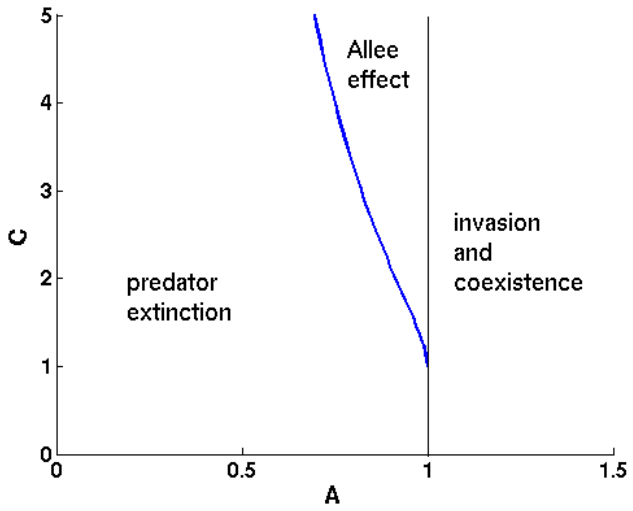

Figure 3.1: Illustration of the possible qualitative behavior of the reduced mutualism model with chemostat dynamics, see (3.3).

The logistic scenario

This time, we choose $G(z) = rz(1 - z/K)$, and h, f as in the previous subsection. After nondimensionalizing, system (3.3) reads

$$\begin{aligned} \frac{dx}{dt} &= x(Az(1 + Cx) - B), \\ \frac{dz}{dt} &= z(1 - z) - xz(1 + Cx), \end{aligned} \tag{3.11}$$

where $A = aK/r$, $B = d/r$ and $C = r\alpha/(2ea)$. The semi-trivial state is unstable when $A > B$. A coexistence state satisfies the cubic equation

$$C^2x^3 + 2Cx^2 + (1 - C)x + \frac{B}{A} - 1 = 0, \tag{3.12}$$

and $z = \frac{B}{A(1+Cx)}$. When $A > B$, then the cubic polynomial has exactly one positive root by Descartes' rule of signs. When $A < B$, then there are zero or two positive roots. By Descartes' rule again, we need $C > 1$ for there to be two positive roots. If $C > 1$, then a saddle-node bifurcation occurs at

$$A^* = \frac{B}{1 + \frac{-4+2\sqrt{1+3C}}{9C}(C - \frac{\sqrt{1+3C}}{3} - \frac{1}{3})}, \tag{3.13}$$

so that the system has two positive steady states whenever $A \in (A^*, B)$.

At a positive steady state, the Jacobi matrix can be reduced to

$$J = \begin{bmatrix} ACxz & Bx/z \\ -z(1 + 2Cx) & -z \end{bmatrix}. \tag{3.14}$$

The trace of this matrix is zero if $x = 1/AC$. Substituting this expression into the steady state equation (3.12), we obtain a curve in parameter space on which a Hopf bifurcation can occur, provided the determinant is positive there, namely

$$C^{**} = \frac{1 + 2A + A^2}{A^3 + (1 - B)A^2}. \tag{3.15}$$

In summary, when $A > B$, then the semi-trivial steady state is unstable. The unique coexistence state is stable when $C < C^{**}$ and unstable with a stable limit cycle when $C > C^{**}$. When $A < B$, the situation is more complex. When C is small, then the predator cannot persist in the system. As C increases, there is a saddle node bifurcation, whereby a stable and unstable coexistence state emerge. Implicitly, the critical value of C is given by (3.13). Increasing C further causes a Hopf bifurcation when $C = C^{**}$ at the larger coexistence state and the appearance of a stable limit cycle; see Figure 3.1. For very large

values of C, the limit cycle disappears in a global bifurcation, and the predator goes extinct; see Figure 3.2.

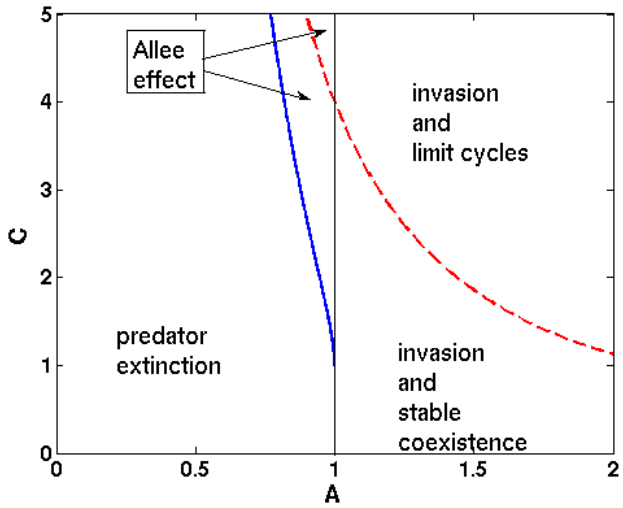

Figure 3.2: Illustration of the possible qualitative behavior of the reduced mutualism model with logistic dynamics. Bifurcation diagram for $B = 1$. To the right of the vertical line, the predator can invade and coexist. To the left of the vertical line, the predator has an Allee effect above the solid curve. At the dashed curve, the coexistence state undergoes a Hopf bifurcation. For even larger values of C, the population can crash (region not shown).

3.2.3 *Facilitation - reduced system*

Another very instructive way to reduce the complexity of model (3.2) is to assume that only one species facilitates resource uptake for the other. There is actually empirical evidence for such interactions in natural systems. For example, the Rufous Babbler (*Pomatostomus iridorei*) foraging technique causes insects to fly out of leaves and tangles. The babbler does not pursue these insects but other species, foraging in close proximity, do (Charnov et al., 1976).

Our setup is as follows. We assume that species x has the lower R^* value in the sense of Tilman (1982), so that it wins the competition in the absence of facilitation. We then assume that species y benefits from the presence of x but not vice versa. We start with the chemostat scenario.

The chemostat scenario

We choose the functions G, h_i, f_i of model (3.2) as in subsection 3.2.2, with $f_1 = 1$. After non-dimensionalizing, we obtain

$$\begin{aligned}\frac{dx}{dt} &= x(A_1 z - 1),\\ \frac{dy}{dt} &= y[A_2 z(1 + Cx) - 1],\\ \frac{dz}{dt} &= 1 - z - z[x + (1 + Cx)y],\end{aligned} \tag{3.16}$$

where $A_i = a_i z_{in}/d$, and $C = \alpha d/e_1 a_1$. The condition that species x has a lower R^* value than species y translates into $A_1 > A_2$.

The resource-only steady state $(0, 0, 1)$ is invasible by x if $A_1 > 1$ and by y if $A_2 > 1$. If $A_2 > 1$, then x can invade the semi-trivial state $(0, A_2 - 1, \frac{1}{A_2})$ since $A_1 > A_2$ by assumption. If $A_1 > 1$, then y can invade the semi-trivial state $(A_1 - 1, 0, \frac{1}{A_1})$ provided

$$C > C^* = \frac{\frac{A_1}{A_2} - 1}{A_1 - 1}. \tag{3.17}$$

In particular, species y can invade of facilitation by species x is strong enough. If the invasion conditions are satisfied, the coexistence state is given explicitly by the expressions

$$x = \frac{1}{C}\left(\frac{A_1}{A_2} - 1\right), \quad y = \frac{A_2}{A_1}(A_1 - 1) + \frac{1}{C}\left(\frac{A_2}{A_1} - 1\right), \quad z = \frac{1}{A_1}, \tag{3.18}$$

see Figure 3.3. We show that this unique coexistence state is stable when it exists. The Jacobian at the coexistence state reads

$$J = \begin{bmatrix} 0 & 0 & A_1 x \\ A_2 C y z & 0 & A_1 y \\ -z(1 + Cy) & -1/A_2 & -A_1 \end{bmatrix}. \tag{3.19}$$

The Routh-Hurwitz conditions for stability require

$$A_1 y + A_2 x > A_2 C x y z (1 - A_1). \tag{3.20}$$

Since the coexistence state only exists if $A_1 > 1$, this condition is always satisfied. We illustrate the coexistence region in terms of C versus A_2 in Figure 3.3 for two different values of A_1. Surprisingly, the two curves intersect. When $A_2 < 1$, the strength, C, with which species x has to support species y to enable persistence decreases as A_1 increases. There are two opposite effects at work. Higher A_1 implies lower resource level $(1/A_1)$ at which species y tries to invade, so that we expect a *higher* value of C would be necessary. However,

with increasing A_1, the steady state level of species x also increases, and the facilitation that species y receives from this increased density more than compensates for the lower resource level. In fact, differentiating the expression in (3.17) with respect to A_1 shows that C increases with A_1 if and only if $A_2 > 1$.

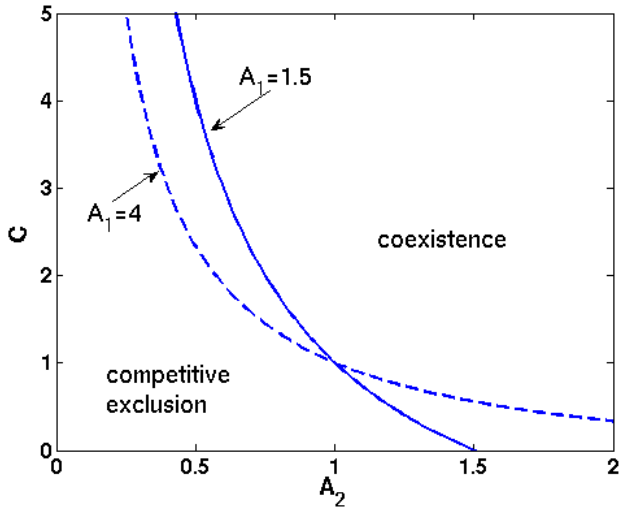

Figure 3.3: Coexistence region of predators with facilitation in the chemostat scenario. Coexistence between all three species is stable above the curve. Below the curve, species x exclude species y from the system.

The logistic scenario

With logistic growth for the prey, the nondimensional equations read

$$\begin{aligned}\frac{dx}{dt} &= x(A_1 z - B_1),\\ \frac{dy}{dt} &= y[A_2 z(1+Cx) - B_2],\\ \frac{dz}{dt} &= z(1-z) - z[x + (1+Cx)y],\end{aligned} \tag{3.21}$$

where $A_i = a_i K/r$, $B_i = d_i/r$ and $C = \alpha r/(e_1 a_1)$. Species x outcompetes species y if $\frac{A_1}{B_1} > \frac{A_2}{B_2}$. We introduce the notation $R_i = B_i/A_i$, so that the assumption about x being the stronger competitor gives Tilman's R^*-rule $R_1 < R_2$ (Tilman, 1982).

The prey-only state $(0, 0, 1)$ is invasible by x if $A_1 > B_1$ and by y if $A_2 > B_2$. Species x invades the semi-trivial state $(0, 1 - R_2, R_2)$ since $R_2 > R_1$. Species y invades the semi-trivial state $(1 - R_1, 0, R_1)$ only if

$$C > C^* := \frac{\frac{R_2}{R_1} - 1}{1 - R_1}. \tag{3.22}$$

Under this condition, the coexistence state is given explicitly by the expressions

$$x = (1 - R_1)\frac{C^*}{C}, \quad y = \frac{R_1}{R_2}(1 - R_1)\left(1 - \frac{C^*}{C}\right), \quad z = R_1, \tag{3.23}$$

All expressions are positive by assumption.

The Jacobian matrix at the coexistence state is

$$J = \begin{bmatrix} 0 & 0 & A_1 x \\ A_2 C R_1 y & 0 & \frac{B_2}{R_1} y \\ -R_1(1 + Cy) & -R_2 & -R_1 \end{bmatrix}. \tag{3.24}$$

The Routh-Hurwitz condition for stability is

$$A_1 C R_1 xy + A_1 R_1 x + \frac{B_2 R_2 y}{R_1} > A_1 A_2 C R_2 xy \tag{3.25}$$

which can be rewritten as

$$\begin{aligned} 0 < A_1 C R_1 xy \left(1 - \frac{B_2}{R_1}\right) + A_1 R_1 x + \frac{B_2 R_2 y}{R_1} = \\ = A_1 C R_1 (1 - R_1)\frac{C^*}{C} y \left(1 - \frac{B_2}{R_1}\right) + A_1 R_1 (1 - R_1)\frac{C^*}{C} + \frac{B_2 R_2 y}{R_1} = \\ = Z\left(1 - \frac{C^*}{C}\right) + A_1 \frac{R_2 - R_1}{C}, \end{aligned}$$

where

$$Z = (1 - R_1)\left[A_1\left(1 - \frac{R_1}{R_2}\right)(R_1 - B_2) + B_2\right]. \tag{3.26}$$

The stability condition is therefore equivalent to

$$\begin{aligned} C &> C^* - \frac{A_1(R_2 - R_1)}{Z} \quad \text{if} \quad Z > 0 \\ C &< C^* - \frac{A_1(R_2 - R_1)}{Z} \quad \text{if} \quad Z < 0. \end{aligned} \tag{3.27}$$

There are two possible cases. If $Z > 0$, then the coexistence state is stable whenever it exists. When $Z < 0$, then the coexistence state can be destabilized by increasing C sufficiently much above C^*; see Figure 3.4. The condition $Z < 0$ is equivalent to

$$A_2 < \frac{B_2}{B_1}\,\frac{A_1(R_1 - B_2) + B_2}{R_1 - B_2}. \tag{3.28}$$

In contrast to Figure 3.3, this case requires higher values of C for coexistence for higher values of A_1. While the increase in x with A_1

at the semi-trivial equilibrium in the chemostat scenario is linear, this increase in bounded in the logistic scenario. Therefore, a higher value of x cannot necessarily alleviate lower prey levels.

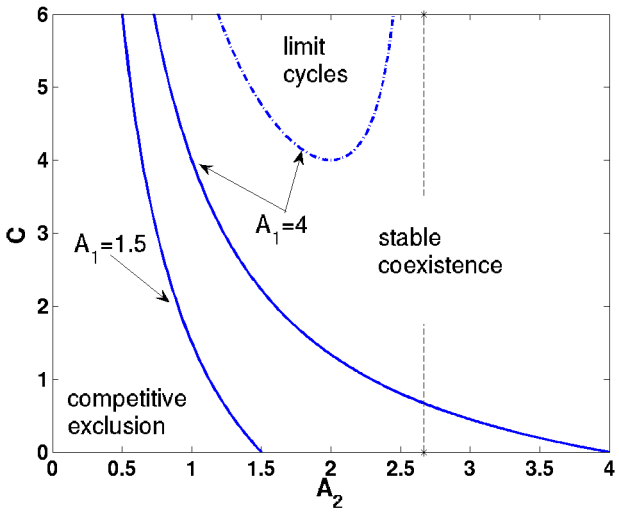

Figure 3.4: Coexistence region of predators with asymmetric mutualism and predation dynamics. Below the solid curve, species x exclude species y from the system. Above the solid curve, the two can coexist. Above the dash-dot curve, coexistence is unstable. The dashed vertical line gives the threshold of A_2 according to (3.28). When $A_1 = 1.5$ condition (3.28) is never satisfied. Parameters B_i are set to unity.

3.2.4 *Nonlinear predation and facilitation*

The linear predation and facilitation functions that we used thus far are not particularly realistic. Predators are saturated, which results in bounded predation functions (e.g. Holling II), and facilitation will eventually level off or even lead to mutual interference when there are too many consumers. Intuition would suggest that with saturating functions for h_i and f_i, similar effects can be observed as in the linear cases discussed above, expect that higher values of C are needed to produce the same dynamic behavior. We confirm this intuition in the case of identical consumers in the chemostat scenario by extending the analysis in subsection 3.2.2.

In addition, a nonlinear functional response can give rise to consumer-resource cycles as in the famous model by Rosenzweig and MacArthur (1963). When we have identical predators in the logistic case, such consumer-resource cycles occur for a wider range of parameters if there is mutualism.

Identical consumers in the chemostat scenario

In system (3.3), we choose monotone, saturating functions for the functional response and the strength of facilitation as

$$h(z) = \frac{az}{1+qz}, \qquad f(x) = 1 + \frac{\alpha x}{1+\beta x}. \tag{3.29}$$

In nondimensional form, the equations read

$$\begin{aligned} \frac{dx}{dt} &= x\left(\frac{Az}{1+Qz}\frac{(1+(D+C)x)}{1+Dx} - 1\right), \\ \frac{dz}{dt} &= 1 - xz - \frac{zx}{1+Qz}\frac{(1+(D+C)x)}{1+Dx}, \end{aligned} \tag{3.30}$$

where $A = az_{in}/d$, $C = \alpha d/(2ae)$, $D = \beta d/(2ae)$, and $Q = qz_{in}$, compare subsection 3.2.2.

The analysis is similar to the previous case, but the expressions are more cumbersome. It turns out that (a) if $A > 1+Q$ then the semi-trivial state is unstable; the consumer can invade, and there is a unique positive stable equilibrium; (b) if $A < 1+Q$, then the semi-trivial state is locally stable; if C is large enough, then the consumer has an Allee effect, i.e. it can persist stably at high enough density. The threshold value for C in the second case is

$$C^* = \frac{1}{A^2}\left[1 + V(AD+1) + 2\sqrt{V(AD+1)}\right], \tag{3.31}$$

where $V = 1+Q-A$. For $D = Q = 0$, this expression reduces to (3.7). The effect of Q and D is that when $A < 1+Q$, higher values of C are required for persistence of the consumer, see Figure 3.5.

Identical consumers in the logistic scenario

The non-dimensionalized system (3.11) with a type II functional response but linear facilitation function reads

$$\begin{aligned} \frac{dx}{dt} &= x\left(\frac{Az(1+Cx)}{1+Qz} - B\right), \\ \frac{dz}{dt} &= z(1-z) - \frac{xz(1+Cx)}{1+Qz}, \end{aligned} \tag{3.32}$$

where $A = aK/r$, $B = d/r$, $C = \alpha r/(2ea$, and $Q = qK$; compare subsection *The logistic scenario* in subsection 3.2.2. For $C = 0$, we obtain the model by Rosenzweig and MacArthur (1963), which has a globally attracting limit cycle, provided $A > \frac{2BQ}{Q-1} + BQ$ and $Q > 1$.

The coexistence equilibria satisfy a cubic equation; compare (3.12). As a result, we obtain the following qualitative behaviors. When $A > B(1+Q)$ then the predator can persist in the system; there is a unique coexistence state. When $A < B(1+Q)$ then the predator can have

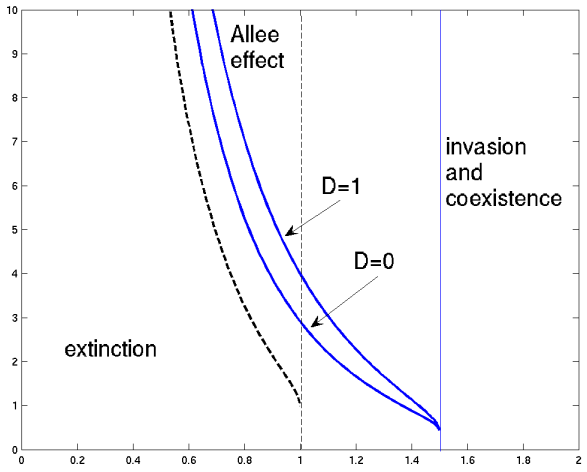

Figure 3.5: Illustration of the effect of nonlinear functional response on the dynamics of the mutualism for identical consumers in the chemostat scenario. Higher values of C are required for persistence when $D, Q > 0$ The solid lines have $Q = 0.5$, and $D = 0, 1$ as indicated. The dashed lines are the reference case $Q = D = 0$.

an Allee effect if C is large enough. The value of C required for a coexistence state in this case increases with Q (Figure 3.6).

The Jacobi matrix at a coexistence state is given by

$$J = \frac{1}{1+Qz}\begin{bmatrix} ACxz & Bx/z \\ -z(1+2C) & z(Q-1)-2Qz^2 \end{bmatrix}. \tag{3.33}$$

Figure 3.6 shows that the Hopf bifurcation occurs for smaller and smaller values of A as the strength of facilitation, C, increases. In fact, even very low mutualism reduced the A-value required for limit cycles dramatically.

3.2.5 *The full model*

In this subsection, we combine the results from the two previous simplified cases to infer the dynamics of the full system of intraguild mutualism. We stick with the linear functional response and mutualism functions.

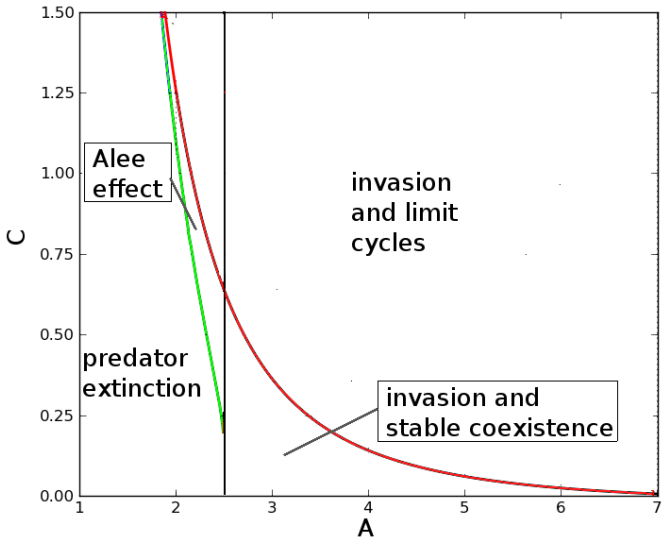

Figure 3.6: Illustration of the effect of nonlinear functional response on the dynamics of the mutualism for identical consumers in the logistic scenario. Higher levels of C are required for persistence, yet cycles appear for lower values of C; compare Figure 3.2. Parameters values are $B = 1, Q = 1.5$. Limit cycles without mutualism appear for $C = 0$ and $A > 7.5$.

The chemostat scenario

The nondimensional system with linear functional response and mutualism function reads

$$\begin{aligned}
\frac{dx}{dt} &= x[A_1 z(1 + C_1 y) - 1], \\
\frac{dy}{dt} &= y[A_2 z(1 + C_2 x) - 1], \\
\frac{dz}{dt} &= 1 - z - z[x(1 + C_1 y) + y(1 + C_2 x)],
\end{aligned} \tag{3.34}$$

A coexistence state is given by the admissible solution of

$$A_1 A_2 C_1 C_2 z^2 - (A_1 A_2 C_1 C_2 + A_1 C_2 + A_2 C_1) z + C_1 + C_2 = 0, \tag{3.35}$$

so that

$$x = \frac{1 - A_2 z}{A_2 C_2 z}, \qquad y = \frac{1 - A_1 z}{A_1 C_1 z}, \tag{3.36}$$

are positive. At a coexistence state, we also have $z + x/A_1 + y/A_2 = 1$.
Case I: $A_1 > A_2 > 1$
Both semi-trivial steady states exist, and species x can invade species

y. In addition, species y can invade species x, leading to coexistence, provided

$$C_2 > \frac{\frac{A_1}{A_2} - 1}{A_1 - 1}, \tag{3.37}$$

see Figure 3.7, panel (a).

Case II: $A_1 > 1 > A_2$
Only species x can persist by itself. Species y can invade and coexist if (3.37) is satisfied; see Figure 3.7, panel (a).

Case III: $1 > A_1 > A_2$
No semi-trivial states exist. The two species have a 'joint Allee effect', meaning that for large enough C_i, the coexistence state exists and is locally stable. Hence, if mutualism is strong enough and if both species have a high enough initial density, then the two species can coexist; see Figure 3.7, panel (b).

We replaced the linear functional responses and mutualism functions with Holling type II functions as in subsection 3.2.4 and explored the qualitative behavior of the system numerically. As expected, stronger mutualism is required, but the same patterns can be observed as with linear functions. The bound of the mutualism functions means that sometimes the strength of mutualism required for coexistence is larger than the bound on the function. Hence, the opportunity for coexistence declines compared to the case of linear functions.

The logistic scenario

The nondimensional system with nonlinear functional response and linear mutualism function reads

$$\begin{aligned}
\frac{dx}{dt} &= x\left[\frac{A_1 z}{1+Q_1 z}(1+C_1 y) - B_1\right], \\
\frac{dy}{dt} &= y\left[\frac{A_2 z}{1+Q_2 z}(1+C_2 x) - B_2\right], \\
\frac{dz}{dt} &= z(1-z) - z\left[\frac{x}{1+Q_1 z}(1+C_1 y) + \frac{y}{1+Q_2 z}(1+C_2 x)\right],
\end{aligned} \tag{3.38}$$

where $A_i = a_i K/r$, $B_i = d_i/r$, $C_i = r\alpha_i/(2e_i a_i)$, and $Q_i = q_i K$.

When $A_1 > B_1(1+Q_1)$, then species x can invade the prey-only state $(0,0,1)$. The semi-trivial state

$$x = \frac{A_1(A_1 - B_1(1+Q_1))}{(A_1 - B_1 Q_1)^2}, \qquad y = 0, \qquad z = \frac{B_1}{A_1 - B_1 Q_1}, \tag{3.39}$$

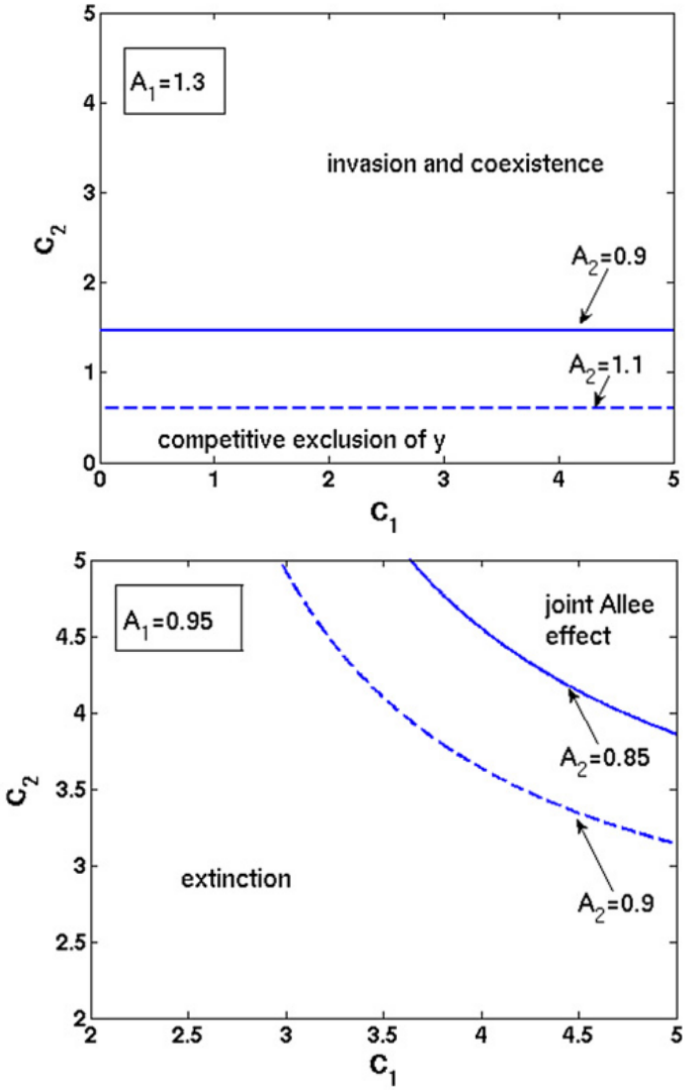

Figure 3.7: Coexistence regions in the three-species system with chemostat dynamics. **Panel (a), top:** $A_1 > 1, A_1 > A_2$. Species y can invade and the two can coexist if C_2 is large enough. **Panel (b), bottom:** $1 > A_1 > A_2$. The two species can coexist if mutualism is high enough and if both have sufficiently high initial density.

is stable in the x-z-plane provided $Q < 1$ or $A_1 < \frac{2B_1Q_1}{Q_1-1} + B_1Q_1$; otherwise there is a stable limit cycle. Species y can invade the semi-trivial state if

$$C_2 > \frac{1}{x}\left[\frac{B_2(1+Q_2z)}{A_2z} - 1\right], \tag{3.40}$$

where x and z are the steady-state values from (3.39). Similar relationships hold when x and y are exchanged by exchanging indices 1 and 2.

A coexistence state is given by the solution of the cubic equation for species z as

$$z^3 - z^2 + \frac{B_1B_2(C_1Q_2 + C_2Q_1) - A_1B_2C_2 - A_2B_1C_1}{A_1A_2C_1C_2}z + \\ + \frac{B_1B_2(C_1 + C_2)}{A_1A_2C_1C_2} = 0. \tag{3.41}$$

From this relation, we obtain several conditions. If $Q_{1,2}$ are large then there are no positive solutions for z. If $Q_{1,2}$ are small enough, then there are positive solutions for z, provided the mutualism coefficients $C_{1,2}$ are large enough.

Investigating the various cases, we find the exact same qualitative behavior as in the chemostat scenario. Specifically, (i) if species x can invade at low density, then the invasion condition for species y is given by (3.40), which leads to a qualitative behavior as in Figure 3.7, left panel. (ii) if no species can invade at low density and if the coefficients $Q_{1,2}$ are small enough, then there is a joint Allee effect, provided the mutualism coefficients $C_{1,2}$ are large enough (from (3.41)). This scenario leads to a qualitative behavior as in Figure 3.7, right panel.

In both cases, with or without joint Allee effect, increasing the strength of mutualism can lead to population cycles. If there is no joint Allee effect, all three species will coexist in a limit cycle. If there is a joint Allee effect, then the two predator species could be driven to extinction if cycles become too large.

Finally, we consider the effect of intraguild mutualism on cyclic coexistence of predators. When $C_{1,2} = 0$, system (3.38) admits for cyclic coexistence via a transcritical bifurcation of limit cycles as follows. With only one predator, the system is a Rosenzweig-MacArthur system and admits a limit cycle. Under certain conditions, the second predator can invade along the limit cycle, and both can coexist in a limit cycle (Kot, 2001). A necessary condition is that one predator does better at low prey density whereas the other grows faster at high prey density (Hsu et al., 1978). This coexistence mechanism depends on a very fine balance and may occur only in a very narrow interval of parameter values. For example, with $A_1 = 8$, $A_2 = 6$, $B_1 = 1$, $B_2 = 0.8$, and $Q_1 = 3$, the two species coexist in the range of

$Q_2 \in [2.63, 2.643]$. Species x does better at low prey density, species y at high density.

Now we add very weak intraguild mutualism of $C_{1,2} = 0.01$. Then the coexistence region along a limit cycle is $Q_2 \in [2.57, 2.704]$, which is much larger than for $C_{1,2} = 0$. Figure 3.8 shows such limit cycles and demonstrates that the two predators are in phase with one another.

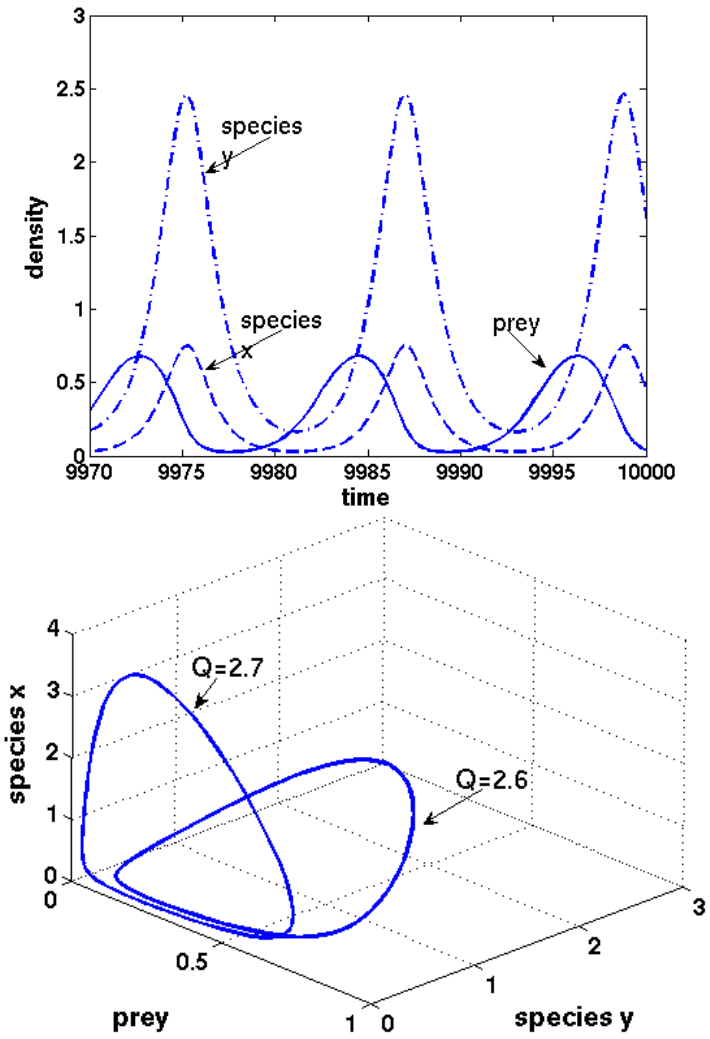

Figure 3.8: Cyclic coexistence of two mutualistic predators on one prey. For $Q_2 < 2.57$ there is a stable limit cycle between y and z with $x = 0$. As Q_2 increases, there is a transcritical bifurcation of limit cycles, and the coexistence limit cycle becomes stable. For Q_2 larger than 2.704, the limit cycle between x and z with $y = 0$ is stable against invasion by y. Parameters are $A_1 = 8$, $A_2 = 6$, $B_1 = 1$, $B_2 = 0.8$, and $Q_1 = 3$.

3.2.6 *Discussion*

Mutualistic interactions between species are well documented empirically but much less studied theoretically than competitive or exploitative interactions (Boucher et al., 1982; Bruno et al., 2003). Intraguild mutualism in particular could be a mechanism for coexistence between competing species, and could therefore contribute to the creation and maintenance of biological diversity (Stachowicz, 2001). Crowley and Cox (2011) propose a theoretical research program on intraguild mutualism, based on studying several community modules. To our knowledge, this work is the first step in this research program towards understanding causes and effects of intraguild mutualism from a modeling perspective.

Even within each of the modules proposed by Crowley and Cox (2011), one has to make modelling decisions as to which processes are affected by mutualism. Gross (2008) assumed that death rates of competing species decreased in the presence of their competitors and found stable coexistence between many competitors on a single resource. Alternatively, based on empirical evidence (e.g. Losey and Denno (1998)), we modeled mutualistic interaction by increased feeding rates in the presence of the mutualist. In the first subcase (subsection 3.2.2), we demonstrated how bistability (Allee effect) can emerge from mutualism. In the second subcase (subsection 3.2.3), we explored how facilitation can lead to coexistence of consumers and to persistence of consumer that would go extinct on its own. In both cases, the dynamics of the logistic case included cyclic behavior, but not in the chemostat case. Nonlinearities did not introduce new behavior in the chemostat case, but did so in the logistic case, where cycles are present in the absence of mutualism, and mutualism enhances the propensity to cycle (subsection 3.2.5). In the final subsection, we put the pieces of the puzzle together and explored some more complex dynamical issues numerically.

One of our results is also that stable coexistence between two intraguild mutualists occurs over a much larger set in parameter space than without mutualistic interactions. Hence, these results by Gross (2008) are robust and independent of the particular mechanism. In addition, we found that mutualism can be a mechanism for destabilization of a stable coexistence state and for emergence of population cycles. This effect only occurred for the logistic scenario. Our results here differ from the results by Gross (2008), who found limit cycles also with linear prey renewal, which corresponds to our chemostat scenario. We speculate that this difference results from the different implementation of mutualism. In our model, enhanced consumption of resources appears in the consumer and in the resource equations. In the model by Gross (2008), the mutualistic reduction of death rates appears only in the consumer equation; the effect on the resource is

only indirect. Since this effect is only indirect, it could act similarly to a delay, which can easily destabilize a steady state. The third effect that we found is that of a joint Allee effect for the consumer species: neither can persist on the given resource alone, but jointly they can with sufficiently high initial density. A similar effect has recently been found theoretically in a plant–pollinator system (Lutscher and Iljon, 2013). We are not aware of empirical evidence for such an effect. However, it is conceivable that so-called "ecosystem engineers" (Cuddington et al., 2009) would show such effects.

The interaction between an Allee effect (joint or not) and population cycles can lead to a catastrophic collapse of a cyclic population when the cycle becomes so large that it drops below the Allee threshold at its low point. A similar effect was already observed by Conway and Smoller (1986) in a predator–prey system with Allee effect of the prey. Hence, intraguild mutualism can lead to a variety of complex patterns that are otherwise absent from a competitive system.

As part of our analysis, we identified two special cases of parameter regimes that correspond to ecologically relevant situations on their own, namely intraspecific facilitation in a two-species model and unidirectional facilitation in a three-species model. The analysis of these two reduced systems provided crucial understanding of possible patterns in the full systems, yet was much simpler to understand. This observation can help uncover similarities between seemingly quite different ecological scenarios through mathematical scaling.

In addition to cyclic coexistence, systems with competing consumers can also show chaotic dynamics (Abrams et al., 2003). The two predator densities are intermediately correlated in such scenarios. Mutualism tends to synchronize cyclic predator populations; see for example Fig. 3.8. This mechanism could be a reason for why we did not see any chaotic dynamics in our simulations, but finding chaos was not our main focus. The question of whether mutualism decreases the likelihood of chaos should be explored in the future.

An important next step in this research is to include spatial movement into the models. We observe that the sign patterns of the Jacobi matrix for the two-dimensional models in subsection 3.2.2 allows for diffusion-induced instability. Hence, we expect spatial patterns to form when we simply add diffusion terms of sufficiently different magnitude to both species. Our preliminary numerical investigations show that the same is true for the full three-species system (plots not shown), see White and Gilligan (1998) for detailed conditions on Turing patterns in three-species systems. An alternative and much more challenging approach would be to model movement behavior of different intraguild mutualist species where one moves in response to the other as well as the prey. In such a movement model, one could study how higher catch rates in the presence of a competing species might emerge as a result of different (optimal?) foraging strategies.

3.3 ECO-EPIDEMIC EFFECTS AND THE RISK OF MALARIA IN THE ATLANTIC FOREST

Plasmodium vivax malaria is a neglected infectious disease that can cause severe symptoms and death in tropical regions. It is associated with an estimated 80-300 million cases of malaria worldwide. Brazilian tropical rain forests are home to a rich community of animals that can influence the dynamics of malaria transmission. In this study, we used a mathematical model parametrized with observation data to study two aspects of biodiversity – the abundance of wild warm-blooded animals, and the abundance of non-malarial mosquitoes – and the effects they have on malaria outbreak threshold. We found that both aspects can help prevent malaria outbreaks in tropical forests. Contrary to what has long been believed, forest conservation and malaria control are not incompatible, and biodiversity issues should be considered in order to achieve the desirable goals of biological conservation and maintenance of low malaria transmission.

3.3.1 *Background*

The dynamics of malaria transmission involve an interaction among vector mosquitoes (*Anopheles* species), protozoan parasites (*Plasmodium* species), and vertebrate hosts. Malaria is endemic in tropical and subtropical regions (Sinka et al., 2011, 2010*a*,*b*). The Global Malaria Eradication Program adopted in the 1950s has failed to meet expectations for malaria control in tropical and subtropical countries. One of the causes of that failure was the lack of an in-depth knowledge of the ecology of malaria-parasite transmission (Ferguson et al., 2010). In addition, *Plasmodium vivax* malaria has been neglected as a chronic disease (Carlton et al., 2011).

In the forested areas of the biogeographical subregion known as the Serra do Mar (mountain range), within the Atlantic Forest of southeastern Brazil, where the levels of insect and vertebrate richness are high (Forattini et al., 1986; Galetti et al., 2009), malaria has a low incidence (Curado et al., 2006; Marrelli et al., 2007; Duarte et al., 2008; Oliveira-Ferreira et al., 2010), with the primary malaria parasite being *Plasmodium vivax* (Couto et al., 2010). In the Atlantic forest, species of the *Anopheles* subgenus *Kerteszia* are the primary malaria vectors. The majority of *Kerteszia* species use bromeliad phytotelmata (small water tanks held by plants) as larval habitats (Zavortink, 1973), and it has been suggested that *Kerteszia* spp. participate in the dynamics of malaria-parasite transmission in Trinidad (Downs and Pittendrigh, 1946) and along the Atlantic coast of Brazil (Lutz, 1903; Smith, 1953). Between 1944 and 1951, there were malaria epidemics in the southern Atlantic Forest within the states of Santa Catarina and Paraná,

the overall incidence for the period being 5% (Smith, 1953). Such epidemics mainly ceased because of deliberate deforestation that eliminated 3,800 km^2 of native forest (Reitz, 1983), removing bromeliads and reducing the number of resting sites for adult mosquitoes within the forest (Smith, 1953).

Although malaria epidemics are currently uncommon, temporal and spatial clustering of cases can occur in the Atlantic Forest. One low-incidence outbreak occurred among outdoor workers in the forested highlands of the state of Espírito Santo between 2001 and 2004 (Cerutti et al., 2007). In 2006, another epidemic occurred in the southern periphery of the city of São Paulo, where residents of the Marsilac district invaded the Serra do Mar Natural Forest Reserve to construct houses (CVE, 2006). Given the presence of *Anopheles* vector species, as well as of infected and susceptible hosts, together with the circulation of *Plasmodium*, it is hypothesized that ecological interactions among *Anopheles* (*Kerteszia*) *cruzii*, *Plasmodium* species, and the local biodiversity are modulating malaria transmission in the Serra do Mar.

Forested areas offer a diverse range of habitats for mosquito species (Shannon, 1931). Consequently, high levels of mosquito species richness and abundance are expected (Forattini et al., 1986). This scenario can decrease the number of infective bites, because multiple vector and non-vector mosquito species would try to feed on a defensive host (Edman and Kale, 1971; Pianka, 1974), decreasing the chances of successful bites by the vector population. In addition, malaria parasite transmission could be affected by an abundance of non-competent hosts that would prevent mosquitoes from transmitting *Plasmodium* parasites to humans (Saul, 2003). This would represent a dilution effect of wild warm-blooded animals, which act as dead-end hosts (Ostfeld and Keesing, 2000). Therefore, diffuse mosquito vector competition and dead-end transmission of parasites are mechanisms in the dynamics of malaria transmission in tropical forests that can decrease the chances of malaria emergence.

The insight that ecological mechanisms can influence the dynamics of malaria parasite transmission supports arguments against human occupation of protected natural areas. Current theory says that biodiversity can have an impact on the emergence and transmission of infectious diseases, which is a new focus of conservation studies (Keesing et al., 2010). Some authors have shown that when biodiversity declines, there is an increased risk of humans contracting schistosomiasis (Johnson et al., 2009), West Nile fever (Swaddle and Calos, 2008), hantavirus infection (Suzán et al., 2009), or Lyme disease (Keesing et al., 2009). Similarly, diseases that affect coral reefs become more widespread when biodiversity is reduced by human activities (Raymundo et al., 2009). The relationship between a decline of biodiversity and an elevated risk of vector-borne disease might be attributable to changes in the abundance of hosts and vectors or to

modified host, vector, or parasite behavior (Keesing et al., 2010). In the Brazilian Amazon, gradual and continuous changes in the natural ecosystems can create ecological conditions that favor a rapid increase in abundance of *Anopheles darlingi*, which have been associated with an increased risk of malaria. Sawyer and Sawyer (1992) coined the term "frontier malaria" to define the dynamics of malaria transmission in recently deforested areas of the Amazon Forest. In those areas, malaria transmission decreases when the natural ecosystem is highly modified, to the point that the maintenance of vector species and *Plasmodium* circulation are not ecologically supported (Sawyer and Sawyer, 1992; De Castro et al., 2006). Therefore, malaria in Amazon and in the Atlantic Forest are both associated with biodiversity, because the larval habitats of *An. darlingi*, the primary vector in Amazon Region, and *An. cruzii*, the primary vector in Atlantic Forest, depend on the presence of forested areas.

Historically, tropical regions have been considered economically underdeveloped hotspots of biodiversity (Wilson, 1988). However, Brazil is an emerging global economy, with indications that its forest cover, along with its biodiversity, will decline rapidly (Metzger et al., 2010). In such a case, frontier malaria would be eliminated, but the risk of rural and urban malaria would increase, because *Anopheles marajoara* could become a vector of *Plasmodium* parasites (Conn et al., 2002; Laporta et al., 2011). Given that malaria cannot be completely eliminated and that there is an urgent need for conservation/restoration of tropical biodiversity, it is important to understand interactions between the dynamics of malaria transmission and the diversity of vertebrates and mosquitoes. Here, we develop a theoretical framework that might explain how biodiversity can modulate malaria epidemics in a tropical rain forest. Our case study site is a protected area within the Atlantic Forest, inhabited by indigenous peoples and fishermen, where *An. cruzii* is present but no malaria cases have been reported in the last 30 years. Our objectives were to propose a novel mathematical model for malaria transmission with explicit mechanisms of diffuse mosquito vector competition and dead-end transmission of parasites, applying this model to this case study site.

3.3.2 *Mathematical model of malaria transmission*

To calculate the risk of malaria parasite transmission, we used our model and the Ross-MacDonald model for the two most populated human settlements, the Guarani village and Marujá. With the Ross-MacDonald model, it was assumed that *An. cruzii* abundance was constant; that is, there were no ecological interactions (Anderson and

May, 1991). Therefore, the model was mathematically expressed as follows (Keeling and Rohani, 2008):

$$\begin{aligned}
\frac{dX_h}{dt} &= -\frac{bT_{hm}X_hY_m}{N} + \gamma Y_h \\
\frac{dY_h}{dt} &= \frac{bT_{hm}X_hY_m}{N} - \gamma Y_h \\
\frac{dX_m}{dt} &= \mu Y_m - \frac{bT_{mh}X_mY_h}{N} \\
\frac{dY_m}{dt} &= \frac{bT_{mh}X_mY_h}{N} - \mu Y_m
\end{aligned} \tag{3.42}$$

where X_h and Y_h are susceptible and infected humans, respectively, and X_m and Y_m are susceptible and infected mosquitoes. $N = X_h + Y_h$ is the total human population, b is the biting rate, T_{hm} and T_{mh} are the transmission probabilities from a biting infected mosquito to a susceptible human, and from a infected human to a biting mosquito, γ is the recovery rate by humans, and μ is the mortality rate of vector mosquitoes.

We introduce two new ingredients to this classical formulation: first, the assumption that the vector mosquito population is regulated by the amount of blood available, that is, the birth rate is proportional to the total biting rate; the second is to take into account ecological mechanisms that affect the biting rate on humans, namely diffuse competition for hosts and dilution of bites among humans and other warm-blooded animals. The model than reads:

$$\begin{aligned}
\frac{dX_h}{dt} &= -\frac{bT_{hm}X_hY_m}{(B+N)\left(1+\frac{1}{h}\frac{C+M}{B+N}\right)} + \gamma Y_h \\
\frac{dY_h}{dt} &= \frac{bT_{hm}X_hY_m}{(B+N)\left(1+\frac{1}{h}\frac{C+M}{B+N}\right)} - \gamma Y_h \\
\frac{dX_m}{dt} &= \frac{\alpha b M}{1+\frac{1}{h}\frac{C+M}{B+N}} - \mu X_m - \frac{bT_{mh}X_mY_h}{(B+N)\left(1+\frac{1}{h}\frac{C+M}{B+N}\right)} \\
\frac{dY_m}{dt} &= \frac{bT_{mh}X_mY_h}{(B+N)\left(1+\frac{1}{h}\frac{C+M}{B+N}\right)} - \mu Y_m \ ,
\end{aligned} \tag{3.43}$$

where $M = X_m + Y_m$ is the total vector mosquito population, α is the conversion rate of each bite to *An. cruzii* adults, h is the biting tolerance exhibited by vertebrate animal and human hosts (assumed to be equal for simplicity), B is the abundance of warm-blooded animals, and C is the abundance of other (non-vector) mosquitoes.

The abundance of *An. cruzii* in equilibrium, X_m^*, is given by:

$$X_m^* = \left(\frac{\alpha b}{\mu} - 1\right) h(B+N) - C \ . \tag{3.44}$$

We can recover the Ross-MacDonald model from ours if we consider that wild warm-blooded animals are either absent or do not

interact with *An. cruzii* (B = 0), non-vector mosquito species are absent or do not interact with *An. cruzii* (C = 0), humans do not react to mosquito bites ($h \to \infty$), and *An. cruzii* abundance is constant ($\alpha b = \mu$).

The analysis of the model consists simply in calculating R_0, the basic reproduction number, which is the expected number of secondary cases arising from a single case in a given susceptible population, and assessing how it is influenced by the different parameters, which correspond either to different conditions or to possible future states.

The value of R_0 predicted by the Ross-MacDonald model is:

$$R_0 = \frac{b}{N}\sqrt{\frac{T_{hm}T_{mh}NX_m}{\gamma\mu}}\,, \tag{3.45}$$

whereas our model predicts an R_0 of:

$$\begin{aligned} R_0 &= \frac{b}{(B+N)\left(1+\frac{1}{h}\frac{C+X_m^*}{B+N}\right)}\sqrt{\frac{T_{hm}T_{mh}NX_m^*}{\gamma\mu}} \\ &= \frac{\mu}{\alpha(B+N)}\sqrt{\frac{T_{hm}T_{mh}NX_m^*}{\gamma\mu}}\,, \end{aligned} \tag{3.46}$$

where X_m^* is given by Equation 3.44. When $R_0 > 1$, the disease can invade and there should be an epidemic episode, what does not occur when $R_0 < 1$.

Notice that the two models have different behaviors with respect to changes in the number of human hosts, N: while the Ross-MacDonald predicts high R_0 at low densities and decreasing (as $\sqrt{N}$) R_0 for high N, our model predicts low R_0 for small N (due to a low number of vectors) and increasing R_0 as N increases, since the dilution among humans is not enough to compensate the increase in the number of hosts.

3.3.3 *Study area*

The Iguape-Cananéia-Paranaguá estuarine lagoon region is a coastal plain area of approximately 600-km^2, situated on the southeastern coast of Brazil, between the Ribeira de Iguape River and the Atlantic Ocean. Three great islands stretch along the coast a hundred kilometers from northeast to southwest, namely Comprida, Cananéia, and Cardoso (Suguiu and Petri, 1973). Cardoso island, hereafter referred to as Parque Estadual da Ilha do Cardoso (PEIC), is a São Paulo State Park within the Atlantic Forest (Tabarelli et al., 2005).

The PEIC is separated from the mainland by the Ararapira Channel, a body of water that is as narrow as 30m wide at places. Therefore, even large animals, such as muriqui (*Brachyteles*) can cross (In-

gberman et al., 2010). Common wild warm-blooded animals include medium to large birds, such as quail (*Odontophorus capueira*), toucans (*Ramphastos* species), guans (*Penelope* species and *Pipile jacutinga*), tinamous (*Tinamus solicarius*), and mammals, such as howler monkeys (*Alouatta* species), agoutis (*Dasyprocta leporina*), and squirrels (*Sciurus ingrami*), as described by Bernardo (São Bernardo, 2004). Vegetation types form a successional gradient from sand dunes at the shore to higher and ancient terrains inland. Along the coastal plain, there is sand dune vegetation, scrubland, and low forests with sandy soil (arboreal restinga, or shoal vegetation).

Descendants of European colonists previously occupied what is now the PEIC, and the major local activities were fishing and family farming (Almeida, 1946). The population density is currently approximately 3.3 people/km^2, which has no relevant impact on local biodiversity. However, tourism has become one of the main sources of income, and thousands of tourists arrive every summer in the fishing village of Marujá, to the south. In addition, the indigenous Guarani Mbya tribe has been settled in the northwestern part of the PEIC since 1992, having the right to engage in subsistence hunting and logging in the forest (Conselho Estadual do Meio Ambiente, 2001; Galetti, 2001).

3.3.4 *Results*

On the basis of collected data and data from the literature, the models described in the previous section were completely parameterized for the case study site. Empirical values were unavailable only for the host tolerance (h) parameter, which was set to a range of reasonable values and submitted to a sensitivity analysis.

The indigenous settlement in the study area (a village occupied by members of the Guarani Mbya tribe) is inhabited by 150 natives in an area of 2.8km^2, whereas 165 people (fishermen and their families) live in Marujá in a an area of 0.8km^2. As can be seen in Table 3.1, the estimated abundance of wild birds and mammals (B) was 172 in the Guarani Mbya village and 47 in Marujá. The estimated abundance of mosquitoes in the Guarani Mbya village and Marujá was $1,514$ and 300 for the malaria vector *An. cruzii* (X_m^*), respectively, compared with $14,101$ and $3,640$ for non-vectors (C).

Data in the literature, from laboratory and field experiments, show that the estimated maximum *An. cruzii* biting rate (b) is 0.5 bites/day (Table 3.1). In the laboratory, we found the estimated gonotrophic cycle to be four days, and our field experiments indicated gonotrophic discordance in natural populations. In our laboratory experiments, *An. cruzii* mortality (μ) was estimated to be 0.8/day. Employing the previously mentioned data from the literature, we estimated the α parameter, which indicates how many new adults will be generated

Table 3.1: Model parameters, their descriptions and estimates.

Parameter simbol	Description	Estimates
Human population size (N)	Total number of inhabitants in the Guarani Mbya village and Marujá	150 and 165, respectively
Abundance of wild warm-blooded animals (B)	Estimates of abundance of avian and mammalian species in the Guarani Mbya village and Marujá	172 and 47, respectively
Abundance of non-vector mosquito species (C)	Estimates of abundance of non-vector mosquito species[a] in the Guarani Mbya village and Marujá	14,101 and 3,640, respectively
Abundance of *Anopheles cruzii* (X_m^*)	Estimates of abundance of *An. cruzii*[b] in the Guarani Mbya village and Marujá	1,514 and 300, respectively
Anopheles cruzii biting rate (b)	Biting rate of each *An. cruzii* female upon a given host per day	0.50
Anopheles cruzii mortality rate (μ)	Mortality rate of *An. cruzii* female population per day	0.80
Anopheles cruzii convertion rate (α)	Convertion rate of a successful bite upon a host to the number of emerging females in the Guarani Mbya village and Marujá	5.5 and 3.1, respectively
Probability of *Plasmodium* transmission from *Anopheles cruzii* to humans (T_{hm})	Probability of *Plasmodium* transmission from *An. cruzii* to humans in low-endemicity malaria transmission dynamics	0.022
Probability of *Plasmodium* transmission from humans to *Anopheles cruzii* (T_{mh})	Probability of *Plasmodium* transmission from humans to *Anopheles cruzii* in low-endemicity malaria transmission dynamics	0.24
Human recovery rate (γ)	Daily human recovery rate, which can be understood as the average duration of the infectious period	0.0035 (286 days)
Host tolerance (h)	Number of bites per day before a host starts a defensive behavior divided by *An. cruzii* biting rate (0.5)	20, i.e., host defensive behavior occur after the 10^{th} bite in a given day

[a]: *Aedes serratus*, *Limatus durhami*, *Runchomyia reversa* and *Wyeomyia quasilongirostris*.
[b]: *Anopheles cruzii* is the primary vector of malaria *P. vivax* and *P. malariae* parasites (Curado et al., 2006).

from a single successful bite of *An. cruzii*, to be 5.5 in The Guarani Mbya village and 3.1 in Marujá (Table 3.1).

The estimated probabilities of *Plasmodium* species transmission and the human recovery rate correspond to the dynamics of transmission in a low-endemicity area. Mosquitoes transmit malaria parasites to humans with a probability of 0.022 (T_{hm}), humans infect mosquitoes with a probability of 0.24 (T_{mh}), and the human recovery rate (γ) is about 0.0035/day, which means that average duration of the infectious period is 286 days (Table 3.1).

The h parameter was derived from two other values: the number of bites/day before a host starts a defensive action (assumed to be about 10 bites/day), divided by the maximum biting rate (0.5 bites/-day for *An. cruzii*). Another way to interpret the h parameter is that host defensive behavior will be stronger when the average biting rate is greater than 10 bites/day. On the basis of our field work experience in tropical forests (mainly the Atlantic Forest), we can state that neither humans nor animals can stand mosquito biting rates much greater than that value before they begin to exhibit defensive behavior (e.g., shaking body parts or, in the case of humans, waving hands and swatting). Therefore, h was set at 20, the interval being 18-35 in the sensitivity analysis. It was found that if h were smaller than 18, *An. cruzii* would be excluded by competition in both human settlements; and that if h were larger than 30 and 35, respectively, the R_0 was > 1 in Marujá and the Guarani Mbya village. Given that competitive exclusion of *An. cruzii* and malaria invasion ($R_0 > 1$) represented less possible situations, diffuse mosquito vector competition and dead-end transmission patterns are assessed at h values of 20-30. As a result, no qualitative changes could be made in the initial interpretations (see the following paragraphs).

If we employ the R_0 estimate relative to the Ross-MacDonald model (eq. 1), the Guarani Mbya village would have an R_0 of 2.18 and Marujá would have an R_0 of 0.93. Using the model employed in the present study (eq. 2), we found the R_0 to be 0.30 for the Guarani Mbya village and 0.39 for Marujá. If the abundances of non-vector mosquito and non-host vertebrate species were reduced by approximately 80% and 70%, respectively, the critical threshold level ($R_0 = 1$) would be exceeded in the Guarani Mbya village (Figure 1). Similarly, a 50% reduction in the abundance of non-vector mosquito species could cause malaria invasion ($R_0 > 1$) in Marujá (Figure 2). However, epidemics would not occur in Marujá even if there were local extinction of all non-host vertebrate species but would occur if the human population increased by approximately 50% (Figure 3).

3.3.5 *Discussion*

Although scarce malaria cases are reported annually in the surrounding area (Curado et al., 2006; Duarte et al., 2008; Couto et al., 2010), no malaria cases have been reported in the last 30 years. Therefore it seems safe to assume that *Plasmodium* transmission does not occur in Parque Estadual da Ilha do Cardoso. The estimated R_0 provided by Ross–Macdonald model ($R_0 = 2.18$) would suggest that malaria parasite transmission is occurring in that region. In contrast, the model proposed estimated a value of $_0$ for the Guarani Mbya village of 0.30, which is in accordance with the fact of no malarial transmission. With this model, we formulate hypothetical scenarios in order

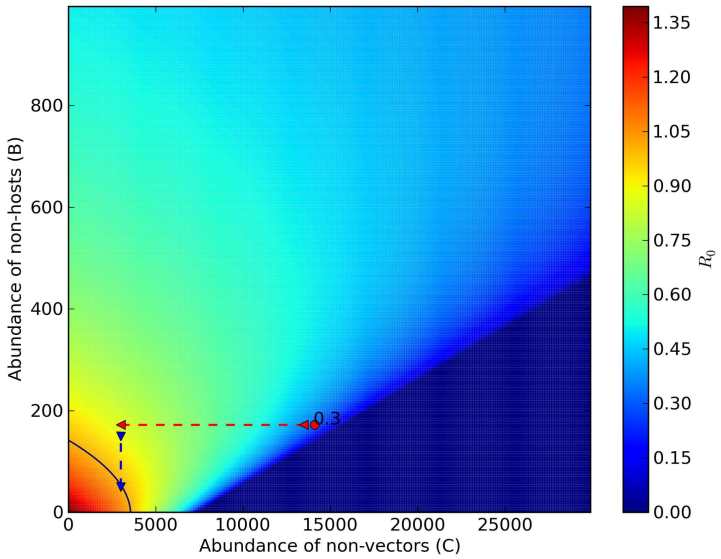

Figure 3.9: Dilution effect and diffuse mosquito vector competition in the Guarani Mbya village. Increase in abundance of non-vector mosquito species and in abundance of wild warm-blooded animals is correlated with decrease in the risk of malaria-parasite transmission. Reduction in abundance of wild warm-blooded animals (blue dashed arrow) and in abundance of non-vector mosquito species (red dashed arrow) can exceed the critical threshold level, $R_0 = 1$, represented by the black isoline. The red circle is the R_0 estimate of our model ($R_0 = 0.3$).

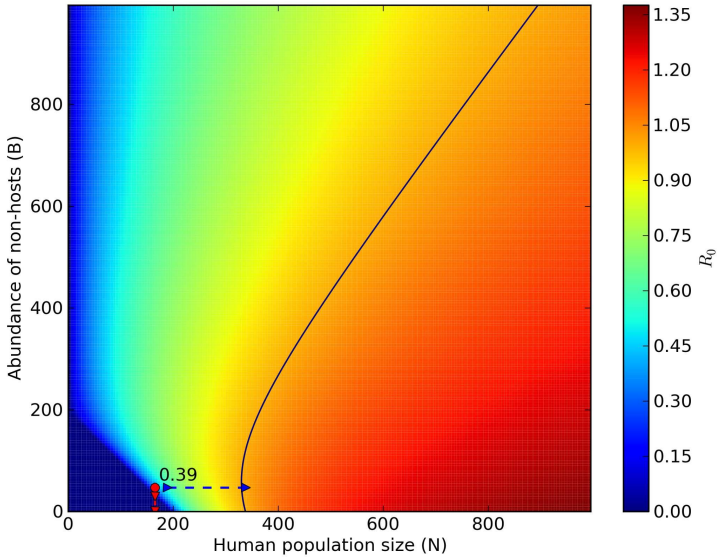

Figure 3.10: Increase in abundance of wild warm-blooded animals can increase or decrease the value of R_0, although not enough, in this case, to exceed the critical threshold level $R_0 = 1$, represented by the black isoline. However, increase in human population size (blue dashed arrow) can exceed the threshold.

to show what would happen with the R_0 estimate value if: 1) Non-vector mosquito populations increase (i.e., effect of diffuse mosquito vector competition), 2) Non-host animals populations increase (i.e., effect of dead-end transmission of parasites), and 3) Human population increases (effect of over-encroachment of human populations). These results provide support for biodiversity preventing the circulation of *P. vivax* in human settlements embedded in natural ecosystems. The absence of malaria cases can be explained by the diffuse mosquito vector competition. Greater abundances of mosquitoes can be correlated with higher levels of biodiversity, which increase ecosystem's functional redundancy, thus decreasing the chances of malaria occurrence, which is in keeping with the insurance hypothesis (McCann, 2000). According to this hypothesis, an insurance effect is the ability of an ecosystem to buffer perturbations, as well as the ability of the species in the community to respond differentially to perturbations. In other words, although our model applies equally when there is a single species of abundant non-vector competitor mosquito species or when there are many species comprising the same total abundance, the insurance effect holds that biodiversity is important to keep this abundance high in response to perturbations, whereas a single competitor species would fail to do same. Therefore, the mechanisms that hinder malaria parasite transmission can be considered services provided by the forest ecosystem.

The results of the model applied in the present study suggest that increasing non-vector mosquito abundance can reduce the number

of *An. cruzii* bites, decreasing malaria parasite transmission in the Atlantic Forest (Figure 3.9). The role of competition between vector and non-vector mosquito species is supported by the fact that there must be an intense selection pressure on hosts to exhibit defensive behavior against biting insects (Kelly, 2001; Edman et al., 1974), and contacts between mosquito species and specific hosts in a community may be influenced more strongly by the presence/absence of hosts than by innate mosquito choices (Chaves et al., 2010). This means blood may be a limiting resource, leading to competition among opportunistic blood-feeder mosquito species. The total abundance of non-vector and not-infected vector mosquito species can have a negative impact on malaria parasite transmission because of apparent competition mediated by host defensive behavior. The effect of apparent competition is a functional response that may be associated with host tolerance to mosquito bites, which results in a larger proportion of unsuccessful bites, with few *Plasmodium*-infective bites. The vector competition effect could also occur within species. For example, when there is more larval habitat available (during the wet season), hatch rates increase, making the proportion of nulliparous females (those that do not reproduce) larger than that of parous females. Host defensive behavior was observed for blacklegged ticks that are killed when feeding on the blood of opossums and squirrels (Keesing et al., 2009). Consequently, diffuse competition is a protective mechanism against infective bites and should therefore be considered a major factor in studies related to the dynamics of malaria transmission. In considering that *Plasmodium* species infection can affect the feeding behavior of anthropophilic mosquitoes (Cohuet et al., 2010), it would be important to understand how the mechanism of diffuse competition can be applied to malaria control strategies in endemic tropical regions.

The abundance of wild warm-blooded animals can decrease the transmission of *Plasmodium* species. Such animals can act as dead-end hosts, diminishing the chances of infective bites in humans, which can be used as an indirect method of malaria control. This might represent a dilution effect mechanism present in natural ecosystems that have a high abundance of warm-blooded animal species. Dilution effect mechanisms (Ostfeld and Keesing, 2000) were observed by Swadle and Calos (Swaddle and Calos, 2008), Johnson et al. (Johnson et al., 2009), and Suzán et al. (Suzán et al., 2009) for West Nile fever, schistosomiasis, and hantavirus infections, respectively. However, a low- to medium-level abundance of dead-end hosts can create a neutral situation in which the dilution effect is either unimportant (Begon, 2008) or harmful (Saul, 2003). Using a computer simulation, Allan Saul showed that the dilution effect (zooprophylaxis) can be harmful when a small number of dead-end hosts increase the risk of malaria parasite transmission by providing blood-feeding opportuni-

ties to vectors (Saul, 2003). Our model predicts that few wild warm-blooded animals can serve as blood sources for mosquito species, increasing the vector population and *Plasmodium* species dissemination. This can be seen in the non-linear (unimodal) relationship between the abundance of non-hosts B and the critical threshold level ($R_0 = 1$) depicted in Figure 3.10. This finding is supported by the work of Randolph and Dobson (2012), who stated that the dilution effect applies only to species-rich host communities in which there is variable reservoir competence. In addition, hunting activities that are allowed for traditional human communities in natural protected conservation units can reduce vertebrate abundance, whereas it increases the density of vegetation and the abundance of invertebrates, resulting in the so-called "empty forest" effect (Terborgh, 2000) and increasing the chances of malaria parasite transmission.

Having the present model as a starting point, two direct extensions can be pursued for studying dynamics of malaria transmission in tropical forests. In respect of the hypothesis suggesting that non-human hosts may be reservoirs of malaria-parasites (Duarte et al., 2008), the present model can be extended with new compartments representing the role of susceptible and infective primates. Moreover, the present model assumes that all host species have the same tolerance to mosquito bites. Considering that animals may have more tolerance to mosquito bites than humans, this assumption is unlikely to be strictly true and thus dilution effect impact is probably underestimated here. It is therefore important to evaluate how primates as *Plasmodium*-reservoirs and tolerance of warm-blooded animals to mosquito bites may affect, positively or negatively, dilution effect predictions in the dynamics of malaria transmission.

Plasmodium-infected *An. cruzii* were found within human domiciles during epidemics occurring in the municipalities of Blumenau, Brusque, Joinvile, and Florianópolis, all located within the Atlantic Forest region, in the 1940s and 1950s. One determinant of the malaria burden in those days was the rapid increase in the population of susceptible humans, which reached 800,000 in a short period of time (Smith, 1953). Another determinant was that humans were immunologically naïve to *Plasmodium* species infection. Consequently, while clearing native forest for agriculture and cattle farming, they lived in the nearby jungle, which increased the contact between humans and infective mosquitoes. It is likely that more recent malaria epidemics in the Amazon Forest occurred because of ecological and social determinants similar to those present in the Machadinho settlement project in the state of Rondônia between 1984 and 1995. Castro et al. observed that the prevalence of malaria increased rapidly in the early stages of settlement and subsequently decayed, reaching a low level 11 years later, which represents the general pattern of frontier malaria in the Amazon (De Castro et al., 2006). One way of avoid-

ing malaria epidemics in tropical regions (mainly in the Amazon) is clearing large areas of forest and rapidly establishing agriculture or farming in order to limit the exposure of new settlers to infective mosquito bites (De Castro et al., 2006). This is in consonance with the traditional approach of forest clearing used in the Atlantic Forest in the 1950s (Smith, 1953). In contrast, the results of the approach taken in the present study suggest that biodiversity contributes to disease control and thus ecosystems in tropical forests can be managed to sustain an equilibrium between high levels of biodiversity and the over-encroachment of human populations. Furthermore, diffuse mosquito vector competition can be considered a novel measure of vector control, especially because some *Anopheles* vector species seem not to be susceptible to indoor residual insecticide spraying and treated bed nets, which are currently the most successful strategies in Africa (Alonso et al., 2011).

Contrary to what has long been believed, forest conservation and malaria control are not incompatible, and biodiversity issues should be considered in order to achieve the desirable goals of biological conservation and maintenance of low malaria endemicity. Although releasing non-vector mosquitoes is not a practical alternative as vector control, conservation of the natural ecosystems may hinder transmission of malaria-parasites. The main application of the present model is to provide a formal framework in which biodiversity conservation and control of the human population size in protected areas are measures that can be taken to control transmission in any malarial endemic settings. The effect of mosquito vector diffuse competition means that policies of removal of native vegetation to eliminate malarial vectors, which were practiced in the past (Smith, 1953), have their shortcomings because they may also decrease non-vector community that buffers malarial transmission. For rural malaria, which includes *Anopheles gambiae* malarial dynamics in Africa, the mosquito vector diffuse competition is also a plausible underlying mechanism because it supports high transmission rates when native fauna is locally depleted by forest removal. Dead-end parasite transmission (dilution effect), by the framework herein proposed, was shown to be highly dependent on host tolerance. Consequently, there are two general predicted scenarios: 1) this mechanism may favour parasite decrease if the most tolerant host is a dead-end and 2) it may increase the vector population if tolerant hosts are present. It is noteworthy that these scenarios are not mutually exclusive. According to the implicit message in Smith and colleagues' work (Smith et al., 2012), scientists of the present century should go beyond the Ross-Macdonald's theory in order to have better insights on the ways that make possible the control of malarial transmission. In addition, the present model also makes qualitative predictions, and not just a correction, about the value of R_0 that are very distinct from the Ross-Macdonald model, e.g., the be-

havior of R_0 when N (i.e., human population) increases: it decreases in the Ross-Macdonald model, but increases in the dynamics of the present model because greater N implies higher vector-host contacts, leading to increase of parasite dissemination. The present model constitutes an essential step for understanding the dynamics of malaria transmission in tropical forest ecosystems that can provide the service of hindering malaria epidemics, allowing to reconcile malaria control with conservation of biodiversity.

4

TEMPERATURE EFFECTS ON STAGE-STRUCTURED POPULATIONS

The work described in this chapter is an ongoing collaboration with Priyanga Amarasekare, professor of Ecology at the University of California, Los Angeles, which started after a mini-course she taught at the ICTP-SAIFR Southern Summer School in Mathematical Biology in 2012. This is a peculiar case, since I had studied delay differential equations during my Master's (Coutinho, 2010) from a mathematical standpoint, but the methods I learned then fit right into the needs for this work. It led to two papers so far: "The intrinsic growth rate as a predictor of population viability under climate warming" (Amarasekare and Coutinho, 2013) and "Effects of Temperature on Intraspecific Competition in Ectotherms"(Amarasekare and Coutinho, 2014).

4.1 INTRODUCTION

Climate warming is predicted to cause many species extinctions and changes to ecosystems. Ectotherm animals (e.g., insects and reptiles) are of particular interest because, since their body temperature is strongly affected by environmental temperature, their metabolic rates are directly affected and so are their life-history traits (birth, death, and maturation rates). Moreover, their life cycle usually include juvenile stages whose development time depends crucially on ambient temperature.

Here we develop a theoretical framework to address how changes in temperature affect populations of ectotherm animals. One great appeal of this project is that the temperature effects occur at the level of individual traits, that can be measured under experimental conditions, and the model formulation provides a mechanistic link between this level and the population level via an application of the framework first developed by Nisbet and Gurney (1983) for stage structured insect populations with varying instar duration. It is also important that this framework accommodates seasonal (intra–annual) fluctuations, which allows one to study issues surrounding seasonal dynamics, as well as long-term temperature changes (climate warming).

4.2 MATHEMATICAL FRAMEWORK

We build a single-species model containing only two stages, juveniles and adults, which is the simplest possible picture of a stage-structured population. Here, we include intra-specific competition, although the linear version, without any density dependence, already has applications, shown in section 4.3.

Elucidating the mechanisms by which temperature affects population dynamics in the presence of intra-specific competition requires three types of information. First, we have to understand how temperature affects life history traits (reproduction, development and survivorship) in the absence of competition. This is important because temperature responses of life history traits determine the physiological optima for reproduction and the lower and upper thermal limits to viability (Van der Have and De Jong, 1996; Van Der Have, 2002; Kingsolver, 2009; Kingsolver et al., 2011). Second, we have to understand how temperature affects intra-specific competition, specifically how it influences the relationship between vital rates (birth, maturation and mortality) and density. Third, we need to know the characteristics of the seasonal temperature regime experienced by the species in question. Of particular importance is the mean habitat temperature in relation to the physiological temperature optima and the amplitude of seasonal fluctuations in relation to the lower and upper thermal limits to viability. For instance, tropical ectotherms tend to experience mean habitat temperatures close to their physiological optima and seasonal fluctuations of relatively small amplitude; Mediterranean and temperate species experience mean habitat temperatures well below their physiological optima and seasonal fluctuations of large amplitude (Deutsch et al., 2008; Amarasekare and Savage, 2012). The extent to which this difference influences temperature effects on competition is an important question.

Effects of temperature on life history traits

Temperature responses of life history traits in the absence of competition have been well-studied for a large number of ectotherm species (Angilletta, 2009; Kingsolver, 2009; Kingsolver et al., 2011) and their mechanistic basis well-understood. Briefly, temperature responses of reproduction, development and mortality are determined by temperature effects on the underlying biochemical processes (e.g., reaction kinetics, hormonal regulation; Johnson and Lewin (1946); Sharpe and DeMichele (1977); Schoolfield et al. (1981); Nijhout (1994); Van der Have and De Jong (1996); Van Der Have (2002); Ratkowsky et al. (2005); Kingsolver (2009); Kingsolver et al. (2011)). For instance, temperature effects on biochemical rate processes (e.g., reaction kinetics and enzyme inactivation) give rise to temperature responses at the organismal level that are either monotonic or left-skewed. Temper-

ature effects on biochemical regulatory processes (e.g., neural and hormonal regulation; Hochachka and David (2002); Long and Fee (2008); Nijhout (1994)) involve negative feedback: rate processes at low and high temperature values push the system towards an intermediate optimum. These effects result in temperature responses that are unimodal and symmetric (e.g., Gaussian). The general shape of the temperature response of these traits is presented in Figure 4.1.

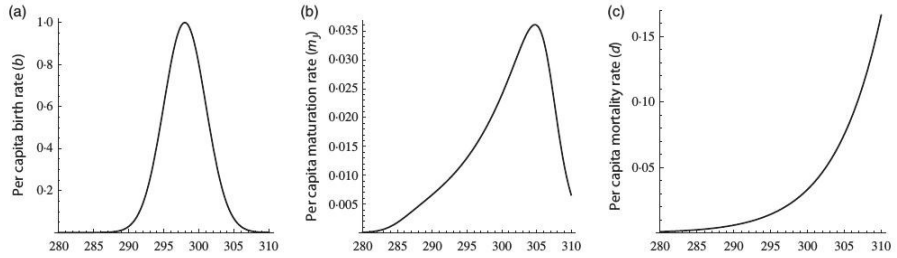

Figure 4.1: Temperature responses of life-history traits – birth, maturation and mortality rates. Parameter values are as follows: $b_{T_{opt}} = 1$, $T_{opt_b} = 298K$, $s_b = 3.0$ for the birth rate, $T_R = 297K$, $m_{J_{TR}} = \frac{1}{60}$ ($\tau = 60$ days at 297K), $A_m = 10500$ for the maturation rate, $d_{X_{TR}} = 0.02$, $A_d = 12000$ for the mortality rate.

Per capita mortality rate of all ectotherms exhibits a monotonic temperature response that is well-described by the Boltzmann-Arrhenius function for reaction kinetics (Van der Have and De Jong, 1996; Gillooly et al., 2002; Savage et al., 2004):

$$d_{X_T}(T) = d_{X_{T_R}} e^{A_{d_X}\left(\frac{1}{T_R} - \frac{1}{T}\right)}, \tag{4.1}$$

where $d_{X_T}(T)$ is the mortality rate of stage X (e.g., juvenile, adult) at temperature T (in K), $d_{X_{T_R}}$ is the mortality rate at a reference temperature (typically between $20 - 30°C$, the commonest being $24 - 25°C$; Sharpe and DeMichele (1977); Schoolfield et al. (1981)) and A_{d_X} is the Arrhenius constant, which quantifies the temperature sensitivity of mortality, i.e., how fast it increases with increasing temperature.

Maturation rate of ectotherms exhibits a left-skewed temperature response (Sharpe and DeMichele, 1977; Schoolfield et al., 1981; Van der Have and De Jong, 1996; Van Der Have, 2002; Kingsolver, 2009; Kingsolver et al., 2011) that results from the reduction in reaction rates at low and high temperature extremes due to enzyme inactivation. This response is well-described by a thermodynamic rate process model (Sharpe and DeMichele, 1977; Schoolfield et al., 1981; Ratkowsky et al., 2005):

$$m(T) = \frac{\frac{m_{T_R} T}{T_R} e^{A_{m_J}\left(\frac{1}{T_R} - \frac{1}{T}\right)}}{1 + e^{A_L\left(\frac{1}{T_{L/2}} - \frac{1}{T}\right)} + e^{A_H\left(\frac{1}{T_{H/2}} - \frac{1}{T}\right)}}, \tag{4.2}$$

where $m(T)$ is the maturation rate at temperature T (in K), m_{T_R} is the maturation rate at the reference temperature T_R at which the enzyme is 100% active, A_{m_J} (enthalpy of activation divided by the universal gas constant R) quantifies temperature sensitivity, $T_{L/2}$ and $T_{H/2}$ are, respectively, the low and high temperatures at which the enzyme is 50% active, and A_L and A_H are the enthalpy changes associated with low and high temperature enzyme inactivation divided by R (Johnson and Lewin, 1946; Schoolfield et al., 1981; Sharpe and DeMichele, 1977; Van der Have and De Jong, 1996; Van Der Have, 2002; Ratkowsky et al., 2005).

Per capita birth rate of most ectotherms exhibits a symmetric, unimodal temperature response that is well-described by a Gaussian function:

$$b(T) = b_{T_{opt}} e^{-\frac{(T-T_{opt_b})^2}{2s_b{}^2}}, \tag{4.3}$$

where T_{opt_b} is the temperature (in K) at which the birth rate is maximized ($b_{T_{opt}}$), and s_b depicts the variability in the temperature response, i.e., the temperature range over which the birth rate decays from the maximum.

Effects of intra-specific competition on life history traits

It is well-established that intra-specific competition for resources (e.g., food, nutrients, space) causes per capita birth rates to decrease and per capita mortality rates to increase with increasing conspecific density (Begon et al., 2006). These density-dependent relationships can be linear or non-linear, with responses leading to overcompensation or undercompensation in the feedback of density on the per capita growth rate (Kot, 2001; Gurney and Nisbet, 1998). The decline in the per capita birth rate is typically non-linear, exhibiting an exponential ($B(A) = be^{-q_b A}$) or hyperbolic ($B(A) = \frac{b}{1+q_b A}$) decline with density (Gurney et al., 1983; Nisbet and Gurney, 1983; Murdoch et al., 2013), where $B(A)$ is a function depicting the density dependence in the per capita birth rate, A is the adult density and b is the per capita birth rate in the absence of intra-specific competition. The parameter q_b is the competition coefficient (quantified as the slope of $B(A)$ vs. A), which determines the magnitude of the negative effect exerted by a single individual on its conspecifics through competition for resources or other limiting factors. The increase in the per capita mortality rate is typically linear ($D(X) = d_x + q_{d_X} X$) or saturating ($D(X) = d_x + \frac{q_{d_X} X}{1+X}$) (Gurney et al., 1983; Murdoch et al., 2013), where $D(X)$ represents the density-dependence in the per capita mortality rate, X is the density of the life stage (e.g., juvenile, adult) at which density-dependent mortality occurs, d_X is the mortality rate in the absence of competition and q_{d_X} is the competition coefficient (the slope of $D(X)$ vs. X).

Effects of temperature on intra-specific competition

Elucidating the effects of temperature on intra-specific competition requires that we understand how temperature modifies the responses of life history traits to density. We currently have no empirical data on how temperature affects these density responses. The first step therefore is to generate expectations about how temperature affects intra-specific competition so that empirical studies can be designed to test specific hypotheses.

There are two hypotheses that provide a starting point for empirical investigations. The first hypothesis, based on metabolic scaling theory (Savage et al., 2004), is that the strength of competition increases monotonically with increasing temperature. This is because higher activity levels at higher temperatures increase the per-individual resource acquisition, which reduces the carrying capacity when resources are limiting. In this case the temperature response of competition should be monotonic:

$$q(T) = q_{T_R} e^{A_q \left(\frac{1}{T_R} - \frac{1}{T}\right)} , \tag{4.4}$$

where $q(T)$ is the competition coefficient at temperature T (in K), q_{T_R} is competition coefficient at a reference temperature T_R, and A_q is the Arrhenius constant that quantifies the temperature sensitivity of competition, i.e., how fast the competition coefficient increases with increasing temperature.

The second hypothesis, based on ecological theory (Murdoch et al., 2013), is that competition is strongest at temperatures that are optimal for reproduction. This is because of the greater demand for resources during periods of high reproductive activity. In this case the temperature response of competition should be unimodal:

$$q(T) = q_{T_{opt}} e^{-\frac{(T - T_{opt_q})^2}{2 s_q{}^2}} , \tag{4.5}$$

where T_{opt_q} is the temperature (in K) at which competition coefficient is the highest ($q_{T_{opt}}$), and s_q depicts the variability in $q(T)$ about the optimum. Note that a Gaussian function is being used for purposes of illustration. Once empirical data become available, any other form of unimodal relationship (e.g., left- or right-skewed) can be used to depict the temperature response.

Joint effects of temperature and competition on life history traits

Building on the above information, we can depict the temperature response of density-dependent fecundity as $B(T, A) = b(T) e^{-q_b(T) A}$ or $B(T, A) = \frac{b(T)}{1 + q_b(T) A}$, where $b(T)$ is the temperature response of density-independent fecundity (Equation (4.3)) and $q_b(T)$ is the temperature response of the competition coefficient, given by Equations

(4.4) or (4.5). Similarly, the temperature response of density-dependent mortality is $D(T,X) = d_x(T)e^{q_{d_X}(T)X}$ or $D(T,X) = d_x(T) + q_{d_X}(T)X$ where $d_x(T)$ and $q_{d_X}(T)$ are, respectively, the temperature responses of the density-independent mortality rate (Equation (4.1)) and the temperature response of the competition coefficient of stage X.

Effects of temperature and competition on population dynamics

The next step is to determine how the joint effects of temperature and competition on life history traits translate into population dynamics. We start with a simple model of the ectotherm life cycle with juvenile and adult stages. Temperature affects all vital rates (birth, maturation, mortality) while intra-specific competition can affect one or more of these traits. Our task is to elucidate how vital rates that are affected only by temperature interact with vital rates that are affected by both temperature and competition to influence population dynamics.

Delay differential equations provide a natural mathematical context for elucidating the effects of developmental delays on population dynamics (Gurney et al., 1983). When temperature affects life history traits, developmental delays (the time it takes for an embryo to develop into a reproductive adult) themselves become functions of temperature. Variable delay models were first derived rigorously by Nisbet and Gurney (1983) to investigate the effects of time-varying parameters on population dynamics. We build on this important early work to develop models in which the time dependence arises from trait responses to temperature. Our novel contribution to the theory is to integrate mechanistic descriptions of trait-level responses with variable delay models of population dynamics.

The key assumption of the framework is that the population can be divided into stages that are dynamically equivalent: individuals in each stage have the same birth and death rates. Moreover, each cohort (the set of individuals born at some time) grows and matures together, that is, there is no variation among individuals, only across different cohorts. Although Nisbet and Gurney (1983) originally defined stages by the mass of individuals, and thus individuals mature to the next class when they reach a threshold mass, we abstract this concept to deal with a generic development time, which need not be connected to biomass.

The dynamics of a two-stage delay model with birth, death and development are given by:

$$
\begin{aligned}
\frac{dJ(t)}{dt} &= B\Big(T(t), A(t)\Big)A(t) - M_J(t) - D_J\Big(T(t), J(t)\Big)J(t) \\
\frac{dA(t)}{dt} &= M_J(t) - D_A\Big(T(t), A(t)\Big)A(t) \\
\frac{dS_J(t)}{dt} &= S_J(t)\left[\frac{m_J(T(t), J(t))D_J(T(t-\tau(t)), J(t-\tau(t)))}{m_J(T(t-\tau(t)), J(t-\tau(t)))} - D_J(T(t), J(t))\right] \\
\frac{d\tau(t)}{dt} &= 1 - \frac{m_J(T(t), J(t))}{m_J(T(t-\tau(t)), J(t-\tau(t)))} \\
M_J(t) &= B\Big(T(t-\tau(t)), A(t-\tau(t))\Big)A(t-\tau(t)) \\
&\quad \times \frac{m_J(T(t), J(t))}{m_J(T(t-\tau(t)), J(t-\tau(t)))} S_J(t)\ ,
\end{aligned}
\tag{4.6}
$$

where J and A depict juvenile and adult densities, $S_J(t)$ is the survival of juveniles to adulthood, and the functions $B\Big(T(t), A(t)\Big)$ and $D_X\Big(T(t), X(t)\Big)$, with $X = J, A$, describe the temperature- and density-dependence of per capita birth and mortality rates. The function $M_J(t)$ is the recruitment rate to the adult stage, which is the product of the recruitment rate into the juvenile stage $\tau(t)$ time units ago and the fraction of juveniles that survive to adulthood. The latter can be density-dependent if intra-specific competition affects juvenile mortality. The function $m_J(t)$ depicts variation in the juvenile maturation rate with time due to the temperature dependence of the juvenile developmental delay (τ). Note that vital rates are both temperature-dependent and time-dependent to accommodate trait responses to variable temperature regimes.

4.3 VIABILITY ANALYSIS UNDER CLIMATE WARMING

The most immediate application of the formalism described in the previous section is to evaluate the Feasibility ectotermos animal species in different projections heating. The viability of a species does not guarantee its persistence, which depends on the interaction with other species, but provides a threshold of extinction, which corresponds to abiotic conditions that do not allow survival of population. From a theoretical point of view, we study how the growth rate average of the population behaves in the absence of biotic factors such as competition intra - specific. Of course, viable populations have rate positive growth as opposed to non-viable populations.

4.3.1 *Climate warming scenarios*

It is expected that climate warming is manifested as an increase in annual mean temperature and amplitude of seasonal fluctuations (Change, 2007). We incorporate the climate warming as a linear increase in the average amplitude, i.e., $M_T(t) = M_{T0} + \gamma t$ and $A_T(t) = A_{T0} + \gamma t$, where M_{T0} and A_{T0} are the annual average temperature and amplitude of the typical seasonal fluctuations. The parameter γ is the daily rate the average and the amplitude increase with time. Thus, the temperature T is given by:

$$T(t) = M_T(t) - A_T(t)\cos\left(\frac{2\pi t}{\text{ano}}\right) , \tag{4.7}$$

We considered three climate warming scenarios: an increase of 0.03°, 0.05° and 0.1°C per year (Change, 2007).

4.3.2 *Model*

Mathematically, we will have a linear model which is characterized by an intrinsic growth rate r. This rate is similar to the Malthusian growth parameter, and, at a constant temperature, it can be calculated as the largest eigenvalue of the linear system, which takes into account all the life stages. In this case, it is well known that the distribution of stages (proportion of population in each stage) reaches a steady state (Kot, 2001). This result obviously is not true when the parameter values vary in time, as in the case of seasonal variations, however, by analogy, we expect a similar conclusion when the variation is periodic, in the sense that the stage distribution is also periodic. An additional problem happens when the seasonal variation is not perfectly periodic, but its average amplitude grows smoothly, as in climate warming scenarios.

We use the model described by equations 4.6 with B, D_J, D_A, and m_J depending only on temperature, not on density. To investigate whether ectotherm animal populations reach a stationary stage distribution under (i) a system with typical seasonal temperature variation and (ii) temperature disturbances caused by climate warming. These analysis are made by means of numerical investigations of the solutions for typical parameters of a species of Mediterranean climate of grasshopper.

4.3.3 *Results*

Constant environment

When the environmental temperature is constant, a population experiencing density-independent population dynamics 4.6 will attain a long-run per capita growth rate that depends on the environmental temperature, given by the largest eigenvalue of the linear system:

$$r(T) = -d_A(T) + \frac{1}{\tau(T)} W\left(b(T)\tau(T)e^{(d_A(T)-d_J(T))\tau(T)}\right) \tag{4.8}$$

and a ratio of juveniles and adults, corresponding to the eigenvector associated to the largest eigenvalue, that also depends on the environmental temperature:

$$\frac{J}{A}(T) = \frac{b(T)(1-e^{-(r(T)+d_J(T)\tau(T))})}{r(T)+d_A(T)} \tag{4.9}$$

Here, W is the principal (positive) branch of the Lambert W function or the product logarithm (Corless et al., 1996) and the functions

$$b(T),\ \tau(T) = \frac{1}{m(T)},\ d_X(T)\ (X = J, A) \tag{4.10}$$

depict the temperature responses of reproduction (Equation (4.3)), development (Equation (4.2)) and mortality (Equation (4.1)), as defined above.

The key point is that we can predict the long-run growth rate and the stable stage distribution achieved under a given temperature for any species for which data on the temperature responses of life-history traits are available.

The expression for r above is the same as that obtained from the Euler-Lotka equation:

$$\int_0^\infty b(a)e^{-r_m a}l(a)da = 1\ , \tag{4.11}$$

where $b(a)$ is the age-specific fecundity and $l(a)$ is the age-specific survivorship. In our model, for instance, we divided the population in two classes: juveniles, which do not reproduce ($b = 0$) and adults of constant fecundity. Since the death rates are linear, survivorship up to age a is simply $l(a) = e^{-da}$, but we have to take into account that juveniles and adults have different mortality rates – thus, $l(a) = e^{-d_J\tau - d_A(a-\tau)}$. The Euler-Lotka equation becomes, then:

$$\int_\tau^\infty be^{-r_m a}e^{-d_J\tau - d_A(a-\tau)}da = \frac{be^{-d_J\tau}e^{-r_m\tau}}{r_m + d_A} = 1\ , \tag{4.12}$$

whose solution for r_m is exactly Equation (4.8). However, the Euler-Lotka equation can be applied in general for any b and l functions, without the need to divide the population into classes and build a delay-differential equation model. On the other hand, it assumes that these functions do not change over time.

Seasonally varying, warming environment

In our analyses, we used parameter values for life-history traits that are realistic for insect species. Since temperature responses are conserved across taxa, thermodynamical constraints dictate that temperature sensitivity parameters such as Arrhenius constants take only a narrow range of values. Indeed, the theory on metabolic scaling (Gillooly et al., 2001, 2002; Brown et al., 2004; Savage et al., 2004) suggests that values of these temperature sensitivity parameters should be largely invariant across taxa. We used parameter values for seasonal temperature variation that represent Mediterranean or temperate environments. We did so because greater seasonal fluctuations in these environments allow for a greater portion of the temperature response functions to be expressed, thus allowing us to obtain a more complete understanding of how seasonal variation influences population dynamics. We use a time-scale of 100 years both because it provides a basis for comparison with previous studies that have used the Euler-Lotka framework to predict climate warming effects on population viability, e.g. (Deutsch et al., 2008), and because it provides sufficient time for a given species, particularly longer-lived ones, to attain a stationary age/stage distribution. Although we have not used parameter values specific to any particular species or seasonal environment, the model we have developed is general and can be parameterized with data for any ectotherm species inhabiting any habitat type or latitude.

When there is seasonal variation in the environmental temperature, $\frac{J}{A}$ achieves a stationary distribution relatively rapidly (within one year for a species with a developmental period of 60 days), as does the daily per capita growth rate. As a consequence, the mean annual per capita growth rate and $\frac{J}{A}$ remains constant across years. The rate of convergence to a stationary stage distribution depends on the relative magnitudes of birth, maturation and death rates, being faster if juvenile and adult mortality rates are low relative to birth and maturation rates.

The Figure 4.2 shows how the distribution of stages and the average growth rate, the mean or amplitude, evolve with the increasing of the temperature. After a period in which the heating increases the average growth rate, this rate decreases rapidly, reaching extinction in about 60 years in the case where the heating rate is $0.1^{\circ}C$ per year. These results, at a first look trivial, differ substantially from the average growth rate calculated using models that do not incorporate the

seasonal fluctuation, whose effect is particularly pronounced when the development time τ is relatively long. Thus, we provide a more robust metric to predict and compare the climate warming effects on a large class of organisms.

4.3.4 *Discussion*

Mounting evidence for climate warming makes it important that we be able to identify species that are at high risk of extinction due to warming. Recent studies have used the intrinsic growth rate calculated from the Euler-Lotka equation (r_m) as a metric for estimating population viability. The Euler-Lotka equation assumes a stable age/stage distribution in a constant environment, which is violated when the environmental temperature changes over time. In order to use r_m to estimate population viability under warming, we need to first establish that ectotherm populations can achieve a stationary age/stage distribution in thermally variable environments.

Here, we investigate this issue using a population model with temperature-dependent vital rates. This is, to our knowledge, the first time that mechanistically derived temperature responses of life-history traits (reproduction, development, mortality) have been incorporated into a population model that realistically captures the variability in time delays induced by temperature effects on development. We report two key findings. First, when there is seasonal variation in temperature, the stage distribution varies within the year but this intra-annual variation occurs in a predictable manner that remains constant between years. As a consequence, the per capita growth rate averaged over the year also remains constant between years.

This finding poses a key question: what mechanisms enable populations to converge to a stable stage distribution in the face of seasonal variation in temperature? The answer lies in the fact that life-history traits exhibit systematic and predictable responses to temperature variation, which, unless the environmental temperature varies in a completely unpredictable manner, will lead to predictable changes in vital rates and hence, population dynamics. The reason why life-history traits exhibit predictable responses to temperature is because temperature effects on the underlying biochemical processes (e.g. reaction kinetics, hormonal regulation) follow basic rules of thermodynamics (e.g. changes in entropy and enthalpy; (Johnson and Lewin, 1946; Sharpe and DeMichele, 1977; Schoolfield et al., 1981; Van der Have and De Jong, 1996; Ratkowsky et al., 2005). These thermodynamical properties define the lower and upper temperature thresholds below and above which reproduction and development cease. Beyond these thresholds, high mortality ensures that population growth is negative. As long as fluctuations in the environmental temperature occur within the thresholds set by the temperature tolerance of repro-

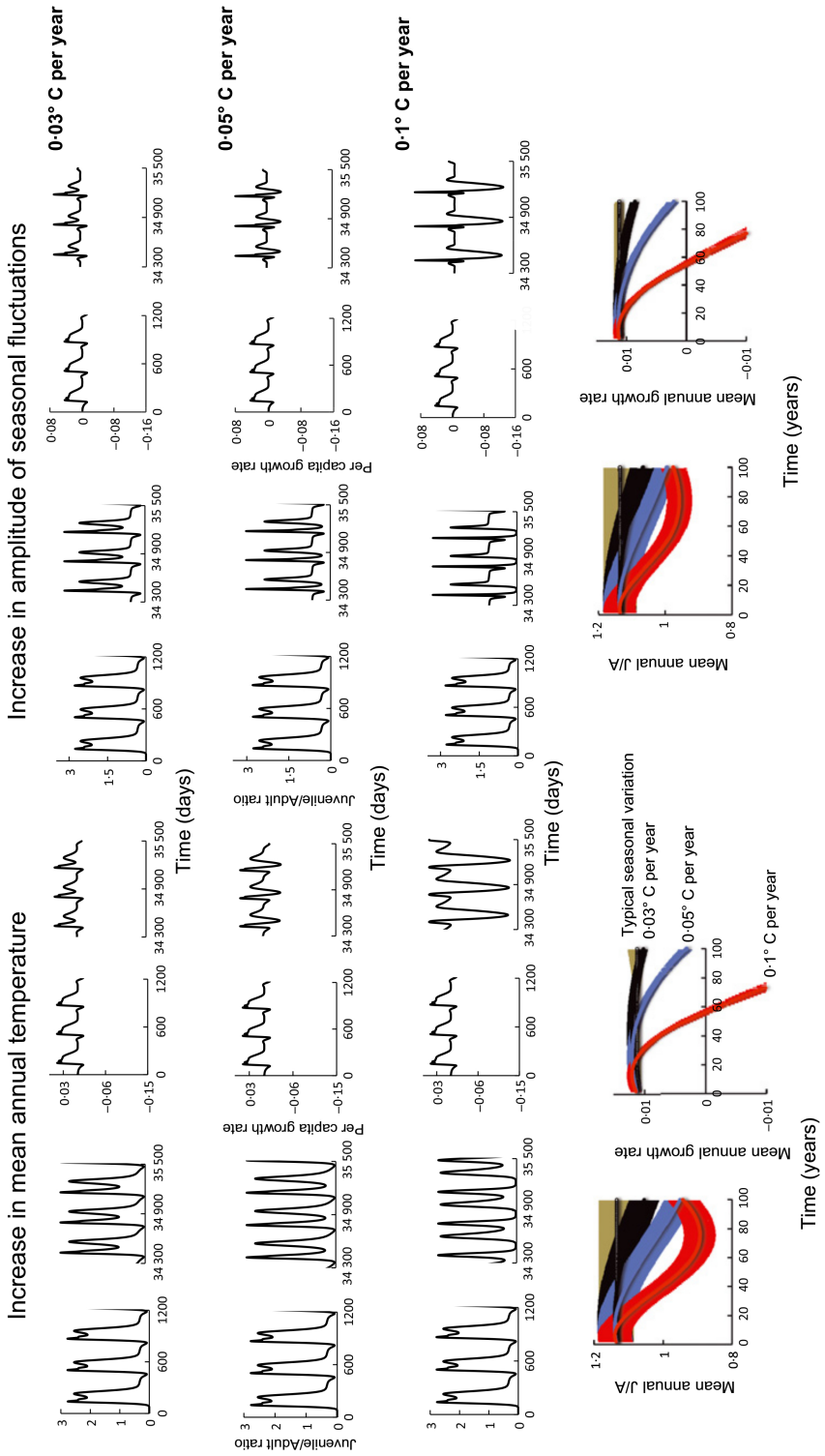

Figure 4.2: Solutions of the linear model 4.6, under the regime of increasing temperature. The first three lines show the effect of the warming under three different (0.03°, 0.05° e 0.1°C per year) on the stage distribution and on the growth rate *per capita*. The last line shows the average annual rate of $\frac{J}{A}$ and the average annual rate of the growth rate *per capita* under the three regimes and warming. The grey, black, blue and red lines correspond to, respectively, an increment of 0.03°, 0.05° and 0.1°C per year, and the error bar (standard deviation) represents the magnitude of the intra–annual variation in which year.

duction and development, the population will be viable and achieve a stationary stage distribution. The key implication is that r_m calculated from the Euler-Lotka equation does provide a valid representation of population growth under typical regimes of seasonal temperature variation.

This suggestion immediately leads to the question of whether r_m provides a realistic representation of population growth under perturbations to the typical thermal environment such as climate warming. We find that a stationary stage distribution can be achieved under climate warming, but only on relatively short (e.g. decadal) time-scales. Effects of warming on reproduction, development and mortality become compounded over time, causing a qualitative change in the stage distribution. Importantly, the time-scale over which this change occurs is the time-scale over which predictions based on r_m are valid. Temperature-induced changes in the stage distribution are informative about the error associated with using r_m to predict times to extinction. As warming proceeds, the amplitude and frequency of intra-annual fluctuations in the juvenile-to-adult ratio increase. The population model that accommodates these fluctuations predicts the mean annual per capita growth rate to decline and approach zero within 100 years when warming is slow relative to the developmental period of the organism (0.03 – 0.05°C per year) and to become negative, causing population extinction, well before 100 years when warming is fast (e.g. 0.1°C per year). The Euler-Lotka equation, which does not take intra-annual variation into account, predicts a slower decline in the intrinsic growth rate when warming is slow and a longer persistence time when warming is fast.

The degree of error associated with using r_m to predict times to extinction depends on both the rate of warming and the developmental period of the organism. Species with short developmental delays relative to warming rate are likely to exhibit longer time periods during which the mean annual r_m remains constant between years. For such species, r_m may be used to predict effects of climate warming on short time-scales (50–60 years) provided the rate of warming is slow (< 0.05°C per year). For ectotherms with long developmental delays, r_m is unlikely to be a reliable predictor of warming effects, even on a decadal time-scale.

Recent studies that have used r_m to predict extinction risk due to climate warming (Deutsch et al., 2008) find that tropical ectotherms, mainly insects, are more at risk of extinction due to climate warming than temperate ectotherms. Given that temperate ectotherms tend to have longer developmental delays than their tropical counterparts, r_m may underestimate their risk of extinction under climate warming. Whether tropical ectotherms remain more susceptible to climate warming than temperate ectotherms once the difference in their de-

velopmental delays is taken into account is an important question that needs to be addressed.

The appeal of using the intrinsic growth rate to estimate population viability lies the fact that it provides a common, an easily quantifiable, metric that applies across diverse ectotherm taxa and obviates the need for constructing explicit age-/stage-structured models of population dynamics for each species of interest, which is infeasible in most cases. A possible alternative to r_m that more accurately reflects the outcomes of population models is to use the temperature responses of life-history traits to compute the lower and upper temperature thresholds below and above which reproduction and development cease. These thresholds provide an estimate of the thermal limits below and above which a population cannot recover from low densities. Since the temperature responses of reproduction and development are driven by biochemical processes whose thermodynamical properties are well characterized and known to be conserved across ectothermic taxa (Johnson and Lewin, 1946; Sharpe and DeMichele, 1977; Schoolfield et al., 1981; Nijhout, 1994; Van der Have and De Jong, 1996; Huey and Berrigan, 2001; Van Der Have, 2002; Frazier et al., 2006; Kingsolver, 2009; Sunday et al., 2011; Kingsolver et al., 2011), they will yield predictions about thermal limits to viability that do not depend on assumptions about stationary age/stage distributions and the predictability of the thermal environment.

The framework we have developed focuses on how temperature variation influences ecological dynamics. It does not take into account the ability of organisms to adapt to changes in the thermal regime. Provided there is sufficient genetic variation in the reaction norms for fecundity, development and survivorship, there may be selection for phenotypes better able to withstand warmer temperature regimes. If thermal responses of life-history traits can evolve over the time-scale of climate warming which, again is more likely for organisms with faster generation times, times to extinction may be longer than that predicted based on ecological dynamics alone. Investigating how temperature responses of life-history traits evolve in the face of perturbations such as climate warming is a key research priority.

4.4 EFFECTS OF TEMPERATURE ON INTRASPECIFIC COMPETITION IN ECTOTHERMS

4.4.1 *Introduction*

It is well known that differential responses to temperature variation (e.g., through differences in emergence times or activity patterns) allow species to coexist by concentrating intra-specific competition relative to inter-specific competition (temporal niches; Chesson (2000)). However, we know little about the mechanisms by which temperature

effects on life history traits (reproduction, development, survivorship) translate into population-level responses. A mechanistic understanding of temperature effects at the level of individual traits is important not only because it allows us to identify the types of life history strategies and temperature regimes that facilitate or constrain species coexistence, but also because it allows us to predict how perturbations to typical thermal environments (e.g., climate warming) influence species diversity in natural communities and biological pest control in agricultural communities.

A trait-based framework for elucidating temperature effects on species interactions necessarily begins with intra-specific competition. This is because intra-specific competition is the major mechanism of negative density-dependent feedback that leads to population regulation, a critical prerequisite for species coexistence.

Empirical studies show that the effects of intraspecific competition on life-history traits is strongly temperature dependent (Ritchie, 1996; Reigada and Godoy, 2006; Nardoni Laws and Belovsky, 2010). However, theoretical work on temperature effects on species interactions has considered intraspecific competition to be temperature independent. For instance, Vasseur and McCann (2005) developed a bioenergetic consumer-resource model without age or stage structure, in which intraspecific competition in the resource species, the source of negative feedback that stabilizes the interaction, is temperature independent. Van de Wolfshaar et al. (2008) and Ohlberger et al. (2011) developed size-structured models that more realistically capture ectotherm life cycles, but they also assumed intraspecific competition in the resource species to be temperature independent. All of these previous studies considered constant thermal environments in which there is no diurnal or seasonal temperature variation. Despite the fact that ectotherms play key roles as resources, predators, parasites, and mutualists in virtually all communities, there is currently no theory that investigates how temperature effects on intraspecific competition influence ectotherm population dynamics in thermally variable environments.

Here we develop a trait-based mathematical framework for how temperature affects intra-specific competition. The novelty of our approach is its strong mechanistic basis. We start with a mechanistic description of temperature responses of life history traits derived from temperature effects on the underlying biochemical processes (e.g., reaction kinetics, enzyme inactivation). We incorporate these responses into population models, described by delay differential equations, that can realistically capture temperature effects on developmental delays. Our goal is to derive testable comparative predictions about how intra-specific competition affects life history traits that can guide empirical studies and inform theory on the conditions under which

the temperature dependence of intra-specific competition should be incorporated into studies of species interactions.

4.4.2 *Model analysis*

We investigate the equilibria and stability of Equation (4.6) under a constant thermal environment (i.e., the organism in question experiences the same temperature, on average, with few or no fluctuations around the mean). We also conduct numerical analyses of Equation (4.6) to understand how population dynamics are affected by seasonal temperature variation.

We incorporate seasonal temperature variation into the population model as $T = s(t)$ where T is the temperature in K, t is time in days, and $s(t)$ depicts seasonal temperature variation. Then

$$s(t) = M_T - A_T \cos\left(\frac{2\pi t}{\text{year}}\right), \tag{4.13}$$

where M_T is the mean annual temperature, A_T is the amplitude of seasonal temperature fluctuations within the year, and year $= 365$ days. We run the model for a period of 100 years and calculate long-term abundances, population variability (Coefficient of variation in abundance) and minimum population size over the last five years.

We analyze four cases along two axes of biological relevance. The first axis is the type of dynamics in the absence of temperature variation, which depends on the life history attributes of the species. Species with low lifetime fecundity and short developmental delays relative to adult longevity attain a stable equilibrium in the absence of temperature variation while species with high lifetime fecundity and long developmental delays relative to adult longevity exhibit delayed feedback cycles when intra-specific competition affects fecundity and single generation cycles when competition affects juvenile mortality (see (Murdoch et al., 2013) for a detailed description of cyclic behavior in delay models). When intra-specific competition affects adult mortality, the equilibrium is stable regardless of life history characteristics unless fecundity exhibits overcompensating density-dependence (Nisbet, 1997).

The second axis is the characteristics of the seasonal temperature regime. We consider two types of seasonal temperature regimes. The first is representative of a tropical habitat, with a mean habitat temperature close to the optimal temperature for reproduction and seasonal temperature fluctuations of low amplitude ($3 - 5°$). The second is representative of a Mediterranean/temperate habitat, with a mean habitat temperature well below the optimal temperature for reproduction and seasonal temperature fluctuations of high amplitude ($9 - 12°$). These values reflect the seasonal temperature regimes experienced by insect species at different latitudes. For instance, the

tropical pod-sucking bug *Clavigralla shadabi* from Benin (Dreyer and Baumgärtner, 1996) experiences a mean annual temperature of 27.2°C (SE = 0.09) and amplitude of seasonal fluctuations (difference between maximum and minimum monthly temperature) of 3.3°. The Mediterranean pod-sucking bug *Murgantia histrionica* in coastal southern California experiences a mean annual temperature of 17.2°C (SE = 0.28) and seasonal fluctuations of 9.5°. The pea aphid *Acyrthosiphon pisum* in eastern England experiences a mean habitat temperature of 9.75°C(SE = 0.41) and seasonal fluctuations of 12.0°. In what follows we focus on a tropical-Mediterranean comparison because ectotherms in these habitats have overlapping generations and can breed continuously, and hence continuous-time models are appropriate for depicting their life history.

4.4.3 *Results*

Effects of temperature and competition on life history traits

Temperature has both direct and indirect effects on life history traits. Direct effects arise from temperature effects on the underlying biochemical processes (e.g., reaction kinetics, enzyme inactivation), which cause birth and maturation rates to decline at both low and high temperatures (ceasing altogether as temperatures reach extreme levels) and the mortality rate to increase with increasing temperature (once temperatures exceed the lower limit for viability; Figure 4.3).

Temperature also affects life history traits indirectly through its effects on intra-specific competition: the decline in birth and maturation rates, and the increase in the mortality rate, with increasing density are now dependent on the environmental temperature. Importantly, the direct and indirect effects of temperature can have a strong impact at the same time or different times depending on the on the mechanism by which temperature affects competition.

When the strength of intra-specific competition increases monotonically with temperature, competition is strongest at temperatures that exceed the optimum for reproduction, at which the per capita birth rate is already declining due to the direct effects of temperature on fecundity. Hence the effects of temperature and competition act synergistically, causing a decrease in the upper temperature limit at which reproduction ceases, and an overall reduction in the birth rate, without altering the qualitative nature of the unimodal temperature response (Fig. 4.3a). A similar outcome is observed in the case of development (Fig. 4.3c). Because the per capita mortality rate increases monotonically with increasing temperature in the absence of competition, temperature effects on competition merely amplify this effect (Fig. 4.3e). The key point is that when the strength of competition increases with increasing temperature, effects of temperature and competition act synergistically to reinforce the decline in birth

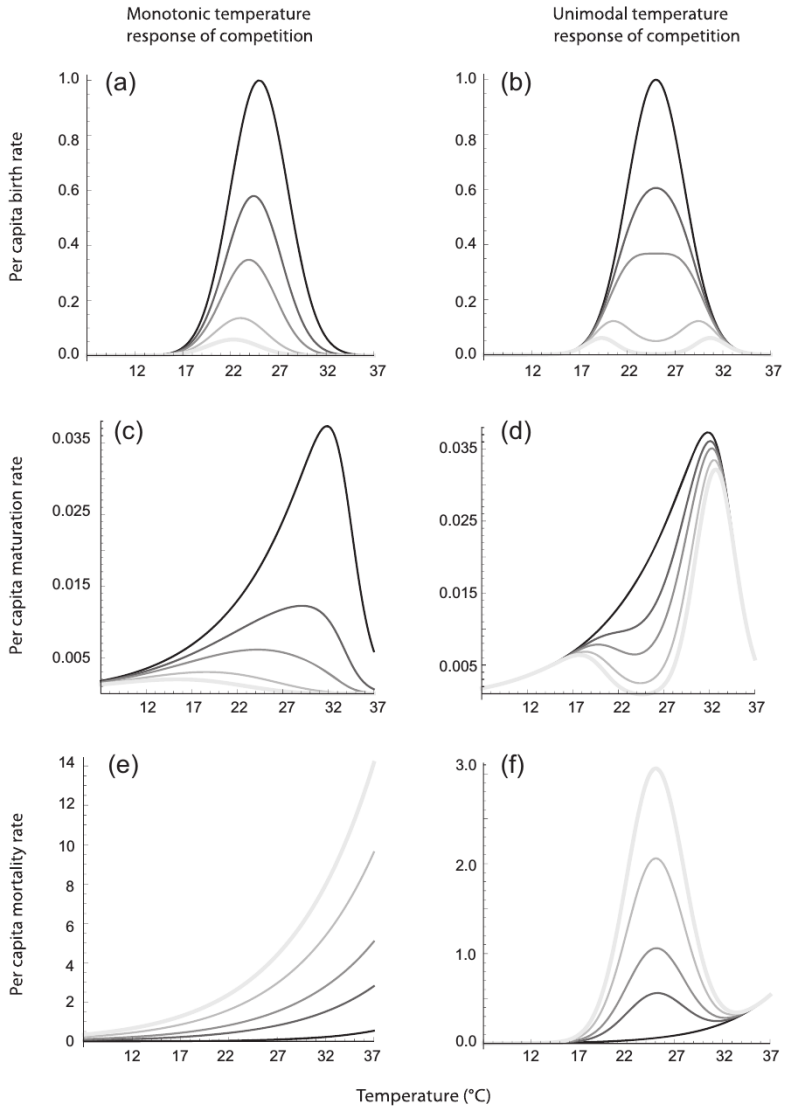

Figure 4.3: Effects of temperature and competition on per capita birth (panels a and b), maturation (panels c and d) and mortality rates (panels e and f) when the strength of intra-specific competition increases monotonically with increasing temperature (panels a, c, e) and when competition is strongest at temperatures optimal for reproduction (panels b, d, f). The dark solid line depicts the temperature response of the trait in the absence of competition, and the grey lines depict the temperature response in the presence of competition, with lighter lines reflecting higher density and hence a stronger competitive response; the population levels used are the same across all panels. Parameter values are: $b_{T_{opt}} = 1.0\text{day}^{-1}$, $T_{opt_b} = T_{opt_q} = 298\text{K}$, $s_b = s_q = 3.0$ for the birth rate, $T_R = 297\text{K}$, $m_{J_{T_R}} = 0.0167\text{day}^{-1}$ ($\tau_{J_{T_R}} = 60$ days), $q_{TR} = 0.2$, $A_m = 10500$, $T_{L/2} = 287\text{K}$, $A_L = -50000$, $T_{H/2} = 307\text{K}$, $A_H = 75000$ for the maturation rate, and $d_{T_R} = 0.02\text{day}^{-1}$, $A_d = 15000$ for the adult and juvenile mortality rates. These parameter values are representative of insect species (Sharpe and DeMichele, 1977; Schoolfield et al., 1981; Kooijman, 1993; Van der Have and De Jong, 1996). In order to facilitate comparisons between different temperature responses of competition, $q_{T_{opt}}$, the maximum value of the competition coefficient when the temperature response of competition is unimodal, was scaled by q_{TR}, the competition coefficient at the reference temperature when the temperature response of competition is monotonic such that $q_{T_{opt}} = q_{TR} e^{A_q \left(\frac{1}{T_R} - \frac{1}{T_{max}}\right)}$ where T_{max} is the maximum temperature experienced by the species calculated as $M_T + 0.5 * A_T$ with M_T and A_T depicting the mean annual temperature and amplitude of seasonal fluctuations.

and maturation rates, and the increase in the mortality rate, that occurs at high temperatures in the absence of competition.

When the strength of competition varies unimodally with temperature, competition is strongest at intermediate temperatures that are optimal for reproduction, at which birth and maturation rates are high and the mortality rate is low. Hence, the effects of temperature and competition act antagonistically, with direct effects of temperature causing birth and maturation rates to decline and mortality rates to increase during periods of low and high temperature extremes, and indirect effects of temperature (mediated via competition) causing birth and maturation rates to decline and mortality rates to increase at temperatures that are favorable to reproduction and development (Fig. 4.3). The key consequence of the antagonistic effects of temperature and competition is an increase in the non-linearity of temperature responses of life history traits. For instance, there is a qualitative change in the temperature response from unimodal to bimodal in the case of birth and maturation rates, and monotonic to unimodal in the case of the mortality rate (Fig. 4.3).

Effects of temperature and competition on population dynamics

CONSTANT THERMAL ENVIRONMENT

When environmental temperatures are constant, the stage-structured model (Equation (4.6)) yields analytical results on equilibrium abundance and stability. There are two key results to note. First, regardless of whether intra-specific competition affects fecundity, juvenile mortality or adult mortality, variation in equilibrium abundance with temperature is greater when competition is strongest at temperatures optimal for reproduction than when the strength of competition increases monotonically with increasing temperature; Figs. 4.4a-c). For instance, when competition affects fecundity and its temperature response is unimodal, equilibrium abundance shows a bimodal pattern with a large peak at low temperatures and a much smaller peak at high temperatures (Fig. 4.4a). This is because while competition is relaxed at higher temperatures, fecundity is lower and mortality is higher (recall that fecundity exhibits a unimodal temperature response while mortality exhibits a monotonic temperature response; Fig. 4.3), thus making for a smaller increase in abundance once temperatures exceed the optimal range for reproduction. A similar outcome is observed when competition affects juvenile mortality, since density-dependence in juvenile mortality reduces the number of juveniles maturing into adults and therefore adult abundance is lowest at intermediate temperatures at which competition is strongest. In this latter case, in contrast to the others, the relationship between the equilibrium juvenile and adult abundances is non-linear (see Appendix 4.A), which causes their maximum to be attained at different temperatures.

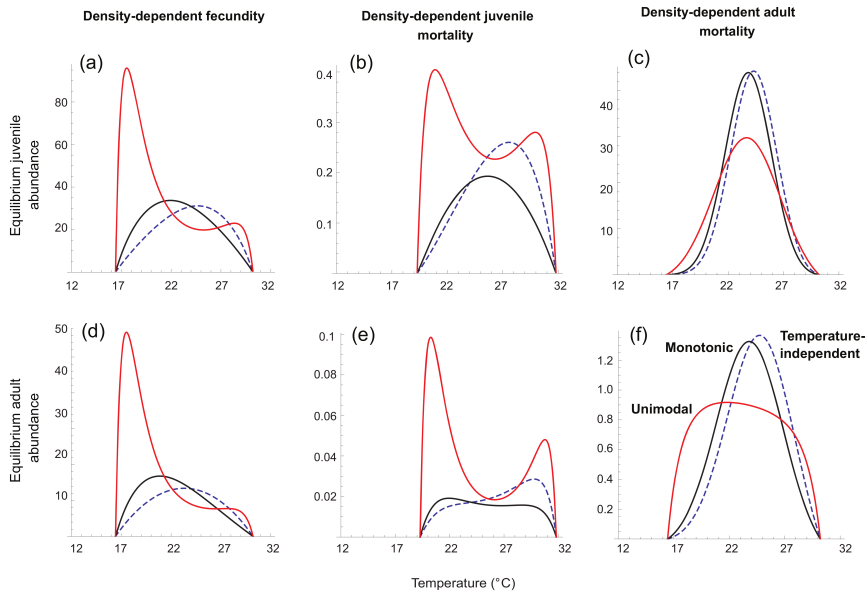

Figure 4.4: Equilibrium abundances of juveniles (panels a-c) and adults (panels d-f) in a constant thermal environment (Equation (4.6)). In all panels, the dashed line gives the outcomes when competition is temperature-independent, the black solid line, when competition strength increases with temperature and the red solid line, when competition is strongest at temperatures optimal for reproduction. Panels (a) and (d) depict equilibrium abundances as a function of temperature when intra-specific competition affects fecundity, panels (b) and (e), when competition affects juvenile mortality, and panels (c) and (f), when competition affects adult mortality. Parameter values are: $d_{J_{T_R}} = d_{A_{T_R}} = 0.02, A_{d_J} = 12000, A_{d_A} = 15000$. Other values are as in Fig. 4.3.

Second, the mechanism by which temperature affects competition determines the temperature at which equilibrium abundance reaches a maximum. When the temperature response of competition is unimodal, abundance is highest at temperatures below the optimum for reproduction regardless of whether it is fecundity or mortality that is affected by competition. This is because mortality is low at temperatures below the optimum for reproduction, at which competition is also weak. When the temperature response of competition is monotonic, abundance peaks at temperatures below the optimum for reproduction when competition affects fecundity or juvenile mortality, and at temperatures near the optimum for reproduction when competition affects adult mortality (Figs. 4.4a-c). The former outcome ensues because when the strength of competition increases with temperature, the upper temperature limit at which reproduction ceases is lowered, with a corresponding decrease in the temperature at which the birth rate is highest (Fig. 4.3a). The latter outcome ensues because increase in the adult mortality rate with increasing temperature is amplified when the temperature response of competition is monotonic (Fig. 4.3e), and reproduction is unconstrained by competition leading to higher abundances at the optimal temperature for reproduction. These results underscore the non-intuitive outcomes arising from the interplay between direct and indirect effects of temperature on life history traits, which could not have been elucidated without the aid of mechanistic mathematical theory.

SEASONALLY VARYING THERMAL ENVIRONMENT

Numerical analysis of the stage-structured model (Equation (4.6)) under seasonal temperature variation leads to three key insights. First, seasonal variation leads to qualitatively different long-term abundance patterns depending on the mechanism by which temperature affects competition: a unimodal temperature response of competition leads to more complex dynamics (greater increase in frequency and amplitude of population fluctuations) than a monotonic temperature response of competition, the nature of which changes depending on the life history trait affected by competition and the type of seasonal regime (tropical vs. Mediterranean/temperate) (Fig. 4.5). Second, intra-annual fluctuations in abundance when the temperature response of competition is monotonic are qualitatively similar to those observed when competition is temperature-independent. In contrast, intra-annual fluctuations when the temperature response of competition is unimodal are qualitatively different from those observed when competition is temperature-independent. Third, despite greater complexity of population dynamics, a unimodal temperature response of competition leads to a higher minimum population size than a monotonic temperature response (Fig. 4.6). Below we explain how these results come about.

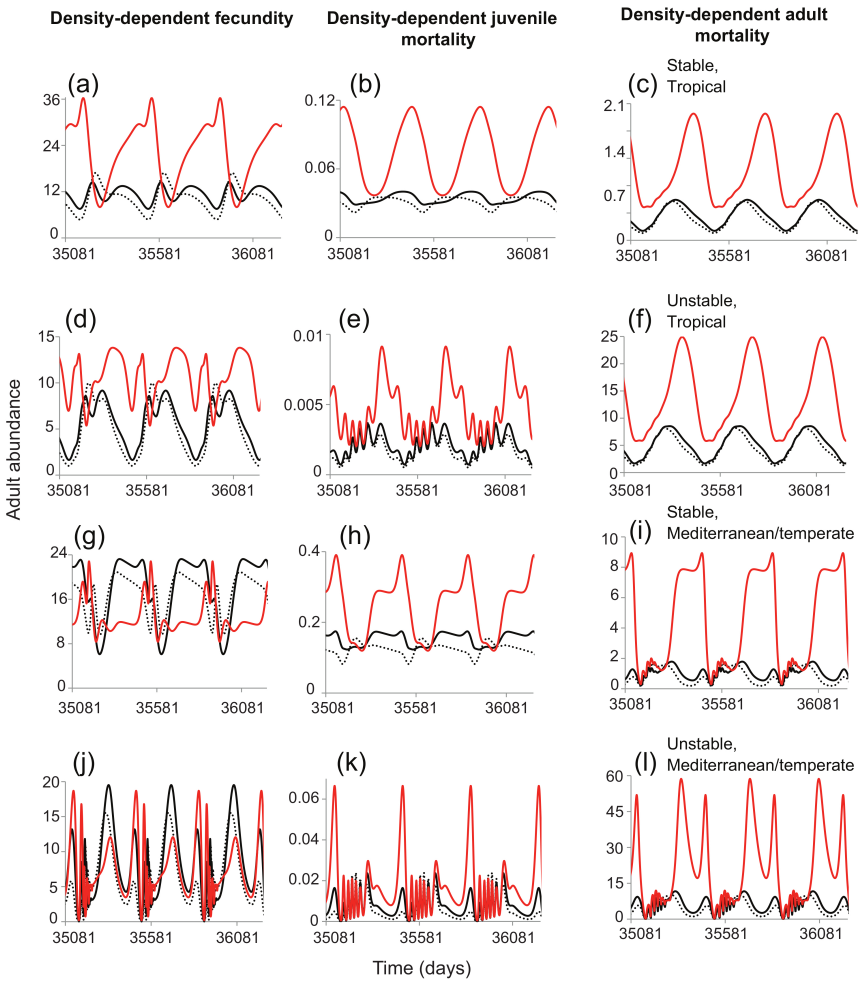

Figure 4.5: Long-term adult abundances in a seasonal environment for species that attain a stable equilibrium (panels a-c and g-i) or population cycles (panels d-f and j-l) in the absence of temperature variation and experience a tropical (panels a-f) or Mediterranean (panels g-l) temperature regime. In each panel, the dashed line depicts abundances when intra-specific competition is independent of temperature, the black solid line, when the temperature response of competition is monotonic and the red solid line, when the temperature response of competition is unimodal. For species experiencing stable dynamics in the absence of temperature variation, $b_{T_{opt}} = 1.0\text{day}^{-1}$, $d_{A_{T_R}} = 0.05\text{day}^{-1}$; for species experiencing unstable dynamics, $b_{T_{opt}} = 5.0\text{day}^{-1}$, $m_{J_{T_R}} = 0.0167\text{day}^{-1}$, $d_{J_{T_R}} = 0.005\text{day}^{-1}$, $d_{A_{T_R}} = 0.5\text{day}^{-1}$. Parameters for the tropical temperature regime are: $M_T = 27°$ C and $A_T = 3.0°$ and for the Mediterranean regime: $M_T = 17°$ C and $A_T = 9.0°$. Other parameters are as in Figs. 4.3 and 4.4.

When temperature affects life history traits but not competition, abundances decline at low and high temperatures because mortality exceeds reproduction and development. They also decline following periods of favorable temperatures for reproduction and development because an excess of birth and recruitment over deaths increases intraspecific competition. When temperature affects both life history traits and competition, the nature of temperature dependence of competition determines how this basic pattern is altered.

When competition is strongest at intermediate temperatures that are optimal for reproduction, intra-annual fluctuations are out of phase with those observed when competition is temperature-independent, with an increase in both the amplitude and frequency of fluctuations (Fig. 4.5). This is because extreme temperatures and strong competition reduce fecundity, development and survivorship at different times, thus increasing the non-linearities in life history traits' response to temperature and density. When the strength of competition increases monotonically with temperature, intra-annual fluctuations in abundance are in phase with those observed when competition is temperature-independent, with a small increase in the amplitude of fluctuations but no change in the frequency (Fig. 4.5). This is because extreme temperatures and strong competition reduce fecundity, development and survivorship at the same times, thus enhancing the existing non-linearities in the temperature responses of life history traits and the density response of the per capita growth rate. The only exception occurs when competition affects juvenile mortality of species that attain a stable equilibrium in the absence of temperature variation (Fig. 4.5, panels b and h). In this case a monotonic temperature response of competition leads to fluctuations that are out of phase with respect to the fluctuations generated by temperature-independent competition, but less so than when the temperature response of competition is unimodal (the degree to which fluctuations are out of phase can be quantified as the correlation between time series; Fig. 4.6.). This difference arises because the fluctuations in abundance are driven by the seasonal variation in temperature (recall that in a constant environment these species attain a stable equilibrium), and intra-specific competition affecting juvenile mortality leads to distinct temperature responses of the equilibrium adult and juvenile abundances (Fig. 4.4). The increase in non-linearity due to stronger seasonal fluctuations shifts the intra-annual relationship between adult and juvenile abundances even further, making it deviate from those under temperature-independent competition even when the temperature response of competition is monotonic.

Somewhat paradoxically, antagonistic effects of temperature and competition lead to more complex dynamics but a higher minimum population size. This is because competition is relaxed at temperatures above the optimum for reproduction causing abundances to in-

crease, which in turn buffers the subsequent decrease in abundance as temperatures decline. The strength of this buffering is determined by how strong the direct effects of temperature (decrease in the birth rate and increase in the mortality rate at temperatures above the optimum) oppose the indirect effects (weaker competition at higher temperatures due to a unimodal temperature response of competition). Species in which the increase in the mortality rate at high temperatures is lower than the decrease in birth rate and the upper temperature limit for viability is high relative to the temperature optimum for reproduction (i.e., greater tolerance of high temperatures) are likely to exhibit a stronger buffering effect.

4.4.4 *Discussion*

We have presented a trait-based mathematical framework for elucidating the mechanisms by which temperature affects intra-specific competition. This framework leads to testable comparative predictions about how intra-specific competition affects reproduction, development and mortality under alternative hypotheses about the temperature dependence of competition. It identifies the conditions under which temperature dependence of intra-specific competition yields population dynamics that are qualitatively different from those observed when competition is temperature-independent.

The novelty of our approach is its strong mechanistic basis, which leads to insights that could not otherwise have been obtained. For instance, we find that the interplay between direct and indirect effects of temperature on life history traits can have qualitatively different effects on population dynamics depending on the mechanism by which temperature affects competition. Direct effects arise from temperature effects on biochemical processes (e.g., reaction kinetics, enzyme inactivation) that underlie the temperature responses of fecundity, development and survivorship, which can be derived from first principles using thermodynamical rate process models Johnson and Lewin (1946); Sharpe and DeMichele (1977); Schoolfield et al. (1981); Van der Have and De Jong (1996); Van Der Have (2002); Ratkowsky et al. (2005). Indirect effects arise from temperature effects on life history traits' response to density, which can be quantified using competition experiments conducted at different temperatures. When the strength of competition increases monotonically with temperature, direct and indirect effects of temperature act synergistically; when competition is strongest at temperatures optimal for reproduction, direct and indirect effects act antagonistically. Antagonistic effects increase the non-linearity in the trait responses to temperature and density, leading to an increase in the frequency and/or amplitude of intra-annual fluctuations. In contrast, synergistic effects enhance existing non-linearities in trait responses, leading to a small increase in the

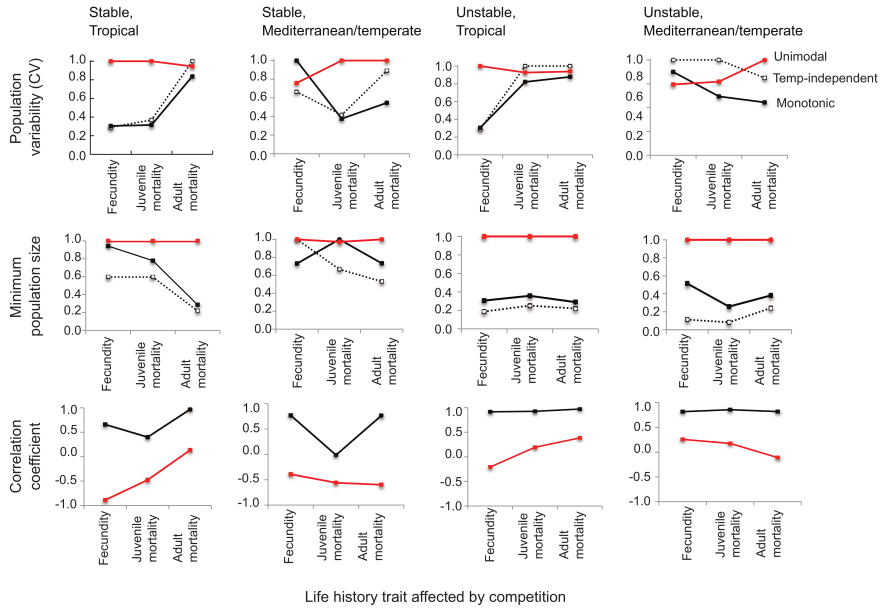

Figure 4.6: Population variability (quantified as the CV of population abundances; first row), minimum population size (second row) and the deviations of intra-annual fluctuations under temperature-dependent competition from those under temperature-independent competition (quantified as the correlation coefficient between time series of adult abundances; third row). The first two columns depict, respectively, these metrics for a species that attain a stable equilibrium in the absence of temperature variation, and the last two columns, for a species that attains population cycles in the absence of temperature variation. Each species experiences a tropical (first and third columns) or Mediterranean (second and fourth columns) temperature regime. In all panels of the first two rows, the dashed line depicts temperature-independent competition, the black solid line, a monotonic temperature response of competition, and the red line, a unimodal temperature response of competition. In panels of the third row, the black line gives the correlation coefficient between time series of abundances (for the last five years of a 100 year run) when competition is temperature independent and when the temperature response is monotonic and the red line, when the temperature response is unimodal. In all panels lines are drawn for ease of visual comparison. Note that when the temperature response of competition is monotonic, population dynamics are in phase with those observed under temperature-independent competition (as indicated by a statistically significant positive correlation; $n = 365, p < 0.005$) but when the temperature response of competition is unimodal, dynamics are out of phase (as indicated by a smaller positive or negative correlation; $n = 365, p < 0.005$). Parameter values used are as in Figs. 4.4 and 4.5.

amplitude of fluctuations without altering the frequency. Counter to intuition, antagonistic effects of temperature and competition lead to a higher minimum population size than synergistic effects, despite the greater tendency for complex dynamics.

These results have important implications for future work. The lack of empirical data on the temperature dependence of intra-specific competition has necessitated theoretical studies to assume that intra-specific competition is temperature-independent (e.g., Savage et al. (2004); Vasseur and McCann (2005)). An important contribution of our work is in identifying the conditions under which temperature dependence of competition should be incorporated into studies of temperature effects on species interactions. We find that intra-annual fluctuations in abundance are qualitatively similar to, and in phase with, those observed when intra-specific competition is independent of temperature when the temperature response of competition is monotonic but not when it is unimodal. Even when the temperature response of competition is monotonic, the degree to which intra-annual fluctuations deviate from those under temperature-independent competition depends on the life history trait affected by competition and the characteristics of the temperature regime experienced by the species. While the assumption that self-limitation is temperature-independent may be reasonable for species in which competition affects fecundity and/or adult mortality and the strength of competition increases with increasing temperature, it may not be reasonable when (i) competition affects juvenile mortality in species that experience a Mediterranean or temperate temperature regime and in which and (ii) when the temperature response of competition is unimodal regardless of the seasonal temperature regime. This finding is particularly important for theoretical investigations of climate warming effects on consumer-resource interactions. Whether warming increases the amplitude of consumer-resource fluctuations that predispose species to stochastic extinction during periods of low abundances will depend crucially on whether self-limitation in resource species, typically the source of negative density-dependence that enables stable consumer-resource coexistence (i.e., at a point attractor; (Nisbet, 1997; Murdoch et al., 2013)), increases with increasing temperature or peaks at intermediate temperatures.

The above findings underscore the urgent need for experimental studies that investigate temperature effects on competition. A second important contribution of our work is in providing testable comparative predictions about the joint effects of temperature and competition on life history traits, which can be tested via controlled experiments. For instance, temperature effects on the strength of intra-specific competition (the parameter q) can be measured by conducting competition experiments at a series of temperatures and using linear or non-linear regression to estimate q as the slope of the relationship between

per capita birth/maturation/mortality rate and density. Values of q thus estimated at a series of temperatures constitute the temperature response of competition for a given life history trait. If temperature effects on competition affect life history traits in the way hypothesized by metabolic scaling or ecological theory, experimentally quantified temperature responses should provide a significant fit to the predicted temperature responses under monotonic (Equation (4.4)) or unimodal (Equation 4.5)) temperature responses of competition (Fig. 4.3). Because the theory makes comparative predictions under alternative hypotheses, experiments can not only quantify the joint effects of temperature and competition, but also identify the mechanisms by which temperature affects competition.

Our framework also provides guidelines for investigating temperature effects on population dynamics using time series data. Depending on the mechanism by which temperature affects competition, long-term abundances exhibit qualitatively different patterns, the nature of which also depends on the life history trait affected by competition and the type of seasonal temperature regime. Thus, our theory predicts distinctive signatures of abundance patterns that statistical methods could potentially detect in real time series data. The model we have developed provides a general representation of ectotherm life cycles that can be modified to incorporate more complex forms of stage-structure. If data on the temperature responses of life history traits and competition are available, the model can be parameterized and its output compared with independent time series data from experiments or field observations. Even if data are unavailable to parameterize a model, statistical analyses could be used to detect the existence of signatures in time series data that are consistent with particular combinations of temperature responses and seasonal temperature regimes.

A particular advantage of the predictions emerging from our framework is their utility for comparative studies of temperature effects on multiple species within a community or the same species in different habitats. Such studies are particularly important in assessing which combinations of life history traits and density responses make species more or less vulnerable to perturbations such as climate warming and in determining the ability of natural enemy species with complementary action to continue to achieve high pest suppression in the face of warming.

In conclusion, our study constitutes a first step in investigating the effects of temperature variation on intra-specific competition in ectotherms. It is intended to provide a predictive framework for future empirical studies on the temperature effects on competition, and a mechanistic basis for future theoretical studies on temperature effects on population dynamics and species interactions.

4.A APPENDIX. LONG-TERM OUTCOMES OF THE STAGE-STRUCTURED VARIABLE DELAY MODEL IN A CONSTANT THERMAL ENVIRONMENT

Intra-specific competition affects fecundity

When intra-specific competition affects fecundity, the per capita birth rate is a decreasing function of density. In a constant thermal environment (i.e., the species experiences the same temperature, on average, over the year), this gives us the following version of Equation (4.6) :

$$\begin{aligned}\frac{dJ(t)}{dt} &= b(T)A(t)e^{-q(T)A(t)} - M_J(t) - d_J(T)J(t)\\ \frac{dA(t)}{dt} &= M_J(t) - d_A(T)A(t)\\ M_J(t) &= b(T)A(t-\tau(T))e^{-q(T)A(t-\tau(T))}e^{-d_J(T)\tau(T)}\end{aligned} \tag{4.14}$$

where the functions $b(T)$, $d_X(T)(X = J, A)$ and $M_J(t)$ depict the density-independent rates of per capita birth, mortality, and recruitment to adult stage at temperature T. Notice that, since development and juvenile mortality rates are no longer time- or density-dependant, development time τ and juvenile survival rate S (equal to, respectively, $e^{-d_J(T)\tau(T)}$ and $\frac{1}{m_J(T)}$) do not change over time, so they become simply constants, instead of state variables.

At equilibrium $\frac{dJ(t)}{dt} = 0$, $\frac{dA(t)}{dt} = 0$, and $J(t) = J(t-\tau(T)) = J^\star$ and $A(t) = A(t-\tau(T)) = A^\star$. The non-trivial equilibrium is given by $J^\star = \frac{d_A(T)\left[\exp\left(\frac{d_J(T)}{m_J(T)}\right)-1\right]\left[\ln\left(\frac{b(T)}{d_A(T)}\right)-\frac{d_J(T)}{m_J(T)}\right]}{d_J(T)q(T)}$ and $A^\star = \frac{\ln\left(\frac{b(T)}{d_A(T)}\right)-\frac{d_J(T)}{m_J(T)}}{q(T)}$. Note that the developmental delay is expressed in terms of the maturation rate, i.e., $\tau(T) = \frac{1}{m_J(T)}$. Figures 4.4(a) and (d) depict the effects of temperature on equilibrium abundance.

As is characteristic of single species models with fixed time delays (Nisbet and Gurney, 1983; Murdoch et al., 2013), the equilibrium is a function of the strength of competition ($q(T)$) but the stability of the equilibrium is not. The local stability criterion, determined by the dominant eigenvalue derived from the characteristic equation of Equation (4.14) around the above equilibrium (Gurney et al., 1980), is $\tau(T) < \frac{\cos^{-1}[(1-q(T)A^*)^{-1}]}{d(T)\sqrt{(1-q(T)A^*)^2-1}}$. As can be seen, stability is driven by the temperature responses of birth, maturation and mortality rates.

Intra-specific competition affects juvenile mortality

When intra-specific competition affects juvenile mortality in a constant thermal environment we have the following version of Equation (4.6) :

$$\begin{aligned}\frac{dJ(t)}{dt} &= b(T)A(t) - M_J(t) - \Big(d_J(T) + q(T)J(t)\Big)J(t)\\ \frac{dA(t)}{dt} &= M_J(t) - d_A(T)A(t)\\ M_J(t) &= b(T)A(t-\tau(T))e^{-\int_{t-\tau(T)}^{t}\left(q(T)J(x)+d_J(T)\right)dx}\end{aligned} \tag{4.15}$$

The non-trivial equilibrium is: $J^\star = \frac{m_J(T)\ln\frac{b(T)}{d_A(T)} - d_J(T)}{q(T)}$, $A^\star = \frac{(d_J(T)+q(T)J^\star)J^\star}{b(T)-d_A(T)}$. Figures 4.4(b) and (e) depict the effects of temperature on equilibrium abundance.

Intra-specific competition affects adult mortality

When intra-specific competition affects adult mortality in a constant thermal environment we have the following version of Equation (4.6):

$$\begin{aligned}\frac{dJ(t)}{dt} &= b(T)A(t) - M_J(t) - d_J(T)J(t)\\ \frac{dA(t)}{dt} &= M_J(t) - \Big(q(T)A(t) + d_A(T)\Big)A(t)\\ M_J(t) &= b(T)A(t-\tau(T))e^{-d_J(T)\tau(T)}\end{aligned} \tag{4.16}$$

with the non-trivial equilibrium $J^\star = \frac{b(T)A^\star\left(1-e^{-d_J(T)\tau(T)}\right)}{d_J(T)}$, $A^\star = \frac{b(T)e^{d_J(T)\tau(T)} - d_A(T)}{q(T)}$. Figures 4.4(c) and (f) depict the effects of temperature on equilibrium abundance. The equilibrium is stable if

$$\tau(T) < \frac{\cos^{-1}\left[\frac{d_A(T)+2q(T)A^*}{b(T)e^{-d_J(T)\tau(T)}}\right]}{\sqrt{(b(T)e^{-d_J(T)\tau(T)})^2 - (d_A(T)+2q(T)A^*)^2}}$$

.

Murdoch et al. (2013) provide a detailed, and accessible, derivation of the fixed delay models and Nisbet and Gurney (1983) provide the formalism for delay models with variable instar duration driven by time-dependent maturation rates.

5

TRAIT DYNAMICS IN INTERACTING POPULATIONS

This chapter portrays the work done in close collaboration with Toni Klauschies, Ph.D. student at the Ecology and Ecosystem Modelling research group of the Institute of Biochemistry and Biology of the University of Potsdam, and Ursula Gaedke, professor and head of the group. I worked in the University of Potsdam from September 2012 to August 2013 as part of a so-called Sandwich Fellowship, in which the student spends one year of his Ph.D. abroad. The work presented here is still unpublished, but many interesting results have been found, and a manuscript is in the process of submission.

5.1 INTRODUCTION

Ecological theory frequently assumes that each species possesses definite characteristics, even if average or approximate, which are translated into fixed parameters in mathematical models. This hypothesis is related to the separation of ecological and evolutionary time scales, supposed to be several orders of magnitude apart, which allows one to neglect evolutionary processes when studying ecological dynamics.

This picture has been overturned in the last decade (Yoshida et al., 2003; Hiltunen et al., 2014) by empirical and theoretical studies that demonstrated rapid evolution, where population functional traits change in the same time scale as ecological dynamics, affecting and being affected by it. In that situation, it is no longer possible to neglect the variation in species' characteristics, either between individuals that compose the population or over time.

Recently, it has been shown that predator-prey systems can exhibit recurrent rapid evolution Becks et al. (2012); Tirok and Gaedke (2010), engendered by the coupling of such rapid evolutionary processes to ecological dynamics, leading to feedback loops, in which changes in populations' biomasses lead to shifts in trait frequencies, which in turn affect population oscillations.

Current theory on functionally diverse populations and communities can be broadly divided into two classes of models. The first, along the lines of traditional community ecology, considers multispecies ensembles, where each species is assigned a fixed trait value, and evolution proceeds through species sorting, that is, changes in community composition are the sole responsible for changes in trait composition.

The second class of models, sometimes called gradient dynamics models, or aggregate models, are analogous to quantitative genetics models, in the sense that the ecological community is a single entity (i.e. a single population), and hypotheses are made about the distribution of traits and how it evolves over time, given ecological constraints (e.g. predator abundance, environmental stress, competition) that may or may not be changing simultaneously. Usually, under this approach functional traits are characterized by their mean and variance, and additional simplifying hypotheses are employed to model the latter.

Both approaches share a fundamental assumption about how the community is structured: all organisms have constraints, and therefore investment in any advantageous trait has to de-emphasize investment in other traits, leading to trade-offs between traits. For instance, production of defensive structures makes prey less vulnerable to predation, but reduces its growth rate. As central as the trade-off is, very little is known yet about the shape these trade-offs take on in natural or even artificial systems.

The two approaches have, however, complementary drawbacks. Multi-species systems require *a priori* knowledge of the community composition, that is, which trait values can be attained, what in practical terms makes its use cumbersome when individual organisms do not have such limitation (i.e. when intra-specific variation is high), so that the community may end up in a state that the model is unable to describe. Aggregate models deal with this issue in a very elegant fashion, requiring information only about the shape of the trade-off. On the other hand, their assumptions render them unable to describe scenarios where the community splits into more than one "cluster" (perhaps due to disruptive evolution) leading to bi-modal, or multi-modal, trait distributions, since this kind of distribution cannot be well approximated only by its mean and variance.

In this study we develop a novel theoretical framework which generalizes current theory by describing how the entire trait distribution of communities evolve in time. Though increasing considerably the model complexity, this choice attempts to overcome the limitations of both types of models identified above. As in other models, we consider a system where prey organisms vary in their intrinsic growth rates and vulnerabilities to predation, while predators differ in respect to their prey selectivity and maximum grazing rate. We consider functional traits instead of species, conflating intra- and inter-specific variation, what confers to this approach its great generality, since it does not restrict the possible trait values, as the shape of the trait distribution at each trophic level is not predefined but evolves continuously. We also assume trade-offs between the traits, i.e. between growth rates and defence against predators, and between predator selectivity and maximum grazing rate.

5.2 MODEL

Building upon the classical Rosenzweig-MacArthur predator–prey model (Rosenzweig and MacArthur, 1963) and its modification to multiple resource types (Murdoch, 1973), we consider a prey community that has a shared carrying capacity, K, and is grazed upon by a predator community. Each predator species has a distinct grazing rate on each prey species, determined by the functional traits of both trophic levels: prey can be more or less susceptible to predation (higher or lower edibility, ϕ), but suffer from a trade-off on their growth rates, that becomes smaller the lower their edibility is. Predators can be more or less selective (higher or lower selectivity, ω), and also have a trade-off, with a respectively lower or higher half-saturation rate (M). These trade-offs have the form expressed in Eq. (5.3).

We use a type II functional response (Holling, 1965) and a very small immigration rate for both prey and predator, which does not affect the dynamics considerably, but prevents complete exclusion of any single trait in the continuous framework (what is necessary since we do not include mutation) and prevents variance from becoming exactly zero in the gradient dynamics framework.

We can describe the change in prey (A) and predator (C) communities' biomasses by the set of equations:

$$\begin{aligned}\frac{dA(\phi)}{dt} &= (r(\phi) + B(\phi))\,A(\phi) - \overbrace{\int g(\phi,\omega)C(\omega)d\omega}^{\text{total consumption by predators}} + I_A \\ \frac{dC(\omega)}{dt} &= C(\omega)\left(e\underbrace{\int g(\phi,\omega)d\phi}_{\text{total prey grazed}} - d + B(\omega)\right) + I_C\ ,\end{aligned} \tag{5.1}$$

where d is the predator mortality rate, e is the conversion efficiency, I_A and I_C are the prey and predator immigration rates, respectively. The function B is introduced when we need to make close parallels between this model and the aggregate model we derive from it – it is a function that is close to zero between 0 and 1, being negligible in most of the range, but decreases quickly close to the border, precluding

species with traits larger than 1 or smaller than 0 to grow. The prey growth rate r and the grazing rate g are given by:

$$\begin{aligned} r(\phi) &= r'(\phi)\left(1 - \underbrace{\frac{\int A(\phi')d\phi'}{K}}_{\substack{\text{intra-community}\\ \text{competition}}}\right) \\ B(x) &= -\left(e^{-wx} + e^{w(x-1)}\right) \\ g(\phi,\omega) &= g_m \frac{q(\phi,\omega)A(\phi)}{M(\omega) + \underbrace{\int q(\phi',\omega)A(\phi')d\phi'}_{\text{sum over all prey}}} . \end{aligned} \tag{5.2}$$

In the equations above, the index ϕ' was used to denote that the integration is done over all prey species, independent of ϕ, that is, of which species' growth rate is calculated. Table 5.1 contains detailed descriptions of the parameters used, as well as typical values for a system of phytoplankton and ciliates. Although the model is general, it is inspired by plankton communities, so we chose to perform the analyses with parameters typical for such systems, where cell or body sizes increase with trophic level and so, by allometry, weight-specific rates decrease with trophic level. The initial conditions chosen were such that the total biomass in each trophic level is 1 $gC\,m^{-2}$ and traits are distributed normally around 0.5. At each instant in time, the model yields the community biomass density as a function of the functional traits. In order to obtain an actual biomass value, we integrate over a range of trait values.

In our model, the traits edibility (ϕ) and selectivity (ω), with values ranging from 0 to 1, determine maximum growth rates (r'), half-saturation constants (M), and grazing preferences (q). For convenience and ease of comparison, the relations between traits were chosen in the same way as in the works by Tirok et al. (Tirok and Gaedke, 2010; Tirok et al., 2011), and their shapes can be seen in Figure 5.6. Due to energy constraints, we assume at first that the maximum growth rate, r', increases linearly with edibility, ϕ, with a minimum value of r_0 and ratio between the maximum and minimum values of m_r. Hence, fast growing prey species are highly vulnerable to grazing and vice-versa. The half-saturation constant M also varies linearly with selectivity, attaining its maximum for the least selective species, for which $M = M_{max}$, while the most selective species has a half saturation constant m_M times smaller. Hence, high food selectivity is connected with the ability to maintain positive net growth at low prey densities. The preference function $q(\phi,\omega)$ is such that all predators have a high preference for perfectly edible prey ($\phi = 1$), while prey of intermediate edibility (e.g. $\phi = 0.5$) will be grazed upon mostly by predators of intermediate to low selectivity ($\omega < 0.5$), and totally inedible prey

Table 5.1: Description and values of parameters used.

Symbol	Description	Value	Unit
K	prey carrying capacity	10	$g\,C\,m^{-2}$
r_0	minimum prey growth rate	0.25	day^{-1}
m_r	ratio between maximum and minimum growth rate minus one	7	-
d	predator mortality rate	0.15	day^{-1}
e	predator growth efficiency	0.2	-
g_m	weight specific maximum grazing rate	2	day^{-1}
M_{max}	maximum half-saturation constant for grazing	8	$g\,C\,m^{-2}$
m_M	one minus ratio between minimum and maximum half-saturation constant	0.875	-
b	trade-off exponent for sharpness of the predator preference q	6	-
c	trade-off coefficient relating ϕ and ω in the preference q	0.9	-
I_A	prey immigration rate	0.001	$g\,C\,m^{-2}day^{-1}$
I_C	predator immigration rate	0.0002	$g\,C\,m^{-2}day^{-1}$

($\phi = 0$) will be grazed only by the completely non-selective predators ($\omega = 0$), as illustrated in Figure 5.1. The parameter c determines for which range of values of edibility ϕ the predators will have high preference – the range generally will be smaller for higher c. Parameter b determines how sharp is the transition of values of q from non-preferred to preferred prey: higher values of b lead to sharper transitions. The explicit expressions of the trade-off relations are given by:

$$\begin{aligned} r'(\phi) &= r_0(1 + m_r\phi) \\ M(\omega) &= M_{max}(1 - m_M\omega) \\ q(\phi, \omega) &= \frac{1}{1 + \exp\left(-b(\phi - c\omega)\right)} \, . \end{aligned} \tag{5.3}$$

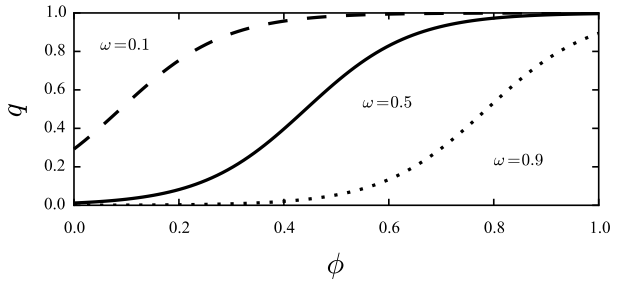

Figure 5.1: Prey edibility ϕ and predator selectivity ω values interact to determine the preference function q: non-selective predators (top curve, low ω) are able to prey efficiently on a wider range of prey, while high-selectivity ones (bottom curve, high ω) graze almost exclusively on highly edible prey (i.e., with ϕ close to 1).

In building this model, we assume a strictly trait–based approach, where organisms are characterized exclusively by their trait values. Furthermore, the model assumes that all individuals beget only new individuals with exactly the same trait value. This is in line with communities predominantly composed by asexually reproducing unicellular organisms or small metazoans, such as rotifers and cladocerans, often dominating freshwater plankton.

Solutions of Equations (5.1-5.3) yield the density along the trait axis of each community as it changes with time. An example is provided in Figure 5.2: in the left panel we see the total community biomasses integrated over all trait values in the top, with the trait distributions in the two bottom panels, changing with time. At each instant, the community trait composition takes a different shape, as shown in the right panel for six different times. At the time labeled (a) in Figure 5.2, total prey biomass is high, with a predominance of prey of low edibility, while predator biomass is low, with its selectivity decreasing in response to a low prey edibility. With the increase of biomass of low selectivity predators at instant (b), prey biomass begins to decline, even as prey of intermediate and high edibility grow. In response to

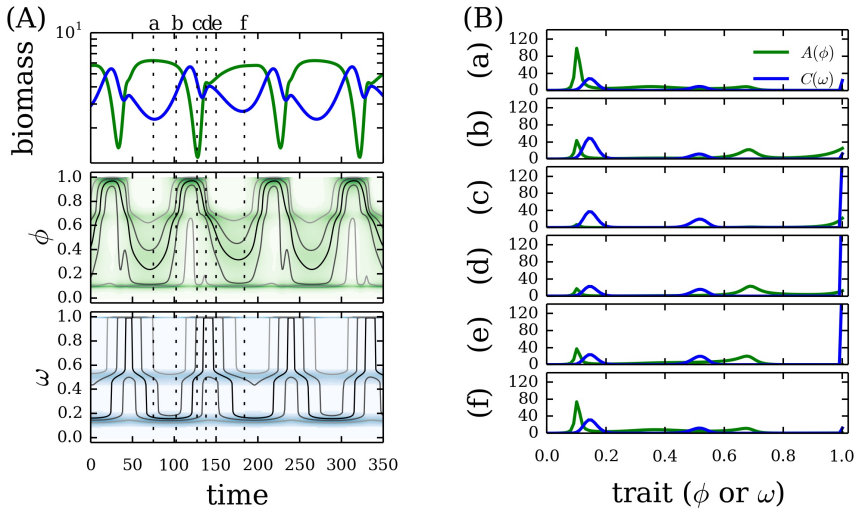

Figure 5.2: **Left.** Top panel shows the total biomass of prey (green) and predator (blue). The two panels below show the distribution of prey edibility, ϕ, and predator selectivity, ω, as a function of time, with dark blue indicating low frequency in the population, and lighter tones followed by yellow and red denoting high frequency of that value. Drawn in continuous gray line is the biomass-weighted average trait value, and in thin black lines are the 10, 30, 50, 70 and 90% percentiles trait percentiles, that is, the trait below which 10% (and 30, 50%, etc.) of the total biomass is found. The vertical dotted lines correspond to the times referred to in the text. **Right.** Sequence of snapshots of the trait distribution of prey (biomass density as a function of edibility, ϕ, in green), and predator (biomass density as a function of selectivity, ω, in blue). The snapshots correspond to the times labeled in the left figure.

that, predators of higher selectivity also increase, leading to a three-peaked distribution of high biomass of predators at instant (c), while prey biomass reaches its lowest level and is dominated by highly edible prey. At instant (d) the prey community recovers due to reduced predator biomass, with intermediate and low edibility prey increasing again, while predator selectivity is still high. At instant (e), prey biomass comes close to the carrying capacity, being composed mostly of low and intermediate edibility species, and now the predator community begins to respond by decreasing its selectivity. It does so very slowly, since the remaining biomass of generalist species is low, and they grow slower than the highly selective ones. Finally, at time (f), prey still has high biomass and low edibility, but predators finally catch up, with low selectivity species becoming the most abundant. From then on the overall pattern is repeated.

Moreover, we see in Figure 5.2 that the predator–prey cycles are out-of-phase, instead of having the quarter-cycle lag of the usual predator-prey dynamics. Those cycles have been shown to be characteristic of eco–evolutionary dynamics Yoshida et al. (2007), resulting from the enhanced ability of prey to evade predation by shifting to a low-edibility trait. Figure 5.4 illuminates how predation strength influences the onset of this kind of dynamics.

In the absence of trait variation in either prey or predator community, that is, when the initial conditions are such that only a single "species" (a single trait value) is present, the variation in the other community quickly vanishes, with a single trait value being selected. On the other hand, when the full range of possible traits is present, both communities keep its functional diversity.

5.3 ANALYSIS OF TOP–DOWN CONTROL EFFECTS

In this section, we explore how dynamics and patterns of the trait distributions change with respect to a control parameter. We chose the predator death rate, d, since it is one of the drivers of the dynamics while not interfering directly with the trade-off functions. As in other predator–prey models, the dynamics would change qualitatively in the same way if we changed, for instance, the carrying capacity K, but with larger K corresponding to smaller d.

We dropped the immigration terms (I_A and I_C), allowing that predator species go extinct, but use instead a sigmoidal functional response Tirok and Gaedke (2010); Baretta-Bekker et al. (1995), which is essentially identical to a type II functional response Holling (1965) for high prey biomasses but is reduced for prey biomasses of the same order or below a critical prey density, A_0, that is always much lower than the scale of the system's carrying capacity. This critical prey density is justified by the existence of resting stages, invulnerable to predation, that may stay in that form for a long time and help

reestablish the population once it reaches low levels. The functional response becomes thus:

$$\begin{aligned} g(\phi,\omega) &= g_m \frac{q(\phi,\omega) f_A(\phi) A(\phi)}{M(\omega) + \int q(\phi',\omega) f_A(\phi) A(\phi') d\phi'} \\ f_A(\phi) &= \frac{A(\phi)}{A_0 + A(\phi)} \end{aligned} \tag{5.4}$$

In the Rosenzweig-MacArthur predator-prey model, increasing predator death rate shortens cycle periods and stabilizes the dynamics for higher values. It also reduces top-down control, with the consequence that predator biomass decreases while prey's goes up. Our simulations confirm that reduced top-down control mediated by higher predator death rates also leads to the same changes in biomass levels (Figure 5.4a) and to traits shifting towards higher edibilities and higher median selectivities (Figure 5.4c), since predators need to increase their gains to compensate a higher mortality. Another point of contact with the traditional theory is that cycles also get shorter as predator mortality increases up to about $d = 0.06$, after which a new mode of oscillation, seen in Figure 5.3 top right panel, appears and eventually dominates the dynamics. These cycles have longer and increasing periods, and exhibit out-of-phase predator-prey oscillations (Figure 5.4f), as well as higher temporal variance in both mean traits and in the numbers of peaks in the trait distribution (Figure 5.4c,e). This kind of oscillation, typical of eco-evolutionary dynamics, is present for a large range of parameters.

Figure 5.3 also shows that, we see that this occurs because it can accommodate solutions with several dominant traits coexisting but with small fluctuations in the trait distribution. To explore this in more detail, we present in Figure 5.4 how the average and standard deviation of the effective number of peaks (described in the Appendix) vary with d – for low mortality, the temporal variance in the peaks is low, increasing together with d, although the mean number of peaks decreases a little, i.e., trait diversity at each instant decreases but temporal variation increases.

This can be clarified by Figure 5.3. In the last two panels at the right, most of the time the biomass distributions are not concentrated around a single value, but are either broad or distributed among several peaks. Compare this with the situation in Figure 5.3a, which shows a situation with low predator mortality rate, and therefore less top-down control, where predator biomass is always dominated by low selectivity species, which synchronize prey dynamics and keeps trait variance down.

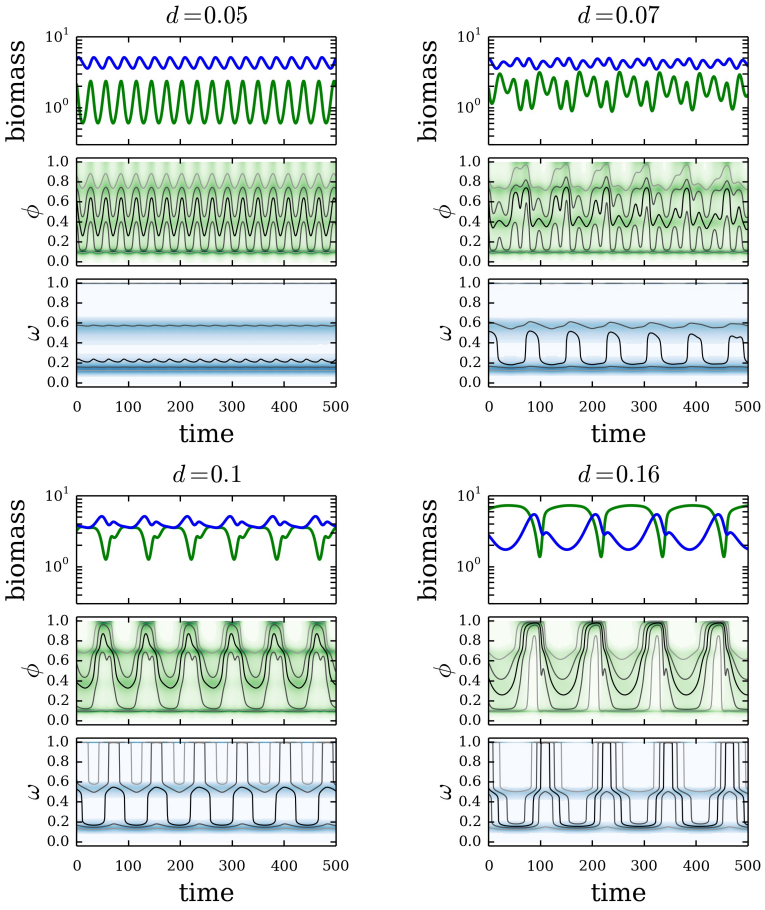

Figure 5.3: Dynamics of predator–prey biomasses and traits change as predator mortality is increased. Simulations were run using parameters from Table 5.1, except the predator mortality d, indicated in the title of each panel. Each panel shows the resulting dynamics, employing the same lines and colors used in Figure 5.2, left panel. **Top left.** At low mortality, predators have higher biomass, cycles are short, regular, and have an almost symmetric shape. Fluctuations in the mean trait distributions are small. **Top right.** At slightly higher mortality, predator–prey cycles become irregular, while predator trait distribution fluctuates more. **Bottom left.** Past a certain threshold, eco-evolutionary cycles set in, as seen by the increased phase difference between the peaks and valleys of prey and predator biomasses. Besides that, prey biomass increases, cycle periods get longer, and fluctuations in traits become very high. **Bottom right.** Finally, at high predator mortality, predator biomass is low while prey biomass is high, fluctuations in the mean values of traits become even more dramatic, cycle periods are longer and the phase lag becomes more marked.

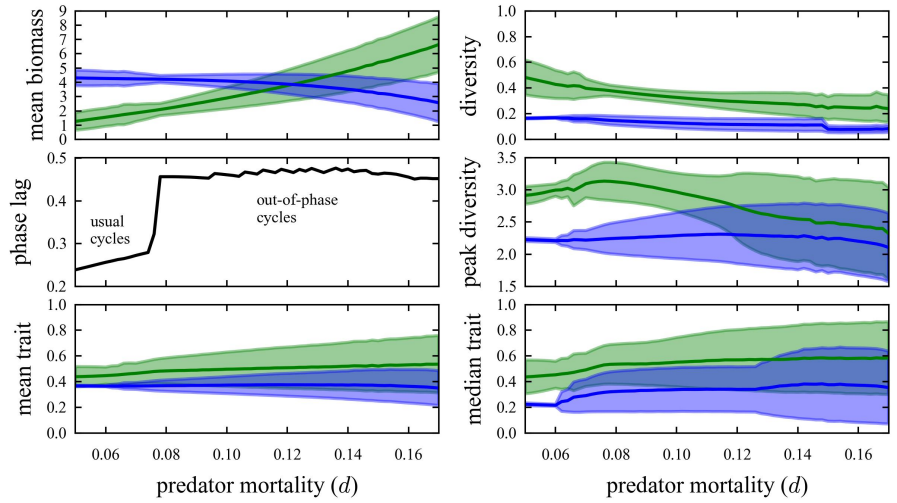

Figure 5.4: All plots are community properties calculated over a long time series taken after a transient, for increasing values of predator mortality rate. Properties belonging to the prey community are colored green and the ones relating to the predator community are in blue. **Left top** Average total biomass for each community, with their respective standard deviations in shade. **Left middle** Average relative phase lag between predator and prey, measured as a fraction of the period. This measure ranges from 0 to 1, so that 0 means synchrony (peaks are simultaneous) and 0.5 means completely out of phase cycles. **Left bottom** Average over time of the mean trait value, with standard deviations in shade. **Right top** Average over time of community diversity, measured by the inverse Simpson index. **Right middle** Average over time of community diversity measured by the inverse Simpson index applied to the aggregated biomasses of the peaks in each community. **Right bottom** Average over time of the median trait value.

5.4 COMPARISON WITH AGGREGATE MODEL

There is increasing empirical evidence that important traits are not necessarily normally distributed, questioning the strong assumption made in aggregate models. For example, it has been shown that phyto- and zooplankton size distributions can be skewed, multimodal (Vergnon et al., 2009; Segura et al., 2013), uniform (Gaedke, 1992) or even bimodal (Chisholm, 1992; Warwick et al., 1986; Tackx et al., 1994) which also holds for more general particle size distributions in oceans (Sheldon et al., 1972). In addition, phyto- and zooplankton size distributions show considerably large variances (e.g. Gaedke (1992)). This is important since size is functioning as a kind of master trait influencing an organism's reproduction, resource acquisition and susceptibility to predation (Litchman and Klausmeier, 2008).

Following the considerable empirical evidence, we have to reevaluate the utility of the aggregate model approach, since predictions about aggregate properties may strongly differ between aggregate models and their underlying multi-species (multiclonal) variants when stabilizing selection does not prevail. For example, sufficiently strong directional selection is expected to impose skewed trait distributions, whereas pronounced disruptive selection will promote bimodal trait distributions. In these cases, the first two central moments of a trait distribution may not accurately predict changes in the aggregate properties since local fitness optimization may differ from the global one.

We show that the aggregate model works well only under strongly stabilizing selection, but not under directional or disruptive selection. We explain this pattern in detail by looking at the trait distributions obtained from the continuous model, that point to multimodal, or even bimodal, distributions with large variances, which the aggregate model is unable to accommodate. We discuss what this means for the current understanding of trait based approaches to ecosystem dynamics.

5.4.1 *Methods*

We build a model based on the aggregate model framework (Norberg et al., 2001) in which we track only the total biomasses of the predator and prey communities (A and C), their mean trait values, ϕ and ω, and their trait variances, ν_ϕ and ν_ω. This kind of model can be derived through a moment closure approximation, that truncates the moment expansion of the trait distribution in the second order (Norberg et al., 2001). In the version described here, we do not use any prior information about the shape of the trait distributions emerging within the continuous model. Instead, as it is usually done, this formulation assumes that the trait values are normally distributed.

The essential feature that distinguishes these models is that in aggregate models only local fitness around the mean trait value, i.e. the local fitness gradient, is relevant for the change in traits, while the continuous model takes into account the whole distribution, and therefore takes into account the full non-linearity inherent to the feeding relationships and trade-offs underlying the system. This is illustrated in Figure 5.5, where we observe a situation where the same prey community is represented in both models – same total biomass, mean trait value and variance – but the traits move in opposite directions.

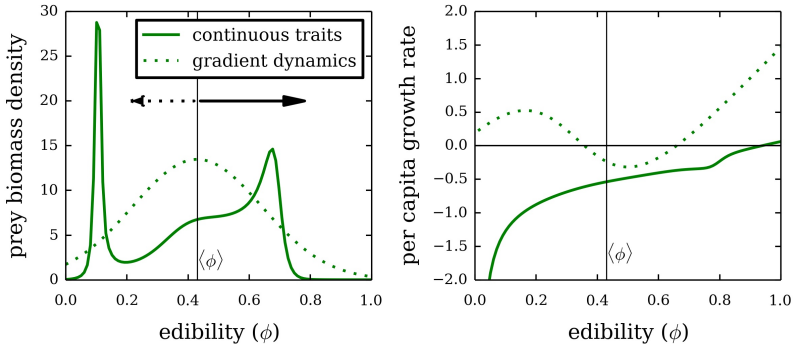

Figure 5.5: Comparison between continuous trait distribution and gradient dynamics models, at one moment in time. The vertical line represents the mean trait value and the arrows indicate its direction and magnitude of change. (a) biomass density distribution with respect to the edibility (ϕ) of prey for the two models, with both possessing the same mean value and variance. (b) fitness landscapes for both models: the *per capita* growth rate (fitness) determines, in both cases, the changes in the trait values, but in the gradient dynamics model the rate of change is proportional to the value of the fitness at the mean trait value, while for the continuous trait model the contribution of all traits is summed over, so that the mean trait value does not necessarily follow the fitness gradient.

The equations for biomass follow basically the same functional forms as in the continuous trait model, while changes in the mean traits and trait variances are determined, respectively, by the first and second derivatives of the *per capita* growth rates evaluated at the respective mean trait values. Following the derivation from Norberg et al. (2001), we included additional terms to the equations to account for non-linear averaging and changes in the location and width of the assumed normal trait distributions via immigration. All the param-

eters are the same as before, described in Table 5.1. Thus, we have

$$\begin{aligned}
\frac{dA}{dt} &= A\left[R_A\left(\bar{\phi},\bar{\omega}\right) + \frac{\nu_\phi}{2}\frac{\partial^2 R_A}{\partial\phi^2}\left(\bar{\phi},\bar{\omega}\right)\right] + I_A \\
\frac{dC}{dt} &= C\left[R_C\left(\bar{\phi},\bar{\omega}\right) + \frac{\nu_\omega}{2}\frac{\partial^2 R_C}{\partial\omega^2}\left(\bar{\phi},\bar{\omega}\right)\right] + I_C \\
\frac{d\bar{\phi}}{dt} &= \nu_\phi\frac{\partial R_A}{\partial\phi}\left(\bar{\phi},\bar{\omega}\right) + \frac{I_A}{A}\left(\frac{1}{2}-\bar{\phi}\right) \\
\frac{d\bar{\omega}}{dt} &= \nu_\omega\frac{\partial R_C}{\partial\omega}\left(\bar{\phi},\bar{\omega}\right) + \frac{I_C}{C}\left(\frac{1}{2}-\bar{\omega}\right) \\
\frac{d\nu_\phi}{dt} &= \nu_\phi^2\frac{\partial^2 R_A}{\partial\phi^2}\left(\bar{\phi},\bar{\omega}\right) + \frac{I_A}{A}\left[\frac{1}{12}-\nu_\phi+\left(\frac{1}{2}-\bar{\phi}\right)^2\right] \\
\frac{d\nu_\omega}{dt} &= \nu_\omega^2\frac{\partial^2 R_C}{\partial\omega^2}\left(\bar{\phi},\bar{\omega}\right) + \frac{I_C}{C}\left[\frac{1}{12}-\nu_\omega+\left(\frac{1}{2}-\bar{\omega}\right)^2\right] .
\end{aligned} \tag{5.5}$$

Following (Klauschies et al.), we introduce a function B which is zero over most of the trait range, from 0 to 1, but steeply increases close to 0 and decreases close to 1, so that $\bar{\phi}$ and $\bar{\omega}$ are restricted to the delimited range. In the same way, $\tilde{B}$ keep the variances bounded between 0 and 0.25, which is the maximum variance possible for a distribution of traits ranging between 0 and 1. The growth and grazing functions are given, in analogy to Eq.(5.2), by

$$\begin{aligned}
r(\phi) &= r'(\phi)\left(1-\frac{A}{K}\right) \\
g(\phi,\omega) &= g_m\frac{q(\phi,\omega)A(\phi)}{M(\omega)+q(\phi,\omega)A(\phi)} .
\end{aligned} \tag{5.6}$$

Finally, R_A and R_C are the instantaneous *per capita* net growth rates of prey and predator:

$$\begin{aligned}
R_A(\phi,\omega) &= \frac{1}{A}\frac{dA}{dt} = r(\phi) - \frac{A}{C}g(\phi,\omega) + B(\phi) \\
R_C(\phi,\omega) &= \frac{1}{C}\frac{dC}{dt} = eg(\phi,\omega) - d + B(\omega) ,
\end{aligned} \tag{5.7}$$

where B is, once again, a border function defined by $B(x) = -\left(e^{-wx} + e^{w(x-1)}\right)$.

This model can be summarized as the closest aggregate model one can build using the same assumptions of the model described in the previous section. The key difference, as we have seen, is how the trait distribution changes: in the aggregate model, the traits follow the fitness landscape around the current mean trait value, with a speed proportional to the local fitness gradient at the mean trait value and to the current trait variance, while in the continuous trait model, the whole fitness landscape shapes the dynamics.

Trade–offs and selection regimes

To manipulate the selection regime exhibited by the prey and predator communities, we systematically altered the shape of the trade-offs between edibility and growth rate, and between selectivity and half-saturation constant, extending equations 5.3 above by introducing a non-linearity parametrized by β:

$$\begin{aligned} r'(\phi) &= r'_0(\beta_r)(1 + m_r \phi^{\beta_r}) \\ M(\omega) &= M'_{max}(\beta_M)(1 - m_M \omega^{\beta_M}) \, . \end{aligned} \tag{5.8}$$

When $\beta = 1$ we recover the linear trade-off curve. The constants m_r and m_M do not depend on β_r and β_M, so the ratio between the maximum and minimum growth rates and half–saturation constants do not change with the degree of non–linearity. On the other hand, we choose the dependence of r'_0 and M'_{max} on β_r and β_M, respectively, in such a way that, given an homogeneous distribution of traits, the averages of prey's maximum growth rate, $\int_0^1 r'(\phi) d\phi$, and of predator's attack rate (i.e. grazing rate at low prey densities), $\int_0^1 \frac{g_m}{M(\omega)} d\omega$ are constant. This is necessary because, otherwise, the direct increase or decrease in prey productivity or in sensitivity of predators to amount of prey would shadow the effect of the non–linearity. These assumptions lead to:

$$\begin{aligned} r'_0(\beta_r) &= \frac{1 + \frac{m_r}{2}}{1 + \frac{m_r}{1+\beta_r}} r_0 \\ M'_{max}(\beta_M) &= \frac{{}_2F_1\left(1, \frac{1}{\beta_M}, 1 + \frac{1}{\beta_M}, m_M\right)}{{}_2F_1(1, 1, 2, m_M)} M_{max} \, , \end{aligned} \tag{5.9}$$

where ${}_2F_1$ is the hypergeometric function. The resulting trade-off curves are shown in Figure 5.6.

We focus on situations with $\beta_r = \beta_M = \beta$, where selection tends to act in the same manner in both prey and predator communities. When β is small, prey growth rate increases quickly for small ϕ, but slowly for high ϕ; selectivity, on the other hand, declines steeply at low ω, but gently for high ω (Figure 5.6). Thus, subject to the same predation functions, mid values of both edibility and selectivity are favored, giving rise to stabilizing selection. In this case, the long–term trait distribution is expected to be strongly concentrated in mid values, exhibiting small trait variances.

As the value of β increases, selection pressures reverse: prey growth rate increases slowly at low edibility and quickly at high edibility, while predator half saturation constant decreases slowly at low selection but steeply for high selectivity, thus favoring extreme trait values in both trophic levels. This constitutes a case of disruptive selection,

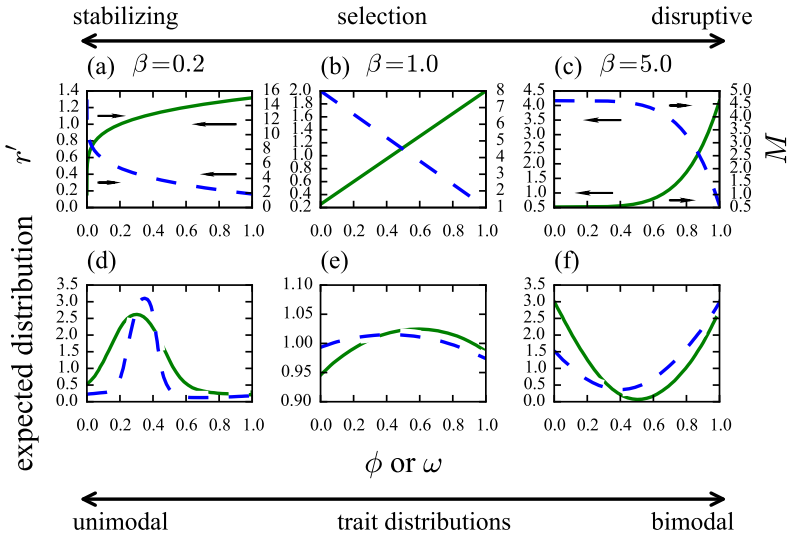

Figure 5.6: The top panels show the trade–off relations between maximum growth rate (r', green solid line) and edibility (ϕ), and between grazing half-saturation constant (M, blue dashed line) and selectivity (ω) for several values of β. The arrows in panels (a) and (c) indicate the tendency of direction of selection on traits, in comparison to the linear case. The bottom panels show how the trade-offs result on distinct expected distributions.

where we expect long–term trait distributions with peaks at both low and high trait values, giving rise to large trait variances.

Analysis

Solutions of the continuous model (Equations (5.1-5.3)) yield the biomass density along the trait axis of each community as it changes with time. An example is provided in the top left part of Figure 5.7: in the left panel we see the total community biomasses integrated over all trait values in the top, with the trait distributions ($A(\phi)$ and $C(\omega)$) in the two panels just below, changing with time. At each instant, the community trait composition takes a different shape, as shown in the bottom panels for four different times. At the time labeled (a) in Figure 5.7, total prey biomass (green) is high, with a predominance of prey of low edibility (ϕ), while predator biomass (blue) is low, with its selectivity (ω) decreasing in response to a low prey edibility. With the increase of biomass of low selectivity predators at instant (b), prey biomass begins to decline, even as prey of intermediate and high edibility grow. In response to that, predators of higher selectivity also increase, leading to a three-peaked distribution of high biomass of predators at instant (c), while prey biomass reaches its lowest level and is dominated by highly edible prey. At instant (d) the prey community recovers due to reduced predator biomass, with intermediate and low edibility prey increasing again, while predator selectivity is still rather high, but begins to respond by decreasing its selectivity.

Since the remaining biomass of non-selective predators is low, they need a long time to recover and control the less edible species. From then onwards the pattern is repeated.

For the given choice of parameters, the same general patterns are seen in the solution of the trait dynamics model (Equations 5.5-5.7), shown in the top right panels of Figure 5.7: prey biomass is initially high, with low edibility, and predator biomass and selectivity are low; then prey selectivity increases, followed after some time by predator selectivity, at which point prey edibility and biomass go down quickly; then predator selectivity and total biomass also decrease, allowing prey biomass to grow again, beginning the cycle anew.

We compare the dynamics and long–term properties of prey and predator communities generated by simulations of both models as the parameter β, that determines the mode of selection, is varied. We observe how long–term mean over time of community biomasses and its coefficient of variation (CV), mean trait values, and trait variances vary, and how that affects the suitability of the aggregate model, by comparing the outcome of both models.

5.4.2 *Results*

At very low β, below 0.25, selection is strongly stabilizing as indicated by small trait variances within both prey and predator communities (Figures 5.6, 5.8). In this case, the two models agree quite well, predicting very similar dynamics and long–term states of the aggregate properties (Figure 5.9a), in which both edibility and selectivity settle at low values, linked to low growth and grazing rates, which promotes stable biomass dynamics.

As β increases, the selection regime changes from stabilizing to directional selection, where different trait values are favored at different times. Indeed, both models show considerable changes in mean trait values and trait variances. The recurrent invasion of fast-growing well edible prey and selective predator species strongly destabilizes community biomasses in both models. However, despite similar trends in the aggregate properties with increasing β initially, the continuous and aggregate models substantially differ in their predictions about the magnitude and variance of the aggregate properties for higher values of β (Figures 5.8, 5.9b). For example, the aggregate model tends to underestimate prey biomass for values of β below 1.5, whereas it overestimates prey biomass for values above that (Figure 5.8). In addition, the aggregate model overestimates predator biomass throughout most of the parameter range. In general, the bias increases with increasing values of β. Furthermore, the aggregate model shows considerably higher variation in the mean trait values and encompasses partially opposite trends with increasing values of β compared to the continuous model. Although both model approaches predict similar

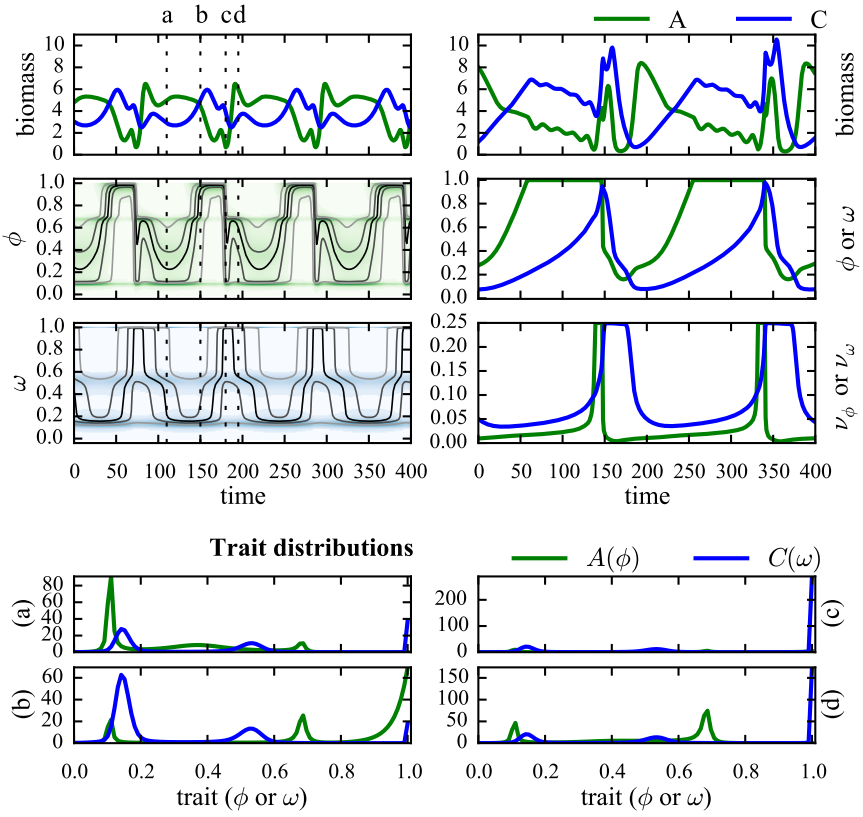

Figure 5.7: Long-term solutions show recurrent trait shifts in both prey and predator communities. Simulation run using parameters from Table 5.1 and $\beta = 1$. **Top Left.** The top panel at left shows the total biomass of prey A (green) and predator C (blue) for the continuous model. The two panels just below show the distributions of prey edibility, ϕ, and predator selectivity, ω, as a function of time, with lighter shades indicating low frequency in the population, and darker ones denoting high frequency of that value. Drawn in continuous gray line is the biomass-weighted average trait value, and in thin black lines are the 10, 30, 50, 70 and 90% trait percentiles, that is, the trait below which 10% (and 30, 50%, etc.) of the total biomass is found. The vertical dotted lines correspond to the times referred to in the text. **Top Right** The top panels at right show the long–term dynamics of the gradient dynamics, with green and blue representing prey and predators' properties, respectively. **Bottom.** Sequence of snapshots of the trait distribution of prey (biomass density as a function of edibility, ϕ, in green), and predator (biomass density as a function of selectivity, ω, in blue). The snapshots correspond to the times labeled in the top left panel.

mean values of the prey's trait variance, the continuous model shows less variation. In addition, the trait variance of the predators is almost linearly increasing in β in the continuous model, whereas the shape looks rather parabolic for the aggregate model.

As β increases to very high values, above 2.25, to scenarios of more disruptive selection, the continuous model tends to relatively stable solutions in both biomasses and mean trait values as indicated by very low CVs, while the aggregate model still exhibits substantial variation in the aggregate properties. Nonetheless, a more detailed look at the dynamics reveals that the aggregate model predicts rather stable prey and predator biomasses for a long time period during which predator's selectivity is continuously increasing; when the predator's selectivity passes a threshold, both the biomass and trait dynamics become unstable for a short period until the previous conditions are reestablished. In contrast to the continuous model predicting intermediate trait values, the aggregate model predicts rather extreme trait values – high edibility of prey and low selectivity of predators – during most of the time which, in addition, leads to very high predator biomass.

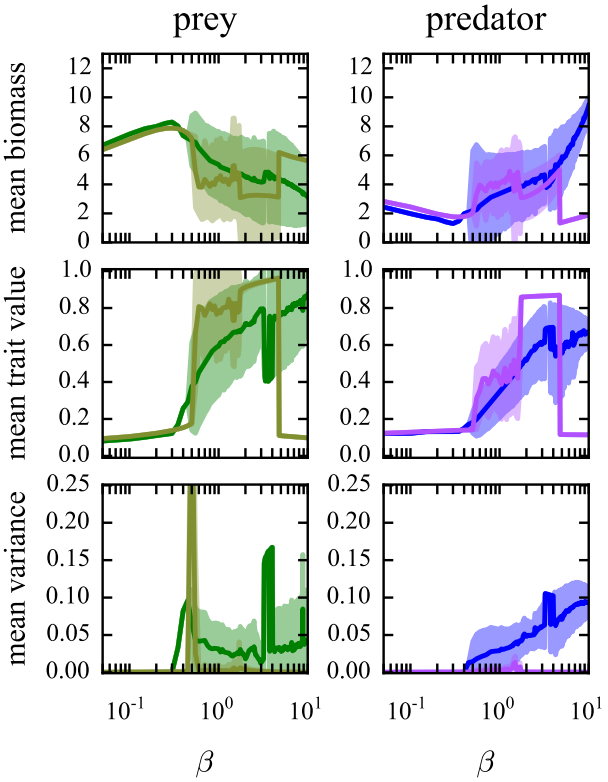

Figure 5.8: Time average of biomass, mean trait, and variance of the solutions of both continuous (green, blue) and gradient dynamics (olive, purple) models as the trade–offs change, that is, as $\beta_r = \beta_M = \beta$ is varied. All parameters are the same as in Table 5.1.

These patterns can be understood by looking at the effects of the trade-offs at the prey and predator communities simultaneously. Whenever there is only a single prey species surviving, competitive exclusion dictates that a single predator type is able to persist; the same is true of the prey community if only a predator type survives. Stabilizing selection, by making extreme phenotypes very unfavorable, inhibits the effect of the trade-offs responsible for coexistence. This, in turn, leads to a single phenotype being predominant in both prey and predator communities, regardless of the model employed, so the continuous model predicts a very narrow, single-peaked distribution (Figure 5.7a). In this limit, the aggregate model is expected to perform quite well and, since the models use the same ingredients and parametrization, they predict almost the same dynamics and long-term states. Although skewness and kurtosis are extremely high, they do not effect much the aggregate properties since overall trait variation is too small.

When stabilizing selection is relaxed, extreme phenotypes are able to invade the community. Notice that this occurs only for higher values of β in the aggregate model because it is not sufficient that some particular phenotype is able to invade: it is necessary that the equilibrium state becomes unstable, that is, phenotypes close to the previously favored one become sufficiently fit, so that the equilibrium phenotype is no longer a maximum of the fitness gradient. In the continuous model, on the other hand, it is enough that some fitter phenotype exists, even if its trait value is far from the previously favored one.

When trade-offs are rather linear, strong predator-prey cycles emerge (Figure 5.7b), giving rise to directional selection, where several different types of prey and predator species can coexist, and shaping the trait distributions in the continuous model. This happens because the ongoing predator-prey cycles change the environment in such a way that each trait value is temporarily favored over the others. As a result, highly skewed trait distributions emerge. However, since the direction of selection is changing in time, the sign of skewness fluctuates as well. In general, when a trait distribution changes its skewness from positive to negative values, or vice-versa, it likely passes through a state in which it is multi- or even bimodal. This assumption is supported by our results, where trait distributions are frequently multimodal (Figure 5.7b). In contrast to disruptive selection, multimodal trait distribution are a combined result of past and present growth and death processes that persist only momentarily. In the aggregate model, such coexistence at a single moment in time is not possible, but it manifests itself by cycling trait values, driven both by the non-linearities in the growth and grazing terms and by the intrinsic predator-prey cycles.

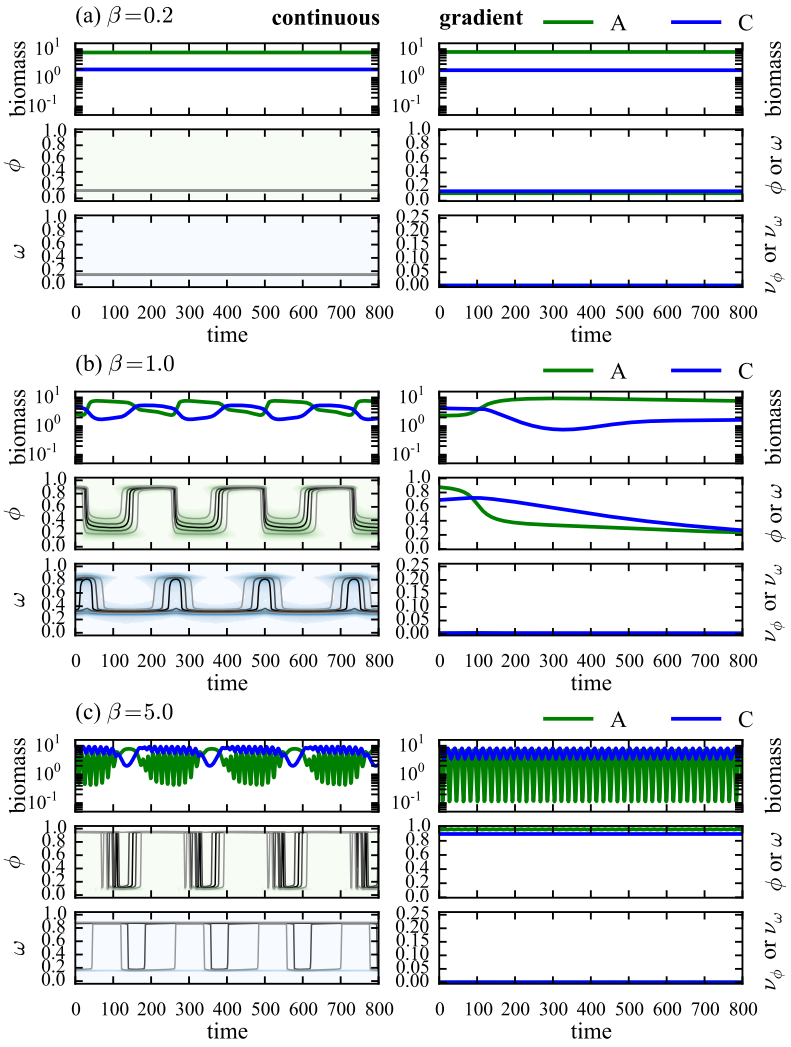

Figure 5.9: Comparison of long-term dynamics of continuous (left) and gradient dynamics (right) models, for $\beta = 0.1$, 1 and 2.5, corresponding to strongly stabilizing, intermediate and strongly disruptive selection. All other parameters are as in Table 5.1. The colors and lines are the same as in Figure 5.7. Notice that the time scale of panel (c) is longer than the others.

The predictions of the two model approaches differ most strongly for disruptive selection, both in terms of the overall magnitude of the aggregate properties and their temporal dynamics. For instance, the predator biomass is overestimated by a factor of three when β equals 2.5. This is a consequence of the prey and predator communities being comprised solely of very productive prey species and rather inefficient predator species during most of the time. This trait composition strongly increases the equilibrium biomass of the predators during the quasi-stable period in the aggregate model (Figure 5.9c), which appears because, under disruptive selection, the extreme traits are favored and thus predator selectivity takes a long time to increase. The difference between the two model approaches is explained by the composition of the prey community, exhibiting a highly skewed but bimodal trait distribution, and predator community being composed of three modes. This configuration of trait distributions has the interesting effect of stabilizing population dynamics, as can be seen visually in Figure 5.7c The aggregate model, in turn, cannot settle down to an equilibrium, but the disruptive selection enables the system to spend longer times at each extreme, and so the cycles become longer and the fluctuations more intense, in complete disagreement with the continuous model.

In accordance with recent model studies, the coupling of trait and biomass cycles leads to so-called out-of-phase cycles (Yoshida et al., 2003), where the predators lag the prey by a phase closer to half the period than one fourth, as in usual predator-prey cycles. This phenomena is considered the "smoking gun" of eco-evolutionary dynamics, but can also be observed in both models presented here for a wide range of parameters. In contrast to previous studies focusing solely on genetic variation within one species, the prey and predator communities in our model represent assemblages of many species and genotypes, which conflate inter- and intraspecific trait variation. However, although both models show a clear feedback between trait and biomass dynamics they do not, in general, lead to the same long-term dynamics or mean values, as we presented in Figure 5.8.

5.5 PERSPECTIVES

In this work, we introduced a new framework that describes the dynamics of the trait distribution of predator-prey communities containing all possible species along a trait axis: edibility for prey, and selectivity for predators. We develop also an analogous model following the gradient dynamics approach, doing a detailed comparison of both models. In particular, we contrast how both models behave in response to varying top-down control and to different forms of the trade-off between prey edibility and growth rate.

The new continuous traits model has the remarkable property of presenting multimodal distributions under a wide range of parameters. Because of the permanent presence of multiple traits, in both prey and predator communities, the continuous traits model is more stable than the corresponding gradient dynamics model, in the sense that both biomasses and mean trait values fluctuate more in time in the latter than in the former. In other words, the diversity of species at both trophic levels stabilizes the dynamics.

Although such trade-offs are thought to be pervasive in nature, little is known yet about their shape, either in natural or artificial systems. We demonstrate here that the choice of modeling framework can have strong effects even on the most basic properties of community dynamics, such as mean biomass and trait values.

A simple extension of the current model allows us to relax the assumption of strict clonal reproduction, by introducing a "mixing" term, whose mathematical expression would be a diffusion of the population in the trait space. This is interpreted as allowing individuals with a certain trait to beget individuals with traits infinitesimally close, but different from their own.

In conclusion, we argue that ecosystem models need to move ahead by accounting for the possibility of complex interactions to generate strongly non-linear fitness landscapes that render aggregate models inaccurate, both due to Jensen's inequality and by giving rise to bimodal trait distributions with large variance. The common assumption that trait distributions reflect only the fitness landscape close to the optimum trait has to be questioned and carefully assessed in each case. With the novel approach presented, we are better equipped to relate trade-off relationships to patterns in trait distributions and in community dynamics.

6

FINAL REMARKS

In this thesis we explored a wide range of ecological systems and modeling approaches. A common thread through the topics explored is the concern of going beyond the comfort zone of developing and analyzing mathematical models, guided by theoretical intuition, and actively looking for opportunities to talk, collaborate, and apply mathematical models to concrete ecological and epidemiological problems. This is not only useful to increase the quality and relevance of the work, but is also a constant source of inspiration.

These cross-disciplinary conversations are rewarding because they involve a perpetual contending between the many complexities of ecological realities and the need to simplify and extract the essential features that will guide understanding. In section 2.3, for instance, we discuss a phenomenon, habitat split, that is possibly interlinked to many others: habitat loss, increase in predation and predator abundance, isolation of subpopulations, among others. Nonetheless, these questions need not figure in our models in order to show how increased mortality of juveniles can lead to extinction. Put that way, this result sounds obvious, but we go further – we explain and quantify the mechanism behind this effect, and link it to the split distance, and at this point we have an outcome that can be fed back into experiments and observations.

A similar remark can be made about the work on seasonal diffusion (section 2.4). There, rainy season length can curb dispersal distance, leading to a maximum dispersal reach limited either by season length or by diffusivity, but the latter cannot determine which is the case. We thus have a measure of functional connectivity that is no longer geometric and static, but depends on the time scales involved, and can be substantially altered by variation in rainy season length across years.

Another consequence of working together with ecologists is that sometimes we can fully parametrize and test the model, even if only *post hoc*. This is always satisfying, notwithstanding reservations about alternative explanations or simply selection bias. In the section about blowfly invasion (2.2), we find a reasonable agreement between predicted and observed invasion speeds, although with large range of possible values. In a sense, blowflies present such a simple behavior, generalist feeding habits, and non-overlapping generations that it feels like the system is simulating the equations. The epidemiologic model for malaria in the Atlantic Forest (section 3.3), on the other hand, included much more refined fitting of parameters, using data

collected by Gabriel Laporta, to reach a conclusion about models: the traditional Ross-MacDonald model seems to overestimate the value of R_0, while ours incorporate ecological mechanisms that correct it. This supports the argument that these mechanisms have to be considered in this kind of transmission dynamics with the possibility of ecological feedbacks.

In the same vein, models can guide future empirical work and generate predictive hypotheses. In chapter 4, we use a seemingly complicated, although conceptually simple, system of delay-differential equations whose parameters relate directly to physiological traits of individuals, measured in laboratory for many ectotherm species. The model connects these traits to population dynamics, allowing better estimates of population viability analysis and predicting the effects of temperature-dependant intra-specific competition under contrasting hypotheses, something valuable in itself, but also as a basis to build more complex scenarios containing more species.

Finally, ecological theory has to respond to new ideas and generalizations arising from observation. The models developed for intraguild mutualism in section 3.2, spurred by growing interest in mutualism as a structuring relationship in communities, show surprising outcomes, demonstrating coexistence of two consumers on a single shared resource for a relatively large range of parameters, something considered exceptional in theory and in practice as well. This showcases the potentially important role of facilitative interactions in promoting coexistence, a topic that only recently captured focused attention from ecologists. In a different context, ecosystem models for plankton communities have relied considerably on moment closure techniques to reduce model complexity, under the assumption of small variance and nearly normal trait distributions. Empirical evidence shows that phyto- and zooplankton communities can deviate far from these limits, presenting multimodality, bimodality and large variances in size distribution. Our approach in chapter 5 then was to show that predictions from a complete description of the system are at variance with the simpler models in most situations, revealing the need to reevaluate their usefulness.

REFERENCES

Abrams, P. A., C. E. Brassil, and R. D. Holt. 2003. Dynamics and responses to mortality rates of competing predators undergoing predator–prey cycles. Theoretical Population Biology 64:163–176. (Cited on page 60.)

Al-Misned, F. A., M. A. Amoudi, and S. S. Abou-Fannah. 2002. Development rate, mortality and growth rate of immature *Chrysomya albiceps* (wiedemann) (diptera: Calliphoridae) at constant laboratory temperatures. J. King Saud Univ. 15:9–58. (Cited on page 17.)

Albuquerque de Moura, P., S.-P. Quek, M. Z. Cardoso, and M. R. Kronforst. 2011. Comparative population genetics of mimetic *Heliconius* in an endangered habitat; Brazil's Atlantic forest. BMC Genetics 12:9. (Cited on page 38.)

Alex Smith, M., and D. M Green. 2005. Dispersal and the metapopulation paradigm in amphibian ecology and conservation: are all amphibian populations metapopulations? Ecography 28:110–128. (Cited on pages 28 and 29.)

Alford, R. A., and S. J. Richards. 1999. Global amphibian declines: a problem in applied ecology. Annual review of Ecology and Systematics pages 133–165. (Cited on page 26.)

Almeida, A. P. 1946. Memória histórica da Ilha do Cardoso. Rev Arq Municipal 111:19–52. (Cited on page 66.)

Alonso, P. L., G. Brown, M. Arevalo-Herrera, F. Binka, C. Chitnis, F. Collins, O. K. Doumbo, B. Greenwood, B. F. Hall, M. M. Levine, et al. 2011. A research agenda to underpin malaria eradication. PLoS Med 8:e1000406. (Cited on page 73.)

Amarasekare, P., and R. M. Coutinho. 2013. The intrinsic growth rate as a predictor of population viability under climate warming. Journal of Animal Ecology DOI: 10.1111/1365-2656.12112. (Cited on page 75.)

———. 2014. Effects of temperature on intraspecific competition in ectotherms. The American Naturalist 184:E50–E65. (Cited on page 75.)

Amarasekare, P., and V. Savage. 2012. A framework for elucidating the temperature dependence of fitness. The American Naturalist 179:178–191. (Cited on page 76.)

Ananthasubramaniam, B., R. Nisbet, W. Nelson, E. McCauley, and W. Gurney. 2011. Stochastic growth reduces population fluctuations in daphnia-algal systems. Ecology 92:362–372. (Cited on page 21.)

Andersen, M. 1991. Properties of some density-dependent integrodifference equation population models. Math. Biosciences. 104:135–157. (Cited on pages 9 and 13.)

Anderson, R. M., and R. M. May. 1991. Infectious diseases of humans: dynamics and control. Wiley Online Library, New York. (Cited on page 63.)

Angilletta, M. J. 2009. Thermal adaptation: a theoretical and empirical synthesis. Oxford University Press. (Cited on page 76.)

Antogiovanni, M., and J. P. Metzger. 2005. Influence of matrix habitats on the occurrence of insectivorous bird species in amazonian forest fragments. Biological Conservation 122:441–451. (Cited on page 30.)

Assaneo, F., R. M. Coutinho, Y. Lin, C. Mantilla, and F. Lutscher. 2012. Dynamics and coexistence in a system with intraguild mutualism. Ecological Complexity 14:64–74. (Cited on page 40.)

Azevedo, F., R. M. Coutinho, and R. A. Kraenkel. 2014. Spatial dynamics of a population with stage-dependent diffusion. Communications in Nonlinear Science and Numerical Simulation 22:605–610.

Baretta-Bekker, J. G., J. W. Baretta, and E. K. Rasmussen. 1995. The microbial food-web in the european-regional-seas-ecosystem-model. Netherlands Journal of Sea Research 33:363–379. (Cited on page 112.)

Baum, K. A., K. J. Haynes, F. P. Dillemuth, and J. T. Cronin. 2004. The matrix enhances the effectiveness of corridors and stepping stones. Ecology 85:2671–2676. (Cited on page 30.)

Baumgartner, D., and B. Greenberg. 1984. The genus *Chrysomya* (diptera: Calliphoridae) in the new world. J Med Entomol 21:105–113. (Cited on pages 8 and 17.)

Becker, C., C. Fonseca, C. Haddad, R. Batista, and P. Prado. 2007. Habitat split and the global decline of amphibians. Science 318:1775–1777. (Cited on pages 19, 26, and 29.)

Becker, C. G., C. R. Fonseca, C. F. Haddad, and P. I. Prado. 2010. Habitat split as a cause of local population declines of amphibians with aquatic larvae. Conservation Biology 24:287–294. (Cited on page 19.)

Becks, L., S. P. Ellner, L. E. Jones, and N. G. Hairston. 2012. The functional genomics of an eco-evolutionary feedback loop: linking gene expression, trait evolution, and community dynamics. Ecology Letters 15:492–501. (Cited on page 105.)

Beebee, T. J., and R. A. Griffiths. 2005. The amphibian decline crisis: a watershed for conservation biology? Biological Conservation 125:271–285. (Cited on page 26.)

Begon, M. 2008. Effects of host diversity on disease dynamics. In: Ostfeld RS, Keesing F, Eviner VT, editors. Infectious disease ecology: The effects of ecosystems on disease and of disease on ecosystems. Princeton: Princeton University Press. (Cited on page 71.)

Begon, M., C. R. Townsend, and J. L. Harper. 2006. Ecology: from individuals to ecosystems. Blackwell Pub. (Cited on page 78.)

Berec, L. 2010. Impacts of foraging facilitation among predators on predator-prey dynamics. Bulletin of mathematical biology 72:94–121. (Cited on page 44.)

Bertness, M. D. 1989. Intraspecific competition and facilitation in a northern acorn barnacle population. Ecology pages 257–268. (Cited on page 44.)

Bertness, M. D., and G. H. Leonard. 1997. The role of positive interactions in communities: lessons from intertidal habitats. Ecology 78:1976–1989. (Cited on page 42.)

Blaum, N., and M. C. Wichmann. 2007. Short-term transformation of matrix into hospitable habitat facilitates gene flow and mitigates fragmentation. Journal of Animal Ecology pages 1116–1127. (Cited on page 30.)

Blaustein, A. R., and L. K. Belden. 2003. Amphibian defenses against ultraviolet-b radiation. Evolution & development 5:89–97. (Cited on page 26.)

Boucher, D. H., S. James, and K. H. Keeler. 1982. The ecology of mutualism. Annual Review of Ecology and Systematics 13:315–347. (Cited on page 59.)

Braack, L., and P. Retief. 1986. Dispersal, density and habitat preference of the blow-flies *Chrysomya albiceps* and *Chrysomya marginalis* (wd.) (diptera: Calliphoridade). Onderstepoort J. vet. Res. 53:13–18. (Cited on pages 15, 16, and 17.)

Brown, J. H., J. F. Gillooly, A. P. Allen, V. M. Savage, and G. B. West. 2004. Toward a metabolic theory of ecology. Ecology 85:1771–1789. (Cited on page 84.)

Brown, K. S. 1981. The biology of *Heliconius* and related genera. Annual Review of Entomology 26:427–456. (Cited on page 31.)

Brown Jr, K. S., and A. V. L. Freitas. 2002. Butterfly communities of urban forest fragments in Campinas, São Paulo, Brazil: structure, instability, environmental correlates, and conservation. Journal of Insect Conservation 6:217–231. (Cited on page 31.)

Bruno, J. F., J. J. Stachowicz, and M. D. Bertness. 2003. Inclusion of facilitation into ecological theory. Trends in Ecology & Evolution 18:119–125. (Cited on pages 41, 42, and 59.)

Bshary, R., A. Hohner, K. Ait-el Djoudi, and H. Fricke. 2006. Interspecific communicative and coordinated hunting between groupers and giant moray eels in the Red Sea. PLoS biology 4:e431. (Cited on page 41.)

Callaway, R. M. 1995. Positive interactions among plants. The Botanical Review 61:306–349. (Cited on page 41.)

Cantrell, R., C. Cosner, and W. Fagan. 1998. Competitive reversals inside ecological reserves: the role of external habitat degradation. Journal of Mathematical Biology 37:491–533. (Cited on page 21.)

Cantrell, R. S., and C. Cosner. 2003. Spatial ecology via reaction-diffusion equations. John Wiley. (Cited on page 31.)

Cardinale, B. J., C. T. Harvey, K. Gross, and A. R. Ives. 2003. Biodiversity and biocontrol: emergent impacts of a multi-enemy assemblage on pest suppression and crop yield in an agroecosystem. Ecology Letters 6:857–865. (Cited on page 41.)

Cardinale, B. J., M. A. Palmer, and S. L. Collins. 2002. Species diversity enhances ecosystem functioning through interspecific facilitation. Nature 415:426–429. (Cited on page 41.)

Cardoso, M. Z. 2010. Reconstructing seasonal range expansion of the tropical butterfly, *Heliconius charithonia*, into texas using historical records. Journal of Insect Science 10: Article 69. (Cited on page 35.)

Carlton, J. M., B. J. Sina, and J. H. Adams. 2011. Why is Plasmodium vivax a neglected tropical disease? PLoS Negl Trop Dis 5:e1160. (Cited on page 61.)

Cerutti, C., M. Boulos, A. F. Coutinho, M. C. L. D. Hatab, A. Falqueto, H. R. Rezende, A. M. R. C. Duarte, W. Collins, and R. S. Malafronte. 2007. Epidemiologic aspects of the malaria transmission cycle in an area of very low incidence in Brazil. Malaria J 6:33. (Cited on page 62.)

Chandrasekhar, S. 1943. Stochastic problems in physics and astronomy. Rev Mod Phys 15:1–89. (Cited on page 12.)

Change, I. P. O. C. 2007. Climate change 2007: The physical science basis. Agenda 6:333. (Cited on page 82.)

Charnov, E. L., G. H. Orians, and K. Hyatt. 1976. Ecological implications of resource depression. The American Naturalist 110:247–259. (Cited on pages 41 and 47.)

Chaves, L. F., L. C. Harrington, C. L. Keogh, A. M. Nguyen, and U. D. Kitron. 2010. Blood feeding patterns of mosquitoes: random or structured? Front Zool 7. (Cited on page 71.)

Chesson, P. 1994. Multispecies competition in variable environments. Theoretical Population Biology 45:227–276. (Cited on page 41.)

———. 2000. General theory of competitive coexistence in spatially-varying environments. Theoretical population biology 58:211–237. (Cited on pages 2, 41, and 88.)

Chisholm, S. W. 1992. Phytoplankton size. Pages 213–237 *in* P. G. Falkowski and A. D. Woodhead, eds. Primary productivity and biogeochemical cycles in the sea. Springer. (Cited on page 116.)

Cohuet, A., C. Harris, V. Robert, and D. Fontenille. 2010. Evolutionary forces on *Anopheles*: what makes a malaria vector? Trends Parasitol 26:130–136. (Cited on page 71.)

Conn, J. E., R. C. Wilkerson, M. N. O. Segura, R. T. L. de Souza, C. D. Schlichting, R. A. Wirtz, and M. M. Póvoa. 2002. Emergence of a new neotropical malaria vector facilitated by human migration and changes in land use. Am J Trop Med Hyg 66:18–22. (Cited on page 63.)

Conselho Estadual do Meio Ambiente. 2001. Plano de manejo do Parque Estadual da Ilha do Cardoso. Secretaria do Meio Ambiente, São Paulo. (Cited on page 66.)

Conway, E., and J. Smoller. 1986. Global analysis of a system of predator-prey equations. SIAM Journal on Applied Mathematics 46:630–642. (Cited on page 60.)

Cooper, N., J. Bielby, G. H. Thomas, and A. Purvis. 2008. Macroecology and extinction risk correlates of frogs. Global Ecology and Biogeography 17:211–221. (Cited on page 28.)

Corless, R. M., G. H. Gonnet, D. E. Hare, D. J. Jeffrey, and D. E. Knuth. 1996. On the lambertw function. Advances in Computational mathematics 5:329–359. (Cited on page 83.)

Coutinho, R. M. 2010. Equações diferenciais com retardo em biologia de populações. Ph.D. thesis. Intituto de Física Teórica - Unesp. (Cited on page 75.)

Coutinho, R. M., W. A. C. Godoy, and R. A. Kraenkel. 2012. Integrodifference model for blowfly invasion. Theoretical Ecology 5:363–371. (Cited on page 6.)

Couto, R. D. A., M. R. D. Latorre, S. M. Di Santi, and D. Natal. 2010. Autochthonous malaria notified in the State of São Paulo: clinical and epidemiological characteristics from 1980 to 2007. Rev Soc Bras Med Trop 43:52–58. (Cited on pages 61 and 68.)

Crowley, P., and J. Cox. 2011. Intraguild mutualism. Trends in ecology & evolution . (Cited on pages 41, 42, and 59.)

Cuddington, K., W. G. Wilson, and A. Hastings. 2009. Ecosystem engineers: feedback and population dynamics. The American Naturalist 173:488–498. (Cited on page 60.)

Curado, I., R. S. Malafronte, A. M. R. C. Duarte, K. Kirchgatter, M. S. Branquinho, and E. A. B. Galati. 2006. Malaria epidemiology in low-endemicity areas of the Atlantic Forest in the Vale do Ribeira, São Paulo, Brazil. Acta Trop 100:54–62. (Cited on pages 61, 67, and 68.)

Cushman, S. A. 2006. Effects of habitat loss and fragmentation on amphibians: a review and prospectus. Biological conservation 128:231–240. (Cited on page 26.)

CVE. 2006. Casos confirmados de malária autóctones. Centro de Vigilância Epidemiológica page Available: http://www.cve.saude.sp.gov.br/htm/zoo/malaria_cautoctone.htm/. Accessed 2011 Oct 18. (Cited on page 62.)

De Castro, M. C., R. L. Monte-Mór, D. O. Sawyer, and B. H. Singer. 2006. Malaria risk on the amazon frontier. Proc Natl Acad Sci U S A 103:2452–2457. (Cited on pages 63, 72, and 73.)

Deutsch, C. A., J. J. Tewksbury, R. B. Huey, K. S. Sheldon, C. K. Ghalambor, D. C. Haak, and P. R. Martin. 2008. Impacts of climate warming on terrestrial ectotherms across latitude. Proceedings of the National Academy of Sciences 105:6668–6672. (Cited on pages 76, 84, and 87.)

Dickman, C. R. 1992. Commensal and mutualistic interactions among terrestrial vertebrates. Trends in ecology & evolution 7:194–197. (Cited on page 41.)

Downs, W. G., and C. S. Pittendrigh. 1946. Bromeliad malaria in Trinidad, British West Indies. Am J Trop Med Hyg 26:47–66. (Cited on page 61.)

Dreyer, H., and J. Baumgärtner. 1996. Temperature influence on cohort parameters and demographic characteristics of the two cowpea coreids clavigralla tomentosicollis and c. shadabi. Entomologia experimentalis et applicata 78:201–213. (Cited on page 91.)

Duarte, A. M. R. C., R. S. Malafronte, C. Cerutti Jr, I. Curado, B. R. Paiva, A. Y. Maeda, T. Yamasaki, M. E. L. Summa, D. V. D. Neves, et al. 2008. Natural *Plasmodium* infections in Brazilian wild monkeys: Reservoirs for human infections? Acta Trop 107:179–185. (Cited on pages 61, 68, and 72.)

Eccard, J. A., J. Pusenius, J. Sundell, S. Halle, and H. Ylönen. 2008. Foraging patterns of voles at heterogeneous avian and uniform mustelid predation risk. Oecologia 157:725–734. (Cited on page 41.)

Edman, J. D., and H. W. Kale. 1971. Host behavior: its influence on the feeding success of mosquitoes. Ann Entomol Soc Am 64:513–516. (Cited on page 62.)

Edman, J. D., L. A. Webber, and A. A. Schmid. 1974. Effect of host defenses on the feeding pattern of culex nigripalpus when offered a choice of blood sources. The Journal of parasitology pages 874–883. (Cited on page 71.)

Ehrlich, P. R. 1984. The structure and dynamics of butterfly populations. Pages 25–40 *in* R. I. Vane-Wright and P. R. Ackery, eds. The Biology of Butterflies. Academic Press, London. (Cited on page 31.)

Ehrlich, P. R., and L. E. Gilbert. 1973. Population structure and dynamics of the tropical butterfly *Heliconius ethilla*. Biotropica 5:69–82. (Cited on pages 31 and 36.)

Eterovick, P. C., A. C. O. de Queiroz Carnaval, D. M. Borges-Nojosa, D. L. Silvano, M. V. Segalla, and I. Sazima. 2005. Amphibian declines in Brazil: An overview. Biotropica 37:166–179. (Cited on page 29.)

Fahrig, L. 2003. Effects of habitat fragmentation on biodiversity. Annual review of ecology, evolution, and systematics pages 487–515. (Cited on pages 19 and 27.)

Ferguson, H. M., A. Dornhaus, A. Beeche, C. Borgemeister, M. Gottlieb, M. S. Mulla, J. E. Gimnig, D. Fish, and G. F. Killeen. 2010. Ecology: a prerequisite for malaria elimination and eradication. PLoS Med 7:e1000303. (Cited on page 61.)

Ferraz, G., J. D. Nichols, J. E. Hines, P. C. Stouffer, R. O. Bierregaard, and T. E. Lovejoy. 2007. A large-scale deforestation experiment: effects of patch area and isolation on Amazon birds. Science 315:238–241. (Cited on page 19.)

Fodrie, F. J., M. D. Kenworthy, and S. P. Powers. 2008. Unintended facilitation between marine consumers generates enhanced mortality for their shared prey. Ecology 89:3268–3274. (Cited on page 41.)

Fonseca, C. R. 2010. The silent mass extinctions of insect herbivores in biodiversity hotspots. Conservation Biology 23:1507–1515. (Cited on page 37.)

Fonseca, C. R., C. G. Becker, C. F. B. Haddad, and P. I. Prado. 2008. Response to comment on "Habitat split and the global decline of amphibians". science 320:874d–874d. (Cited on page 19.)

Fonseca, C. R., R. M. Coutinho, F. Azevedo, J. M. Berbert, G. Corso, and R. A. Kraenkel. 2013. Modeling habitat split: landscape and life history traits determine amphibian extinction thresholds. PLOS ONE 8:e66806. (Cited on page 7.)

Fonseca, C. R., G. Ganade, R. Baldissera, C. G. Becker, C. R. Boelter, A. D. Brescovit, L. M. Campos, T. Fleck, V. S. Fonseca, S. M. Hartz, et al. 2009. Towards an ecologically-sustainable forestry in the Atlantic Forest. Biological Conservation 142:1209–1219. (Cited on page 29.)

Forattini, O. P., A. C. Gomes, D. Natal, and J. L. F. Santos. 1986. Observações sobre atividade de mosquitos Culicidae em mata primitiva da encosta no Vale do Ribeira, São Paulo, Brasil. Rev. Saúde Pública 20:1–20. (Cited on pages 61 and 62.)

Frazier, M., R. B. Huey, and D. Berrigan. 2006. Thermodynamics constrains the evolution of insect population growth rates:"warmer is better". The American Naturalist 168:512–520. (Cited on page 88.)

Gaedke, U. 1992. The size distribution of plankton biomass in a large lake and its seasonal variability. Limnology and Oceanography 37:1202–1220. (Cited on page 116.)

Galetti, M. 2001. Indians within conservation units: lessons from the Atlantic Forest. Conserv Biol 15:798–799. (Cited on page 66.)

Galetti, M., H. C. Giacomini, R. S. Bueno, C. S. S. Bernardo, R. M. Marques, R. S. Bovendorp, C. E. Steffler, P. Rubim, S. K. Gobbo, C. I. Donatti, et al. 2009. Priority areas for the conservation of Atlantic forest large mammals. Biol Conserv 142:1229–1241. (Cited on page 61.)

Gardner, T. A., J. Barlow, and C. A. Peres. 2007. Paradox, presumption and pitfalls in conservation biology: the importance of habitat change for amphibians and reptiles. Biological Conservation 138:166–179. (Cited on page 26.)

Gilbert, L. E. 1984. The biology of butterfly communities. Pages 41–54 *in* R. I. Vane-Wright and P. R. Ackery, eds. The Biology of Butterflies. Academic Press, London. (Cited on page 31.)

———. 1991. Biodiversity of a central american *Heliconius* community: pattern, process, and problems. Pages 403–427 *in* P. W. Price, T. M. Lewinsohn, G. W. Fernandes, and W. W. Benson, eds. Plant-animal interactions: evolutionary ecology in tropical and temperate regions. New York, Wiley. (Cited on page 31.)

Gillooly, J. F., J. H. Brown, G. B. West, V. M. Savage, and E. L. Charnov. 2001. Effects of size and temperature on metabolic rate. Science 293:2248–2251. (Cited on page 84.)

Gillooly, J. F., E. L. Charnov, G. B. West, V. M. Savage, and J. H. Brown. 2002. Effects of size and temperature on developmental time. Nature 417:70–73. (Cited on pages 77 and 84.)

Giuggioli, L., G. Abramson, V. M. Kenkre, G. Suzán, E. Marcé, and T. L. Yates. 2005. Diffusion and home range parameters from rodent population measurements in panama. Bull Math Biol 67:1135–1149. (Cited on page 18.)

Glista, D. J., T. L. DeVault, and J. A. DeWoody. 2008. Vertebrate road mortality predominantly impacts amphibians. Herpetological Conservation and Biology 3:77–87. (Cited on page 29.)

Godoy, W., F. Von Zuben, C. Von Zuben, and S. dos Reis. 2001. Spatio-temporal dynamics and transition from asymptotic equilibrium to bounded oscillations in *Chrysomya albiceps* (diptera, calliphoridae). Mem. Inst. Oswaldo Cruz 96(5):627–634. (Cited on pages 9 and 14.)

Goodwin, B. J., and L. Fahrig. 2002. How does landscape structure influence landscape connectivity? Oikos 99:552–570. (Cited on page 30.)

Gross, K. 2008. Positive interactions among competitors can produce species-rich communities. Ecology Letters 11:929–936. (Cited on pages 42 and 59.)

Guimarães, J. H., A. P. Prado, and G. M. Buralli. 1979. Dispersal and distribution of three newly introduced species of *Chrysomya* robineau-desvoidy in brazil (diptera: Calliphoridae). Revista Brasileira de Entomologia 23:245–255. (Cited on page 18.)

Guimarães, J. H., A. P. Prado, and A. X. Linhares. 1978. Three newly introduced blowfly species in southern brazil (diptera: Calliphoridae). Revista Brasileira de Entomologia 22:53–60. (Cited on page 8.)

Gurney, W., S. Blythe, and R. Nisbet. 1980. Nicholson's blowflies revisited. Nature 287:17–21. (Cited on page 102.)

Gurney, W., R. Nisbet, and J. Lawton. 1983. The systematic formulation of tractable single-species population models incorporating age structure. The Journal of Animal Ecology pages 479–495. (Cited on pages 78 and 80.)

Gurney, W., and R. M. Nisbet. 1998. Ecological dynamics. Oxford University Press, Oxford. (Cited on page 78.)

Haddad, C., and R. Castro. 1998. Biodiversidade dos anfíbios no estado de são paulo. Biodiversidade do Estado de São Paulo, Brasil: síntese do conhecimento ao final do século XX 6:15–26. (Cited on page 29.)

Hanski, I. 1991. Single-species metapopulation dynamics: concepts, models and observations. Biological Journal of the Linnean Society 42:17–38. (Cited on page 19.)

Hanski, I., and I. A. Hanski. 1999. Metapopulation ecology, vol. 232. Oxford University Press Oxford. (Cited on pages 19, 29, and 41.)

Hanski, I., and C. D. Thomas. 1994. Metapopulation dynamics and conservation: a spatially explicit model applied to butterflies. Biological Conservation 68:167–180. (Cited on page 19.)

Harrison, S. 1991. Local extinction in a metapopulation context: an empirical evaluation. Biological journal of the Linnean Society 42:73–88. (Cited on page 19.)

Harrison, S., and E. Bruna. 1999. Habitat fragmentation and large-scale conservation: what do we know for sure? Ecography 22:225–232. (Cited on page 19.)

Harrison, S., D. D. Murphy, and P. R. Ehrlich. 1988. Distribution of the bay checkerspot butterfly, *Euphydryas editha bayensis*: evidence for a metapopulation model. American Naturalist pages 360–382. (Cited on page 19.)

Hay, M. E. 1986. Associational plant defenses and the maintenance of species diversity: turning competitors into accomplices. American Naturalist pages 617–641. (Cited on page 42.)

Heyer, W. R., A. S. Rand, C. A. G. da Cruz, and O. L. Peixoto. 1988. Decimations, extinctions, and colonizations of frog populations in southeast Brazil and their evolutionary implications. Biotropica pages 230–235. (Cited on page 29.)

Hiltunen, T., N. G. Hairston, G. Hooker, L. E. Jones, and S. P. Ellner. 2014. A newly discovered role of evolution in previously published consumer–resource dynamics. Ecology letters . (Cited on page 105.)

Hochachka, P., and G. N. S. David. 2002. Biochemical Adaptation: Mechanism and Process in Physiological Evolution: Mechanism and Process in Physiological Evolution. Oxford University Press. (Cited on page 77.)

Hoeck, H. N. 1989. Demography and competition in hyrax. Oecologia 79:353–360. (Cited on page 42.)

Holling, C. 1959. The components of predation as revealed by a study of small-mammal predation of the european pine sawfly. The Canadian Entomologist 91:293–320. (Cited on page 43.)

———. 1965. The functional response of predators to prey density and its role in mimicry and population regulation. Memoirs of the Entomological Society of Canada 45:1–60. (Cited on pages 107 and 112.)

Holt, R. D. 1984. Spatial heterogeneity, indirect interactions, and the coexistence of prey species. American Naturalist pages 377–406. (Cited on page 41.)

Holyoak, M., and S. P. Lawler. 1996. Persistence of an extinction-prone predator-prey interaction through metapopulation dynamics. Ecology pages 1867–1879. (Cited on page 19.)

Hsu, S., S. Hubbell, and P. Waltman. 1978. A contribution to the theory of competing predators. Ecological Monographs pages 337–349. (Cited on page 57.)

Huey, R. B., and D. Berrigan. 2001. Temperature, demography, and ectotherm fitness. The American Naturalist 158:204–210. (Cited on page 88.)

Ingberman, I., R. Fusco-Costa, C. C. Cheida, E. C. Nakano-Oliveira, R. G. Rodrigues, and E. L. A. Monteiro-Filho. 2010. Was there ever a Muriqui (*Brachyteles*) population in the Ilha do Cardoso State Park in southeastern Brazil? Neotrop Primates 17:21–24. (Cited on page 65.)

Johnson, F. H., and I. Lewin. 1946. The growth rate of e. coli in relation to temperature, quinine and coenzyme. Journal of Cellular and Comparative Physiology 28:47–75. (Cited on pages 76, 78, 85, 88, and 98.)

Johnson, P. T. J., P. J. Lund, R. B. Hartson, and T. P. Yoshino. 2009. Community diversity reduces *Schistosoma mansoni* transmission, host pathology and human infection risk. Proc R Soc Lond B Biol Sci 276:1657. (Cited on pages 62 and 71.)

Joly, P., C. Miaud, A. Lehmann, and O. Grolet. 2001. Habitat matrix effects on pond occupancy in newts. Conservation Biology 15:239–248. (Cited on page 29.)

Kats, L. B., and R. P. Ferrer. 2003. Alien predators and amphibian declines: review of two decades of science and the transition to conservation. Diversity and Distributions 9:99–110. (Cited on page 26.)

Kayano, M. T., and R. V. Andreoli. 2009. Clima da região nordeste do Brasil. Pages 213–233 *in* I. F. A. Cavalcanti, N. J. Ferreira, M. G. A. J. Silva, and M. A. F. S. Dias, eds. Tempo e Clima no Brasil. São Paulo, Oficina de Textos. (Cited on page 31.)

Keeling, M. J., and P. Rohani. 2008. Modeling infectious diseases in humans and animals. Princeton University Press, Princeton. (Cited on page 64.)

Keesing, F., L. K. Belden, P. Daszak, A. Dobson, C. D. Harvell, R. D. Holt, P. Hudson, A. Jolles, K. E. Jones, C. E. Mitchell, et al. 2010. Impacts of biodiversity on the emergence and transmission of infectious diseases. Nature 468:647–652. (Cited on pages 62 and 63.)

Keesing, F., J. Brunner, S. Duerr, M. Killilea, K. LoGiudice, K. Schmidt, H. Vuong, and R. S. Ostfeld. 2009. Hosts as ecological traps for the vector of lyme disease. Proc R Soc Lond B Biol Sci 276:3911. (Cited on pages 62 and 71.)

Kelly, D. W. 2001. Why are some people bitten more than others? Trends Parasitol 17:578–581. (Cited on page 71.)

Kingsolver, J. G. 2009. The well-temperatured biologist. The American Naturalist 174:755–768. (Cited on pages 76, 77, and 88.)

Kingsolver, J. G., H. A. Woods, L. B. Buckley, K. A. Potter, H. J. MacLean, and J. K. Higgins. 2011. Complex life cycles and the responses of insects to climate change. Integrative and Comparative Biology page icr015. (Cited on pages 76, 77, and 88.)

Klauschies, T., D. A. Vasseur, and U. Gaedke. ???? Intraspecific trait variation promotes species coexistence. In prep. (Cited on page 118.)

Koch, A. L. 1974. Competitive coexistence of two predators utilizing the same prey under constant environmental conditions. Journal of Theoretical Biology 44:387–395. (Cited on page 43.)

Kooijman, S. A. L. M. 1993. Dynamic energy budgets in biological systems. Cambridge university press. (Cited on page 92.)

Korpimaki, E., V. Koivunen, and H. Hakkarainen. 1996. Microhabitat use and behavior of voles under weasel and raptor predation risk: predator facilitation? Behavioral Ecology 7:30–34. (Cited on page 41.)

Kot, M. 1992. Discrete-time travelling waves: Ecological examples. J. Math. Biol. 30:413–436. (Cited on pages 6, 9, 10, 12, and 13.)

———. 2001. Elements of mathematical ecology. Cambridge University Press. (Cited on pages 43, 57, 78, and 82.)

Kot, M., M. Lewis, and P. Van Den Driessche. 1996. Dispersal data and the spread of invading organisms. Ecology 77:2027–2042. (Cited on pages 8, 12, 13, and 18.)

Kricher, J. 1997. A Neotropical Companion. Princeton University Press . (Cited on page 31.)

Kronforst, M. R., and L. E. Gilbert. 2008. The population genetics of mimetic diversity in *Heliconius butterflies*. Proceedings of the Royal Society of London B 275:793–500. (Cited on page 38.)

Kuefler, D., B. Hudgens, N. M. Haddad, W. F. Morris, and N. Thurgate. 2010. The conflicting role of matrix habitats as conduits and barriers for dispersal. Ecology 91:944–950. (Cited on page 30.)

Laan, R., and B. Verboom. 1990. Effects of pool size and isolation on amphibian communities. Biological Conservation 54:251–262. (Cited on page 28.)

Laporta, G. Z., P. I. K. L. de Prado, R. A. Kraenkel, R. M. Coutinho, and M. A. M. Sallum. 2013. Biodiversity can help prevent malaria outbreaks in tropical forests. PLoS Neglected Tropical Diseases 7. (Cited on page 40.)

Laporta, G. Z., D. G. Ramos, M. C. Ribeiro, and M. A. M. Sallum. 2011. Habitat suitability of *Anopheles* vector species and association with human malaria in the Atlantic Forest in south-eastern Brazil. Mem Inst Oswaldo Cruz 106:239–245. (Cited on page 63.)

Laurance, W. F., and R. O. Bierregaard. 1997. Tropical forest remnants: ecology, management, and conservation of fragmented communities. University of Chicago Press. (Cited on page 19.)

Lehtinen, R. M., S. M. Galatowitsch, and J. R. Tester. 1999. Consequences of habitat loss and fragmentation for wetland amphibian assemblages. Wetlands 19:1–12. (Cited on page 28.)

Levin, S. 1970. Community equilibria and stability, and an extension of the competitive exclusion principle. American Naturalist pages 413–423. (Cited on page 41.)

Levins, R., and D. Culver. 1971. Regional coexistence of species and competition between rare species. Proceedings of the National Academy of Sciences 68:1246–1248. (Cited on page 41.)

Lima, S. L., and P. A. Zollner. 1996. Towards a behavioral ecology of ecological landscapes. Trends in Ecology and Evolution 11:131–134. (Cited on page 30.)

Lindström, T., N. Håkansson, and U. Wennergren. 2011. The shape of the spatial kernel and its implications for biological invasions in patchy environments. Proc. R. Soc. B . (Cited on page 19.)

Lips, K. R., F. Brem, R. Brenes, J. D. Reeve, R. A. Alford, J. Voyles, C. Carey, L. Livo, A. P. Pessier, and J. P. Collins. 2006. Emerging infectious disease and the loss of biodiversity in a neotropical amphibian community. Proceedings of the national academy of sciences of the United States of America 103:3165–3170. (Cited on pages 26 and 28.)

Litchman, E., and C. A. Klausmeier. 2008. Trait-based community ecology of phytoplankton. Annual Review of Ecology, Evolution, and Systematics 39:615–639. (Cited on page 116.)

Loman, J. 1988. Breeding by *Rana temporaria*; the importance of pond size and isolation. Memoranda Societatis pro Fauna et Flora Fennica 64:113–115. (Cited on page 27.)

Lomolino, M. V. 1986. Mammalian community structure on islands: the importance of immigration, extinction and interactive effects. Biological Journal of the Linnean Society 28:1–21. (Cited on page 19.)

Long, M. A., and M. S. Fee. 2008. Using temperature to analyse temporal dynamics in the songbird motor pathway. Nature 456:189–194. (Cited on page 77.)

Losey, J. E., and R. F. Denno. 1998. Positive predator-predator interactions: enhanced predation rates and synergistic suppression of aphid populations. Ecology 79:2143–2152. (Cited on pages 41 and 59.)

Lutscher, F., and T. Iljon. 2013. Competition, facilitation and the allee effect. Oikos 122:621–631. (Cited on page 60.)

Lutz, A. 1903. Waldmosquitos und waldmalaria. Centralbl Bakt 33:282–292. (Cited on page 61.)

MacArthur, R. H., and E. O. Wilson. 1967. The theory of island biogeography: monographs in population biology. Princeton University . (Cited on page 19.)

Maciel, G. A., and F. Lutscher. 2013. How individual movement response to habitat edges affects population persistence and spatial spread. The American Naturalist 182:42–52. (Cited on page 5.)

Mallet, J. 1986. Dispersal and gene flow in a butterfly with home range behavior: *Heliconius erato* (lepidoptera: Nymphalidae). Biotropica 68:210–21. (Cited on page 36.)

Marrelli, M. T., R. S. Malafronte, M. A. M. Sallum, and D. Natal. 2007. *Kerteszia* subgenus of *Anopheles* associated with the Brazilian Atlantic rainforest: current knowledge and future challenges. Malaria J 6:127. (Cited on page 61.)

Marsh, D. M., and P. C. Trenham. 2001. Metapopulation dynamics and amphibian conservation. Conservation Biology 15:40–49. (Cited on pages 19 and 29.)

May, R. M., and G. F. Oster. 1976. Bifurcations and dynamic complexity in simple ecological models. The American Naturalist 110:573–599. (Cited on page 11.)

McCann, K. S. 2000. The diversity–stability debate. Nature 405:228–233. (Cited on page 70.)

Melbourne, B. A., and A. Hastings. 2009. Highly variable spread rates in replicated biological invasions: Fundamental limits to predictability. Science 325:1536–1539. (Cited on page 14.)

Metzger, J. P., T. M. Lewinsohn, C. A. Joly, L. M. Verdade, L. A. Martinelli, and R. R. Rodrigues. 2010. Brazilian law: full speed in reverse? Science 329:276–277. (Cited on page 63.)

Meyer, J. J., and J. E. Byers. 2005. As good as dead? sublethal predation facilitates lethal predation on an intertidal clam. Ecology Letters 8:160–166. (Cited on page 41.)

Mistro, D. C., L. A. D. Rodrigues, and W. C. Ferreira-Jr. 2005. The africanized honey bee dispersal: a mathematical zoom. Bull. Math. Biol. 67:281–312. (Cited on page 18.)

Mittermeier, R. A., N. Myers, C. G. Mittermeier, P. Robles Gil, et al. 1999. Hotspots: Earth's biologically richest and most endangered terrestrial ecoregions. CEMEX, SA, Agrupación Sierra Madre, SC. (Cited on page 29.)

Moretti, T., R. Coutinho, R. Moral, C. Ferreira, and W. Godoy. 2013. Quantitative and qualitative dynamics of exotic and native blowflies (diptera: Calliphoridae) with migrations among municipalities. Community Ecology 14:249–257.

Murdoch, W. W. 1973. Functional response of predators. Journal of Applied Ecology 10:335–342. (Cited on page 107.)

Murdoch, W. W., C. J. Briggs, and R. M. Nisbet. 2013. Consumer-Resource Dynamics (MPB-36). Princeton University Press. (Cited on pages 78, 79, 90, 100, 102, and 103.)

Muriel, S. B., and G. H. Kattan. 2009. Effects of patch size and type of coffee matrix on ithomiine butterfly diversity and dispersal in

cloud-forest fragments. Conservation Biology 23:948–956. (Cited on page 31.)

Murray, J. D. 2002. Mathematical Biology II: Spatial models and biomedical applications. 3rd ed. Springer, New York, NY, USA,. (Cited on page 5.)

Nardoni Laws, A., and G. E. Belovsky. 2010. How will species respond to climate change? examining the effects of temperature and population density on an herbivorous insect. Environmental entomology 39:312–319. (Cited on page 89.)

Nash, D. R., D. J. Agassiz, H. Godfray, and J. H. Lawton. 1995. The pattern of spread of invading species: Two leaf-mining moths colonizing great britain. J. Anim. Ecol. 64:225–233. (Cited on page 18.)

Nathan, R., W. M. Getz, E. Revilla, M. Holyoak, R. Kadmon, D. Saltz, and P. E. Smouse. 2008. A movement ecology paradigm for unifying organismal movement research. Proceedings of the National Academy of Sciences (USA) 105:19052–19059. (Cited on page 30.)

Nathaniel Holland, J., and D. L. DeAngelis. 2009. Consumer-resource theory predicts dynamic transitions between outcomes of interspecific interactions. Ecology letters 12:1357–1366. (Cited on page 42.)

Neubert, M. G., M. Kot, and M. A. Lewis. 1995. Dispersal and pattern formation in a discrete-time predator-prey model. Theor Popul Biol 48:7–43. (Cited on page 12.)

Neubert, M. G., and I. M. Parker. 2004. Projecting rates of spread for invasive species. Risk Analysis 24:817–831. (Cited on page 18.)

Nijhout, H. 1994. Insect hormones. (Cited on pages 76, 77, and 88.)

Nimer, E. 1972. Climatologia do brasil. Instituto Brasileiro de Geografia e Estatística . (Cited on page 30.)

Nisbet, R., and W. Gurney. 1983. The systematic formulation of population models for insects with dynamically varying instar duration. Theoretical Population Biology 23:114–135. (Cited on pages 75, 78, 80, 102, and 103.)

Nisbet, R. M. 1997. Delay-differential equations for structured populations. Pages 89–118 *in* Structured-population models in marine, terrestrial, and freshwater systems. Springer. (Cited on pages 90 and 100.)

Norberg, J., D. P. Swaney, J. Dushoff, J. Lin, R. Casagrandi, and S. A. Levin. 2001. Phenotypic diversity and ecosystem functioning in changing environments: a theoretical framework. Proceedings of the National Academy of Sciences 98:11376–11381. (Cited on pages 116 and 117.)

Ogden, N., A. Casey, N. French, J. Adams, and Z. Woldehiwet. 2002. Field evidence for density-dependent facilitation amongst ixodes ricinus ticks feeding on sheep. Parasitology 124:117–125. (Cited on page 44.)

Ohlberger, J., E. Edeline, L. A. Vøllestad, N. C. Stenseth, and D. Claessen. 2011. Temperature-driven regime shifts in the dynamics of size-structured populations. The American Naturalist 177:211–223. (Cited on page 89.)

Okubo, A., and S. A. Levin. 1989. A theoretical framework for data analysis of wind dispersal of seeds and pollen. Ecology 70:329–338. (Cited on page 12.)

Oliveira-Ferreira, J., M. V. G. Lacerda, P. Brasil, J. L. B. Ladislau, P. L. Tauil, and C. T. Daniel-Ribeiro. 2010. Review Malaria in Brazil: an overview. Malaria J 9:115. (Cited on page 61.)

Orbach, R. 1986. Dynamics of fractal networks. Science 231:814–819. (Cited on page 27.)

Ostfeld, R. S., and F. Keesing. 2000. Biodiversity series: the function of biodiversity in the ecology of vector-borne zoonotic diseases. Can J Zool 78:2061–2078. (Cited on pages 62 and 71.)

Ovaskainen, O., and I. Hanski. 2004. From individual behavior to metapopulation dynamics: unifying the patchy population and classic metapopulation models. American Naturalist 164:364–377. (Cited on page 30.)

Pachepsky, E., and J. Levine. 2011. Density dependence slows invader spread in fragmented landscapes. Am Naturalist 177:18–28. (Cited on pages 11 and 14.)

Pennington, R. T., D. E. Prado, and C. A. Pendry. 2000. Neotropical seasonally dry forests and quaternary vegetation changes. Journal of Biogeography 27:261–273. (Cited on page 30.)

Pianka, E. P. 1974. Niche overlap and diffuse competition. Proc Natl Acad Sci U S A 71:2141–2145. (Cited on page 62.)

Pounds, J. A., M. R. Bustamante, L. A. Coloma, J. A. Consuegra, M. P. Fogden, P. N. Foster, E. La Marca, K. L. Masters, A. Merino-Viteri, R. Puschendorf, et al. 2006. Widespread amphibian extinctions from epidemic disease driven by global warming. Nature 439:161–167. (Cited on page 26.)

Prevedello, J. A., and M. V. Vieira. 2010. Does the type of matrix matter? A quantitative review of the evidence. Biodiversity and Conservation 19:1205–1223. (Cited on page 30.)

Prout, T., and F. McChesney. 1985. Competition among immatures affects their adult fertility: Population dynamics. The American Naturalist 126:521–558. (Cited on page 9.)

Ramos, R. R., and A. V. L. Freitas. 1999. Population biology and wing color variation in *Heliconius erato phyllis* (nymphalidae). Journal of the Lepidopterists' Society 53:11–21. (Cited on page 31.)

Randolph, S. E., and A. Dobson. 2012. Pangloss revisited: a critique of the dilution effect and the biodiversity-buffers-disease paradigm. Parasitology 139:847–863. (Cited on page 72.)

Ratkowsky, D. A., J. Olley, and T. Ross. 2005. Unifying temperature effects on the growth rate of bacteria and the stability of globular proteins. Journal of theoretical biology 233:351–362. (Cited on pages 76, 77, 78, 85, and 98.)

Raymundo, L. J., A. R. Halford, A. P. Maypa, and A. M. Kerr. 2009. Functionally diverse reef-fish communities ameliorate coral disease. Proc Natl Acad Sci U S A 106:17067. (Cited on page 62.)

Reigada, C., and W. Godoy. 2006. Larval density, temperature and biological aspects of chrysomya megacephala (diptera: Calliphoridae). Arquivo Brasileiro de Medicina Veterinária e Zootecnia 58:562–566. (Cited on page 89.)

Reitz, R. 1983. Bromeliáceas e a malária-bromélia endêmica. Itajaí: Herbário Barbosa Rodrigues. (Cited on page 62.)

Relyea, R. A. 2005. The lethal impact of roundup on aquatic and terrestrial amphibians. Ecological applications 15:1118–1124. (Cited on pages 26 and 28.)

Remsburg, A. J., and M. G. Turner. 2009. Aquatic and terrestrial drivers of dragonfly (odonata) assemblages within and among north-temperate lakes. Journal of the North American Benthological Society 28:44–56. (Cited on page 19.)

Ribeiro, M. C., J. P. Metzger, A. C. Martensen, F. J. Ponzoni, and M. M. Hirota. 2009. The Brazilian Atlantic forest: how much is left, and how is the remaining forest distributed? implications for conservation. Biological Conservation 142:1141–1153. (Cited on pages 29 and 37.)

Richards, C., I. Paterson, and M. Villet. 2008. Estimating the age of immature *Chrysomya albiceps* (diptera: Calliphoridae), correcting for temperature and geographical latitude. Int J Legal Med 122:271––279. (Cited on page 17.)

Richards, C., K. Williams, and M. Villet. 2009. Predicting geographic distribution of seven forensically significant blowfly

species (diptera: Calliphoridae) in south africa. Afr Entomol 17:170–182. (Cited on pages 11 and 18.)

Ricker, W. E. 1954. Stock and recruitment. J Fish Res Board Can 11:559–623. (Cited on page 11.)

Ricketts, T. H. 2001. The matrix matters: effective isolation in fragmented landscapes. American Naturalist 158:87–99. (Cited on page 30.)

Ritchie, M. E. 1996. Interaction of temperature and resources in population dynamics: an experimental test of theory. Frontiers of population ecology. CSIRO Publishing, Melbourne pages 79–91. (Cited on page 89.)

Roland, J. N. K., and S. Fownes. 2000. Alpine parnassius butterfly dispersal: effects of landscape and population size. Ecology 81:1642–1653. (Cited on pages 30 and 37.)

Rosenzweig, M., and R. MacArthur. 1963. Graphical representation and stability conditions of predator-prey interactions. The American Naturalist 97:209–223. (Cited on pages 51, 52, and 107.)

São Bernardo, C. S. 2004. Abundância, densidade e tamanho populacional de aves e mamíferos cinegéticos no Parque Estadual Ilha do Cardoso, SP, Brasil. Universidade de São Paulo [Master's thesis], Piracicaba. (Cited on page 66.)

Sakai, A., F. W. Allendorf, J. S. Holt, D. M. Lodge, J. Molofsky, K. A. With, S. Baughman, R. J. Cabin, J. E. Cohen, N. C. Ellstrand, D. E. McCauley, P. O. ando Ingrid M. Parker and1 John N. Thompson and1, and S. G. Weller. 2001. The population biology of invasive species. Ann. Rev. Ecol. System. . 32:305–332. (Cited on page 9.)

Saul, A. 2003. Zooprophylaxis or zoopotentiation: the outcome of introducing mortality while searching. Malaria J 2:32. (Cited on pages 62, 71, and 72.)

Savage, V. M., J. F. Gillooly, J. H. Brown, G. B. West, and E. L. Charnov. 2004. Effects of body size and temperature on population growth. The American Naturalist 163:429–441. (Cited on pages 77, 79, 84, and 100.)

Sawyer, D. R., and D. O. Sawyer. 1992. The malaria transition and the role of social science research. Pages 105—122 *in* L. C. Cheng, ed. Advancing the Health in Developing Countries: The Role of Social Research. Westport, Auburn House. (Cited on page 63.)

Sberze, M., M. Cohn-Haft, and G. Ferraz. 2010. Old growth and secondary forest site occupancy by nocturnal birds in a neotropical landscape. Animal Conservation 13:3–11. (Cited on page 30.)

Schoolfield, R., P. Sharpe, and C. Magnuson. 1981. Non-linear regression of biological temperature-dependent rate models based on absolute reaction-rate theory. Journal of Theoretical Biology 88:719–731. (Cited on pages 76, 77, 78, 85, 88, 92, and 98.)

Segura, A., C. Kruk, D. Calliari, F. García-Rodriguez, D. Conde, C. Widdicombe, and H. Fort. 2013. Competition drives clumpy species coexistence in estuarine phytoplankton. Scientific reports 3. (Cited on page 116.)

Shannon, R. C. 1931. The environment and behavior of some Brazilian mosquitoes. Proc Ent Soc Wash 33:1–26. (Cited on page 62.)

Sharpe, P. J., and D. W. DeMichele. 1977. Reaction kinetics of poikilotherm development. Journal of theoretical biology 64:649–670. (Cited on pages 76, 77, 78, 85, 88, 92, and 98.)

Sheldon, R., A. Prakash, and W. Sutcliffe. 1972. The size distribution of particles in the ocean. Limnol. Oceanogr 17:327–340. (Cited on page 116.)

Shigesada, N., and K. Kawasaki. 1997. Biological Invasions: Theory and Practice. Oxford Univ. Press, Oxford(UK). (Cited on page 8.)

Shigesada, N., K. Kawasaki, and E. Teramoto. 1986. Traveling periodic waves in heterogeneous environments. Theor Popul Biol 30:143–160. (Cited on page 11.)

Silva, S. S. L., C. S. Zickel, and L. A. Cestaro. 2008. Vascular flora and physiognomic profile of an area of restinga vegetation along the southern coast of Pernambuco State, Brazil. Acta Botanica Brasilica 22:1123–1135. (Cited on page 30.)

Sinka, M. E., M. J. Bangs, S. Manguin, T. Chareonviriyaphap, A. P. Patil, W. H. Temperley, P. W. Gething, I. R. F. Elyazar, C. W. Kabaria, R. E. Harbach, et al. 2011. The dominant *Anopheles* vectors of human malaria in the Asia-Pacific region: occurrence data, distribution maps and bionomic précis. Parasit Vectors 4:89. (Cited on page 61.)

Sinka, M. E., M. J. Bangs, S. Manguin, M. Coetzee, C. M. Mbogo, J. Hemingway, A. P. Patil, W. H. Temperley, P. W. Gething, C. W. Kabaria, et al. 2010*a*. The dominant *Anopheles* vectors of human malaria in Africa, Europe and the Middle East: occurrence data, distribution maps and bionomic précis. Parasit Vectors 3:117. (Cited on page 61.)

Sinka, M. E., Y. Rubio-Palis, S. Manguin, A. P. Patil, W. H. Temperley, P. W. Gething, T. Van Boeckel, C. W. Kabaria, R. E. Harbach, and S. I. Hay. 2010*b*. The dominant *Anopheles* vectors of human malaria

in the Americas: occurrence data, distribution maps and bionomic précis. Parasit Vectors 3:72. (Cited on page 61.)

Skellam, J. 1951. Random dispersal in theoretical populations. Biometrika 38:196–218. (Cited on page 5.)

Smith, D. L., K. E. Battle, S. I. Hay, C. M. Barker, T. W. Scott, and F. E. McKenzie. 2012. Ross, macdonald, and a theory for the dynamics and control of mosquito-transmitted pathogens. PLoS pathogens 8:e1002588. (Cited on page 73.)

Smith, H. L. 1995. The theory of the chemostat: dynamics of microbial competition, vol. 13. Cambridge university press. (Cited on page 42.)

Smith, L. B. 1953. Bromeliad Malaria. Rep Smithson Inst 1952 pages 385–398. (Cited on pages 61, 62, 72, and 73.)

So, P.-M., and D. Dudgeon. 1989. Larval growth dynamics ofhemipyrellia ligurriens (calliphoridae) andboettcherisca formosensis (sarcophagidae) in crowded and uncrowded cultures. Researches on Population Ecology 31:113–122. (Cited on page 44.)

Stachowicz, J. J. 2001. Mutualism, facilitation, and the structure of ecological communities positive interactions play a critical, but underappreciated, role in ecological communities by reducing physical or biotic stresses in existing habitats and by creating new habitats on which many species depend. Bioscience 51:235–246. (Cited on page 59.)

Stuart, S. N., J. S. Chanson, N. A. Cox, B. E. Young, A. S. Rodrigues, D. L. Fischman, and R. W. Waller. 2004. Status and trends of amphibian declines and extinctions worldwide. Science 306:1783–1786. (Cited on page 26.)

Suguiu, K., and S. Petri. 1973. Stratigraphy of the Iguape-Cananéia lagoonal region sedimentary deposits, São Paulo State, Brazil. Bol Inst Geo 4:1–20. (Cited on page 65.)

Sunday, J. M., A. E. Bates, and N. K. Dulvy. 2011. Global analysis of thermal tolerance and latitude in ectotherms. Proceedings of the Royal Society B: Biological Sciences 278:1823–1830. (Cited on page 88.)

Suzán, G., E. Marcé, J. T. Giermakowski, J. N. Mills, G. Ceballos, R. S. Ostfeld, B. Armién, J. M. Pascale, and T. L. Yates. 2009. Experimental evidence for reduced rodent diversity causing increased hantavirus prevalence. PLoS One 4:e5461. (Cited on pages 62 and 71.)

Swaddle, J. P., and S. E. Calos. 2008. Increased avian diversity is associated with lower incidence of human West Nile infection: observation of the dilution effect. PLoS One 3:e2488. (Cited on pages 62 and 71.)

Swift, T. L., and S. J. Hannon. 2010. Critical thresholds associated with habitat loss: a review of the concepts, evidence, and applications. Biological Reviews 85:35–53. (Cited on page 27.)

Tabarelli, M., L. P. Pinto, J. M. C. Silva, M. Hirota, and L. Bedê. 2005. Challenges and opportunities for biodiversity conservation in the Brazilian Atlantic Forest. Conserv Biol 19:695–700. (Cited on page 65.)

Tackx, M., P. Herman, P. Van Rijswijk, M. Vink, and C. Bakker. 1994. Plankton size distributions and trophic relations before and after the construction of the storm-surge barrier in the Oosterschelde estuary. Springer. (Cited on page 116.)

Terborgh, J. 2000. The fate of tropical forests: a matter of stewardship. Conserv biol 14:1358–1361. (Cited on page 72.)

Tilman, D. 1982. Resource competition and community structure., vol. 17. Princeton University Press, Princeton, N. J. (Cited on pages 41, 47, and 49.)

Tirok, K., B. Bauer, K. Wirtz, and U. Gaedke. 2011. Predator-prey dynamics driven by feedback between functionally diverse trophic levels. PLoS ONE 6:e27357. (Cited on page 108.)

Tirok, K., and U. Gaedke. 2010. Internally driven alternation of functional traits in a multispecies predator-prey system. Ecology 91:1748–1762. (Cited on pages 105, 108, and 112.)

Tockner, K., M. Pusch, D. Borchardt, and M. S. Lorang. 2010. Multiple stressors in coupled river–floodplain ecosystems. Freshwater Biology 55:135–151. (Cited on page 28.)

Turner, J. R. G. 1971. Experiments on the demography of tropical butterflies. ii. longevity and home-range behavior in *Heliconius erato*. Biotropica 3:21–31. (Cited on page 36.)

Ullyett, G. C. 1950. Competition for food and allied phenomena in sheep-blowfly populations. Philos T R Soc B 234:77–174. (Cited on page 9.)

Van de Wolfshaar, K., A. De Roos, and L. Persson. 2008. Population feedback after successful invasion leads to ecological suicide in seasonal environments. Ecology 89:259–268. (Cited on page 89.)

Van Der Have, T. 2002. A proximate model for thermal tolerance in ectotherms. Oikos 98:141–155. (Cited on pages 76, 77, 78, 88, and 98.)

Van der Have, T., and G. De Jong. 1996. Adult size in ectotherms: temperature effects on growth and differentiation. Journal of Theoretical Biology 183:329–340. (Cited on pages 76, 77, 78, 85, 88, 92, and 98.)

Vasseur, D. A., and K. S. McCann. 2005. A mechanistic approach for modeling temperature-dependent consumer-resource dynamics. The American Naturalist 166:184–198. (Cited on pages 89 and 100.)

Vergnon, R., N. K. Dulvy, and R. P. Freckleton. 2009. Niches versus neutrality: uncovering the drivers of diversity in a species-rich community. Ecology letters 12:1079–1090. (Cited on page 116.)

Warwick, R., N. Collins, J. Gee, and C. George. 1986. Species size distributions of benthic and pelagic metazoa: evidence for interaction. Mar. Ecol. Prog. Ser 34:63–68. (Cited on page 116.)

Wederkinch, E. 1988. Population size, migration barriers, and other features of *Rana dalmatina* populations near Koege, Zealand, Denmark. Memoranda societatis pro fauna et flora fennica 64:101–103. (Cited on page 27.)

Wells, K. D. 2010. The ecology and behavior of amphibians. University of Chicago Press. (Cited on page 28.)

Weygoldt, P. 1989. Changes in the composition of mountain stream frog communities in the Atlantic mountains of Brazil: frogs as indicators of environmental deteriorations? Studies on Neotropical Fauna and Environment 24:249–255. (Cited on page 29.)

White, K. A. J., and C. A. Gilligan. 1998. Spatial heterogeneity in three-species, plant–parasite–hyperparasite, systems. Phil. Trans. R. Soc. Lond. B 353:543–557. (Cited on page 60.)

Wiens, J. A. 1989. Spatial scaling in ecology. Functional Ecology 3:385–397. (Cited on page 30.)

Williamson, M. 1999. Invasions. Ecography 22:5–12. (Cited on page 8.)

Wilson, E. O. 1988. Biodiversity. National Academy Press, Washington. (Cited on page 63.)

Wuethrich, B. 2007. Reconstructing Brazil's Atlantic Rainforest. Science 315:1070–1072. (Cited on page 29.)

Yoshida, T., S. P. Ellner, L. E. Jones, B. J. Bohannan, R. E. Lenski, and N. G. Hairston Jr. 2007. Cryptic population dynamics: rapid evolution masks trophic interactions. PLoS Biology 5:e235. (Cited on page 112.)

Yoshida, T., L. E. Jones, S. P. Ellner, G. F. Fussmann, and N. G. Hairston. 2003. Rapid evolution drives ecological dynamics in a predator–prey system. Nature 424:303–306. (Cited on pages 105 and 126.)

Zavortink, T. J. 1973. Mosquito studies (Diptera, Culicidae) XXIX. A review of the subgenus *Kerteszia* of *Anopheles*. Contrib Am Entomol Inst 9:1–54. (Cited on page 61.)